

Fractal Coagulation Kinetics

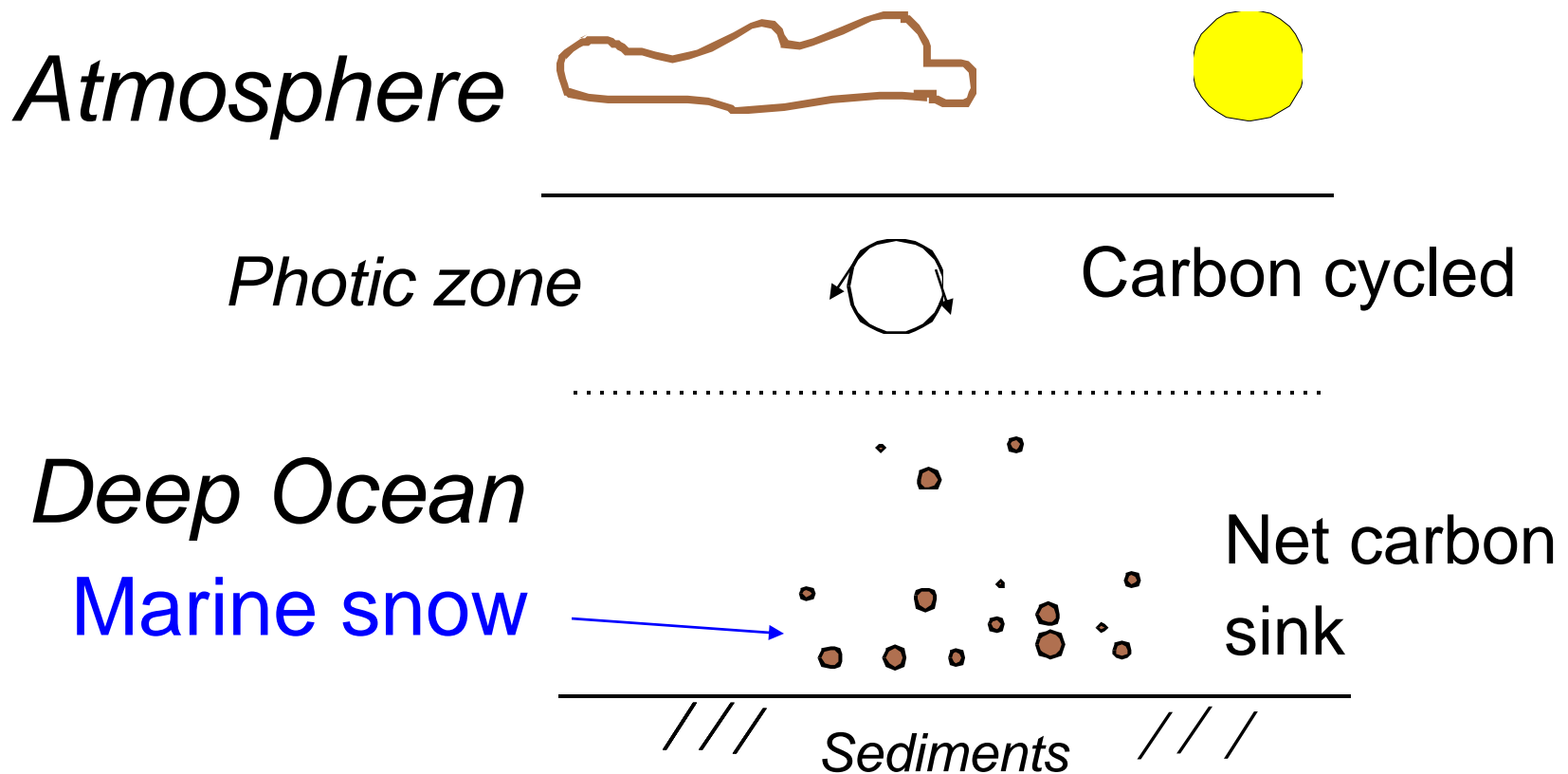
Bruce E. Logan

**Department of Civil & Environmental Engineering
The Pennsylvania State University**

Email: blogan@psu.edu

<http://www.engr.psu.edu/ce/enve/logan.html>

Global Carbon Cycling

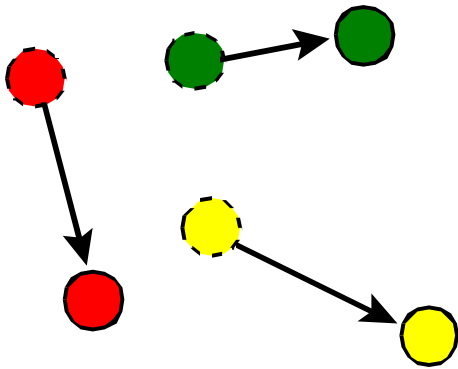


Marine snow can't form...

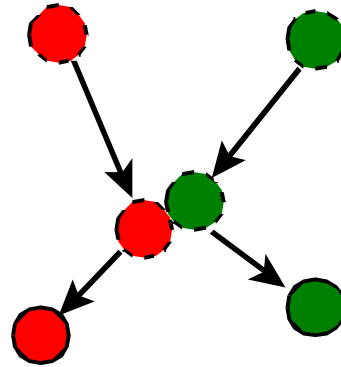
but it does!

- Too few particles (phytoplankton), and therefore too few collisions to make **large** aggregates.
- Marine snow aggregates exist, so our calculations must be wrong.
- How can basis of calculations be improved?

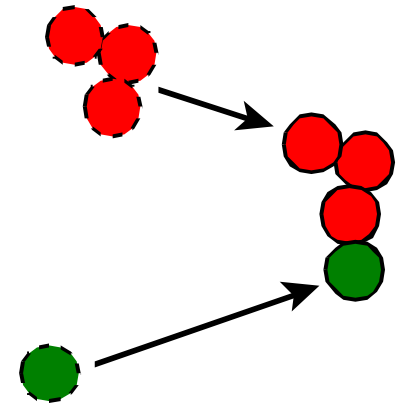
Coagulation



No collisions



**Unsuccessful
collisions**

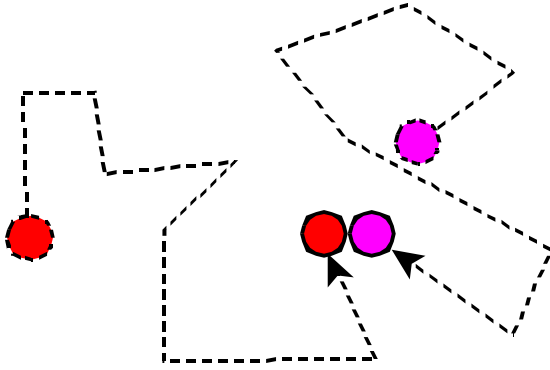


**Successful
collisions &
coagulation**

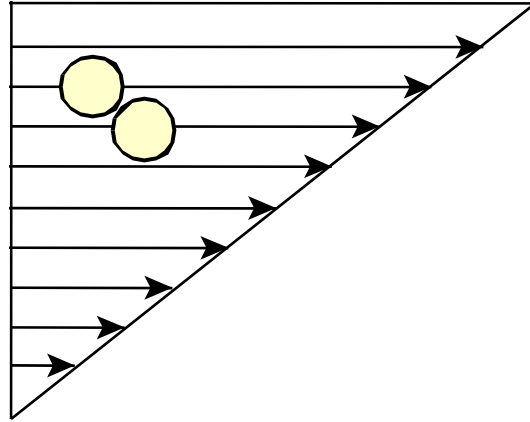
Coagulation Theory

- Coagulation theory is quite old, dating back to Schmoluchowski (1917)
- Coagulation rate proportional to particle concentration squared.
- All particles are spheres.

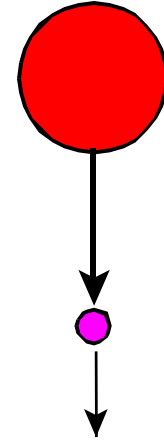
Coagulation mechanisms



Brownian
motion



Fluid
shear

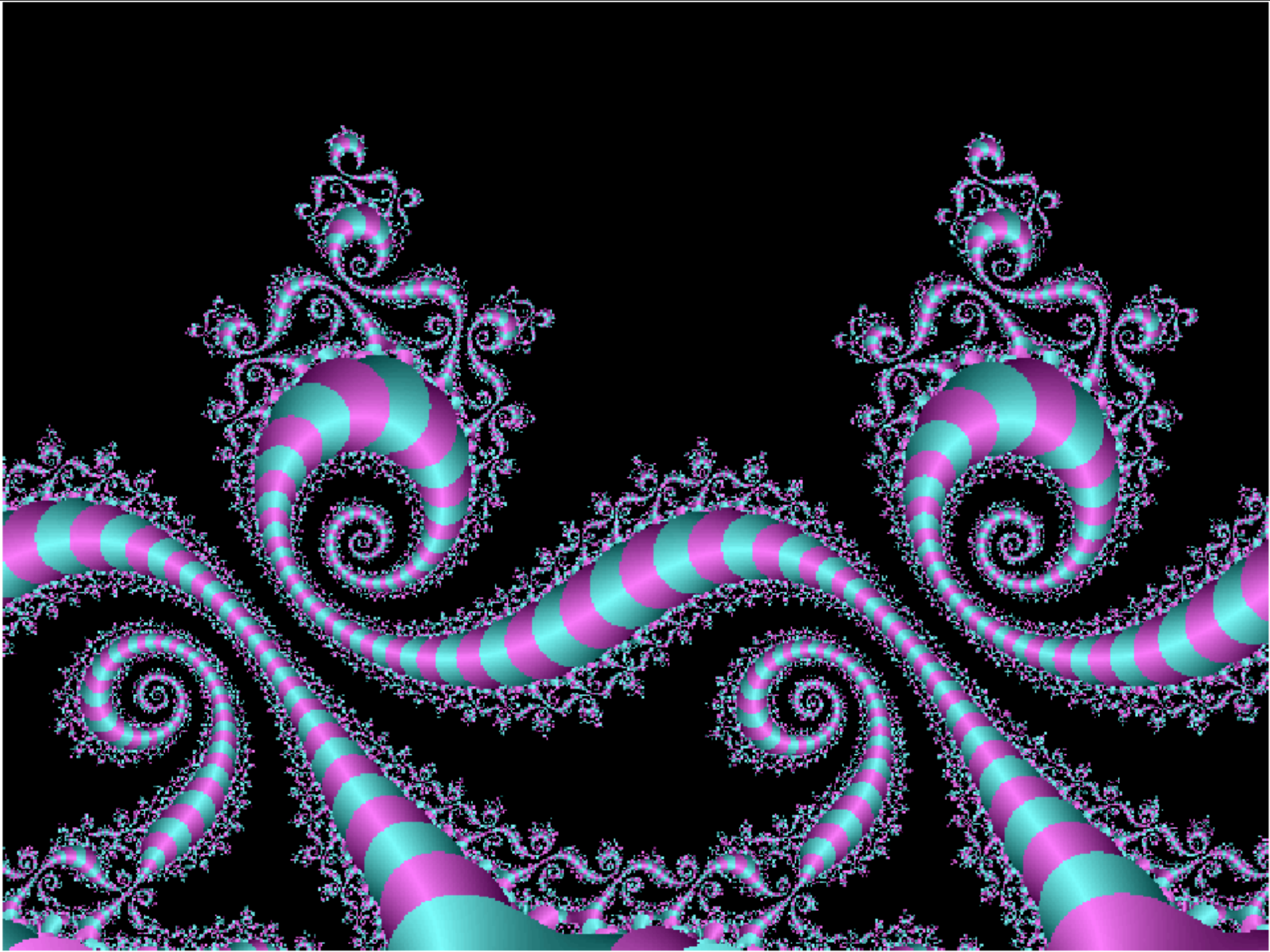


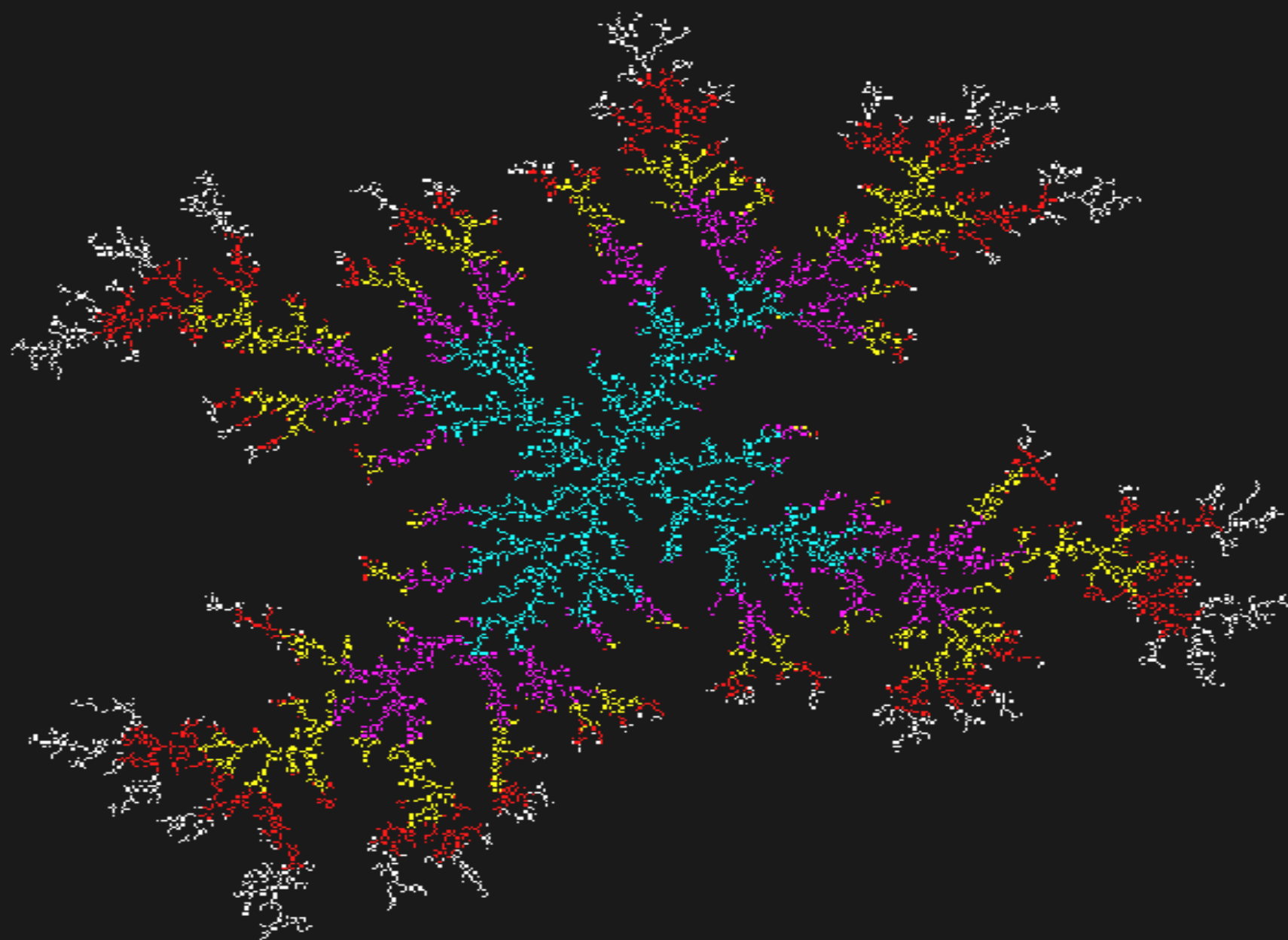
Differential
sedimentation

**What paradigm shift is needed
to explain the formation of
marine snow?**

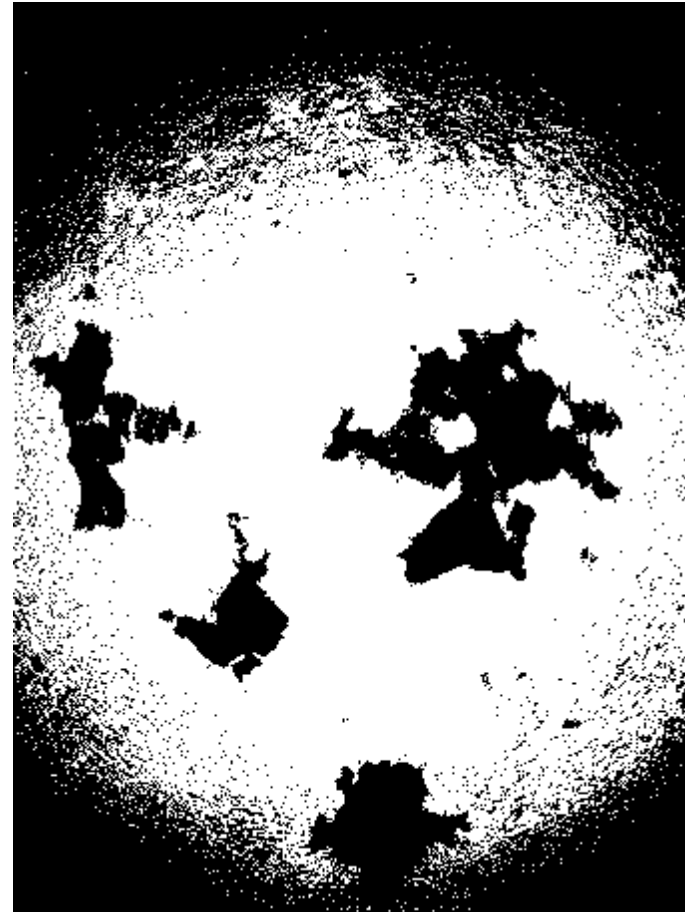
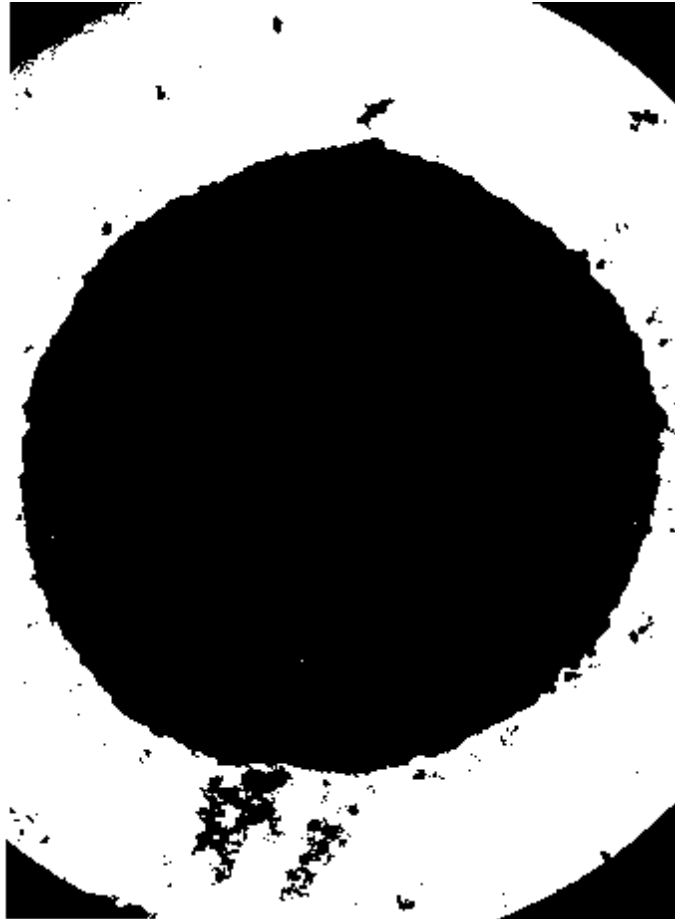
Birth of Fractal Geometry

- In 1982, Benoit Mandelbrot publishes “Fractal Geometry” and fractal mathematics is born.
- Fractal scaling relationships are observed to apply in a variety of fields including geography, hydrology, turbulence, and mathematical solution sets.
- Colorful fractal pictures are developed.





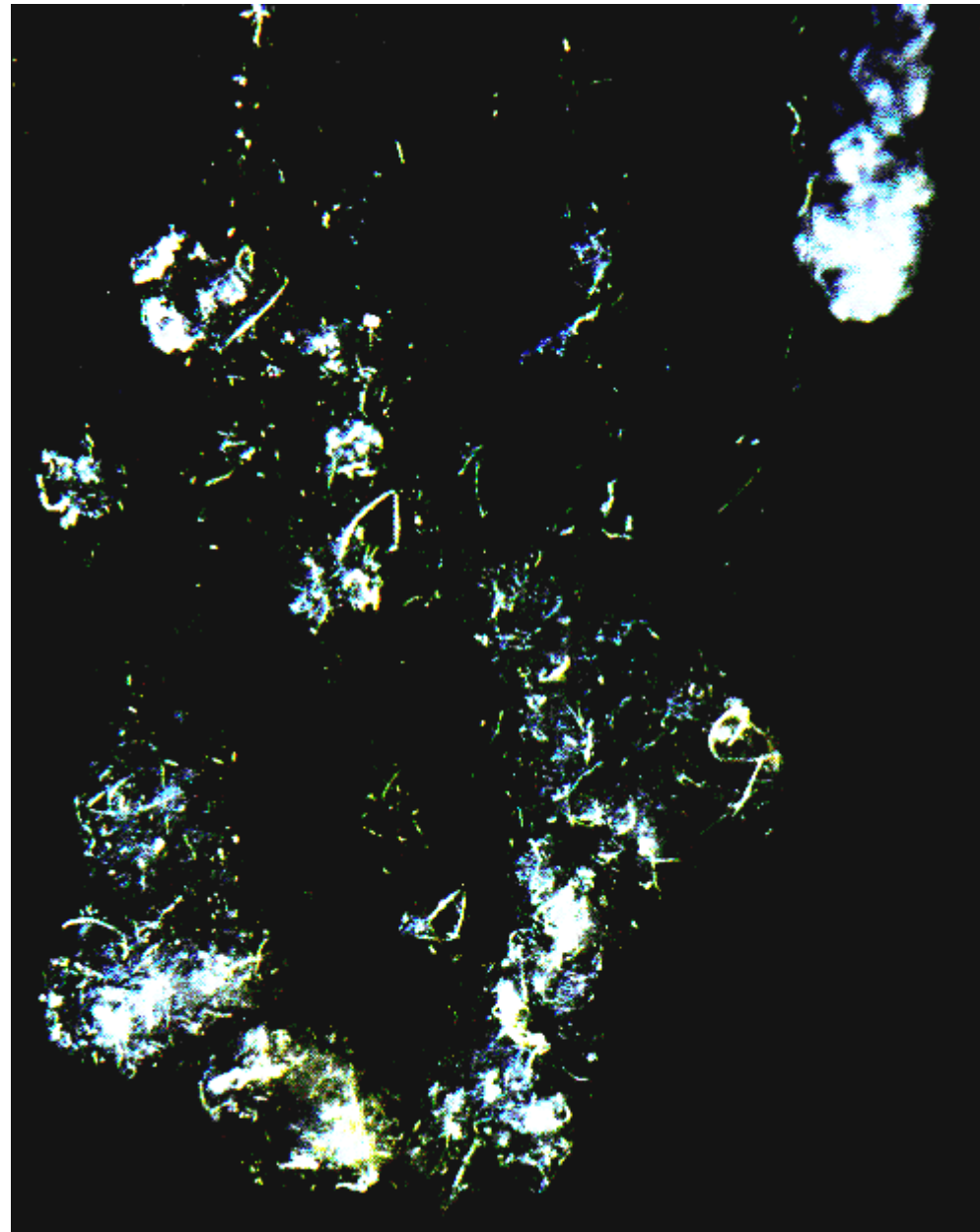
Bacterial aggregates produced in the laboratory have a variety of shapes



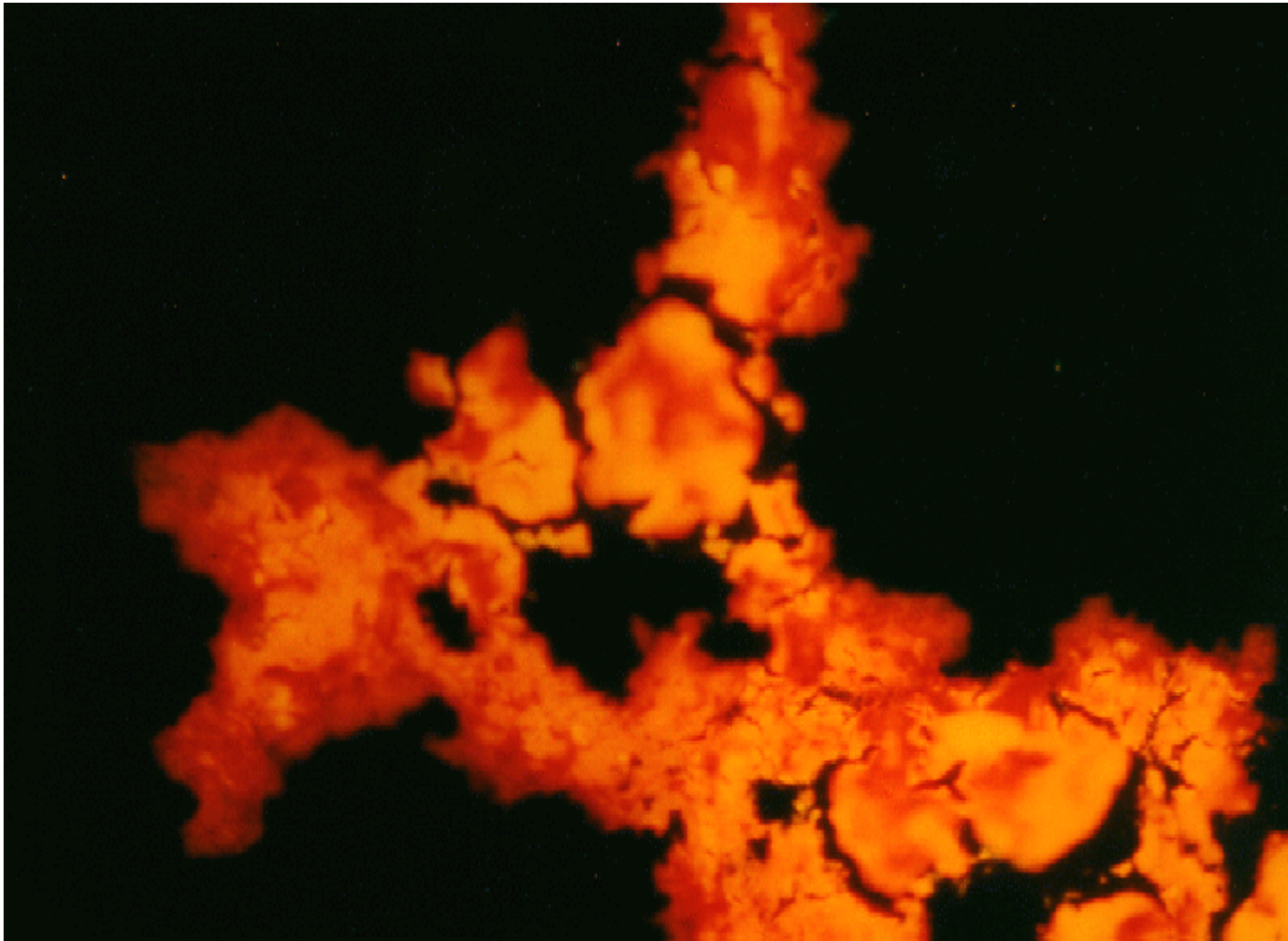
Shewanella putrifaciens grown on two different growth substrates under otherwise identical mixing and media conditions.

Particles that coagulate in nature are not spheres...

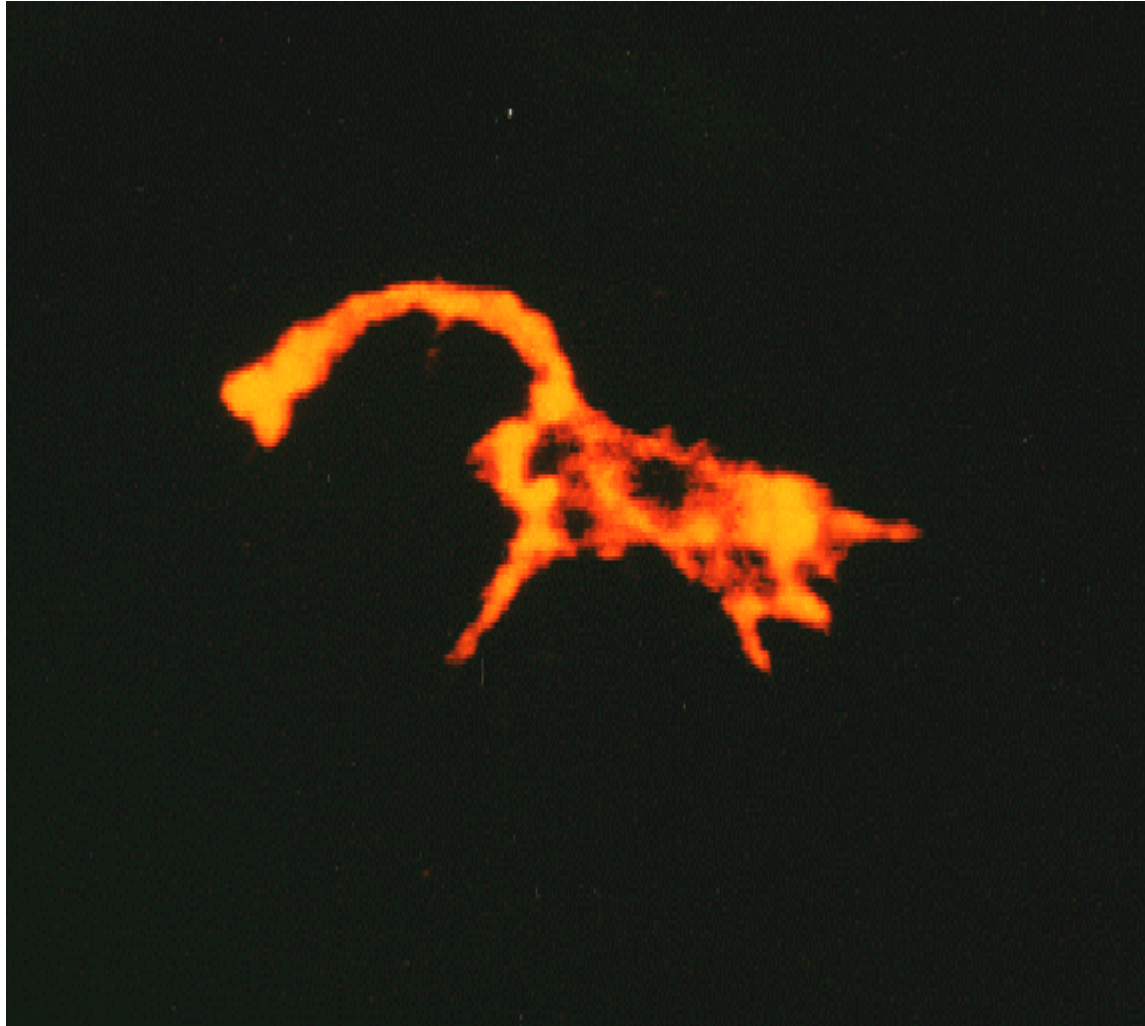
Source: Cover photograph of
Deep-Sea Res. II 42(1), 1995;
photograph by A.L. Alldredge



**Acridine orange staining shows large holes
in non-spherical biological aggregates...**



...and acridine orange staining reveals interesting shapes of fractal objects!



Objectives

- Mathematically define “fractal” and “fractal dimension”
- Demonstrate that biological aggregates formed by shear and differential coagulation in the laboratory are fractal...
- ... and that marine snow aggregates formed in nature are fractal.
- Show coagulation rates of fractal aggregates can be 1 million times faster than those of spheres.

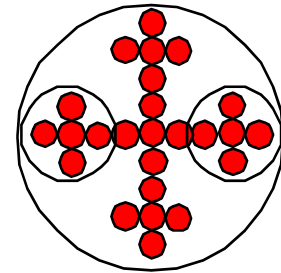
Fractal:

An object that is similar to the whole (in some fashion).

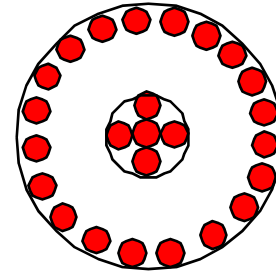
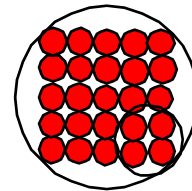


Fractal
generator

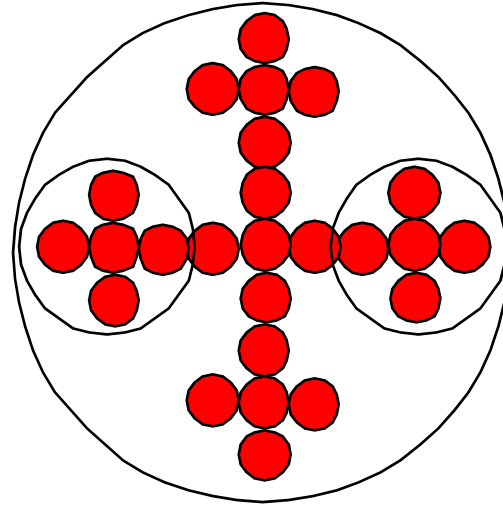
Fractal object



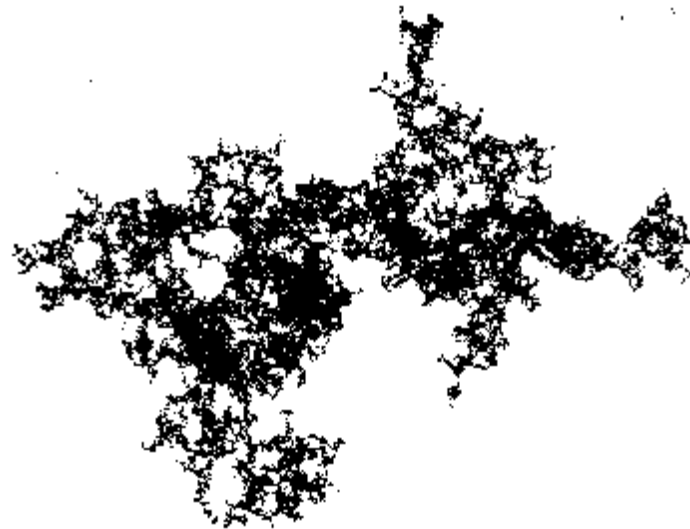
Objects that
are not fractal



Deterministic
fractal



Stochastic
fractal



Fractal dimension: definition

Definition: Power (D_n) that characterizes how an aggregate property changes with size.

Examples: $N \sim l^{D_3}$ and $m \sim l^{D_3}$

$$A \sim l^{D_2}$$

$$P \sim l^{D_1}$$

where: n = value of D for Euclidean object
 N = number of particles in aggregate
 m = mass of aggregate
 A = cross sectional area of aggregate
 P = perimeter of aggregate.

Aggregate Properties: Euclidean Geometry

Volume (encased)

$$V_e = \frac{\Pi}{6} d^3 = \xi d^3$$

Number of
particles in an
aggregate

$$N^* = \varsigma \frac{V_p}{V_e} = \varsigma \frac{\frac{\pi}{6} d^3}{\frac{\pi}{6} d_0^3} = \left(\frac{\varsigma_0 \xi}{\xi_0} \right) d^3$$

where:

ξ = shape factor

ς = packing factor

Aggregate Properties: Fractal Geometry

Number of particles

$$N^* = b_D \left(\frac{l_{ag}}{l_p} \right)^{D_3}$$

Volume

$$V_{ag} = \xi_p l_p^3 b_D \left(\frac{l_{ag}}{l_p} \right)^{D_3}$$

Mass

$$m_{ag} = \rho_p \xi_p l_p^3 b_D \left(\frac{l_{ag}}{l_p} \right)^{D_3}$$

where: $b_D = \left(\frac{\xi \xi}{\xi_0} \right)^{D_3}$

Fractal Property

Fractal Scaling Relationship

Solid volume

$$V = a_v l^{D_3}$$

Mass

$$m = a_m l^{D_3}$$

Area

$$A = a_A l^{D_2}$$



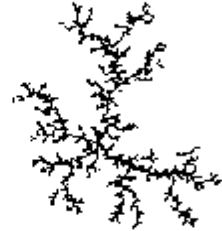
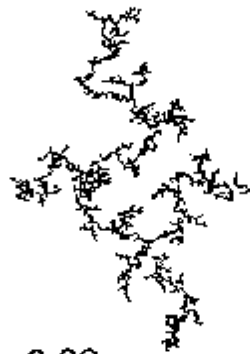
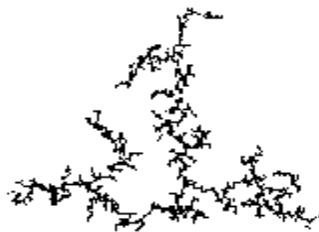
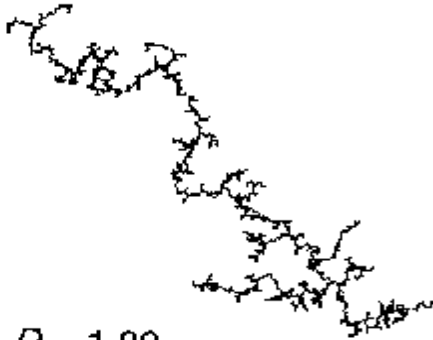
Density

$$\rho = a_p l^{D_3-3}$$

Porosity

$$\varepsilon = a_\varepsilon l^{D_3-3}$$

Simulations demonstrate a variety of fractal dimensions possible for Colloidal-Sized Aggregates

	Reaction-limited	Ballistic	Diffusion-limited
Monomer-cluster	Eden  $D = 3.00$	Vold  $D = 3.00$	Witten-Sander  $D = 2.50$
Cluster-cluster	RLCA  $D = 2.09$	Sutherland  $D = 1.95$	DLCA  $D = 1.80$

“Universality” of fractal scaling relationships for Colloidal-Sized Aggregates

- For colloidal aggregates formed by Brownian motion, fractal dimensions independent of type of colloid (gold, silica, latex spheres)
- Diffusion-limited aggregation (DLA)
 $D_3=1.8$
- Reaction-limited aggregation (RLA)
 $D_3=2.1$
- When $D_3 < 2$, then: $D_3 < D_2$

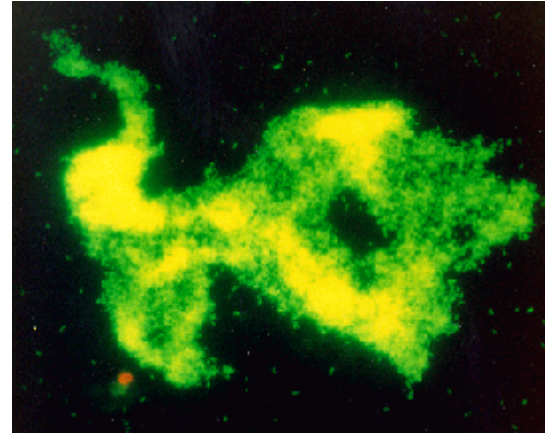
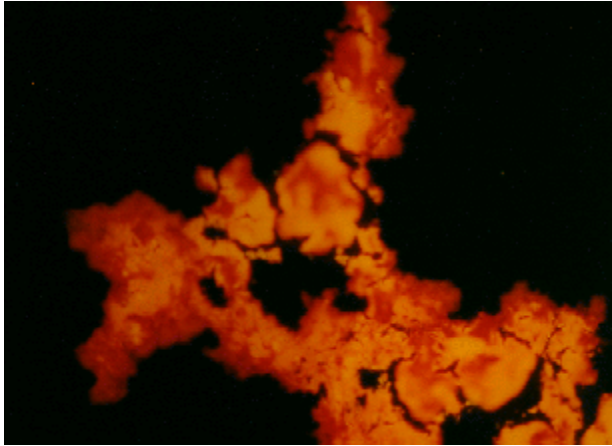
Is there a “universality” of fractal dimensions for aggregates formed by mechanisms other than Brownian motion?

Type of particle

- 👍 Bacteria
- 👍 Yeast
- 👍 Inorganic microspheres

Coagulation mechanism

- 👍 Laminar shear
- 👍 Turbulent shear
- 👍 Differential sedimentation



Laboratory studies:

Biological aggregates

Methods to calculate fractal dimensions

👍 Power law relationships:

💡 $A \sim l^{D_2}$

💡 $N \sim l^{D_3}$

👍 Size Distributions:

💡 Steady State (SS)

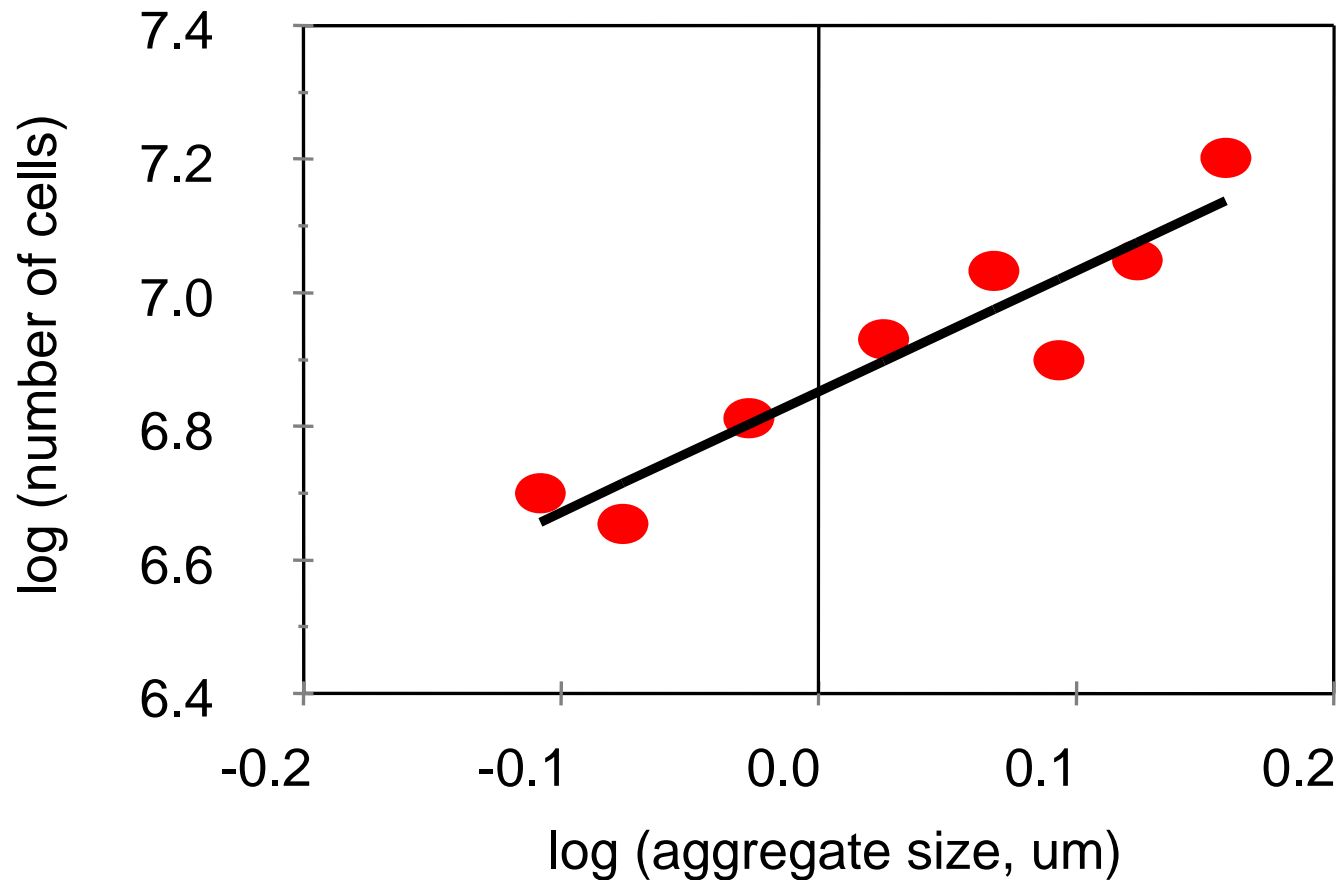
💡 Two slope method (TSM)

💡 Particle concentration technique (PCT)

Fractal dimensions of biological aggregates

- 👍 Aggregates using pure cultures
(*Zoogloea ramigera*, *Saccharomyces cerevisiae*)
- 👍 Aggregates sized, dispersed, and cells counted using acridine orange staining
- 👍 Fractal dimensions determined from log-log plots of:
 - size (l) and
 - number of particles (N) or Area (A)

Bacterial aggregates (*Zoogloea ramigera*)



Fractal Dimensions of Different Biological Aggregates

Microbe	Reactor	D_2 (\pm S.D.)	D_3 (\pm S.D.)
<i>S. cerevisiae</i>	Test tubes (rotating)	1.92 (± 0.08)	2.66 (± 0.34)
<i>Z. ramigera</i>	Aerated bioreactor	1.78 (± 0.11)	2.99 (± 0.36)
<i>Z. ramigera</i>	Test tubes (rotating)	1.69 (± 0.08)	1.79 (± 0.28)

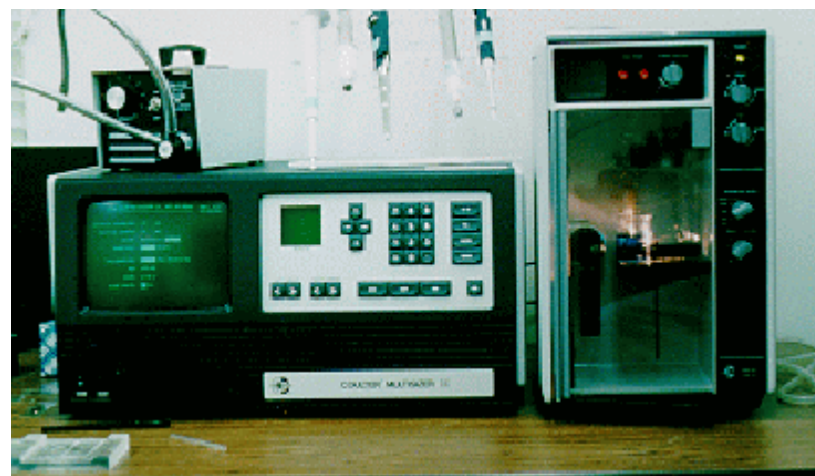
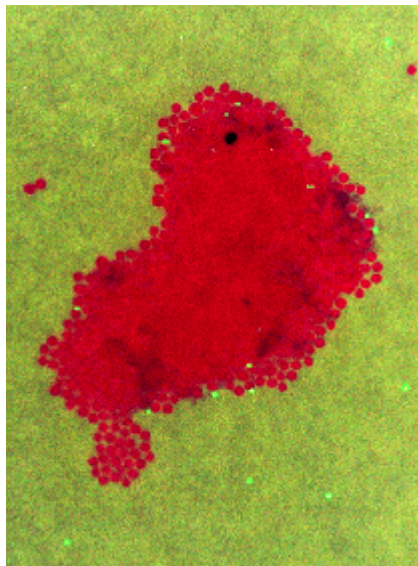
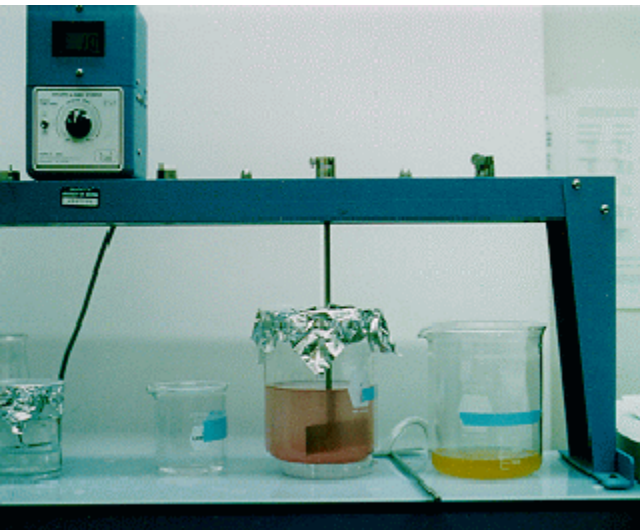
Observations:

- D varies for different microorganisms
- D is a function of growth conditions

Hypothesis:

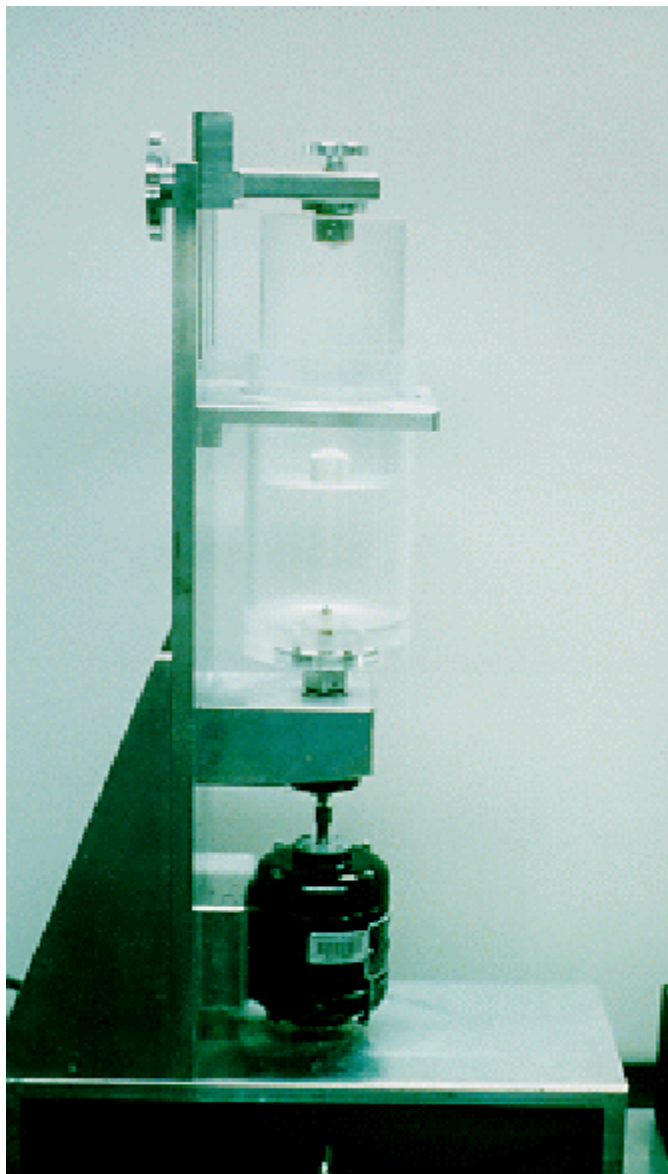
Values of D are a function of the fluid mechanical environment

- Laminar shear (couette device)
- Turbulent shear (paddle mixer)
- Sedimentation (rolling cylinder)



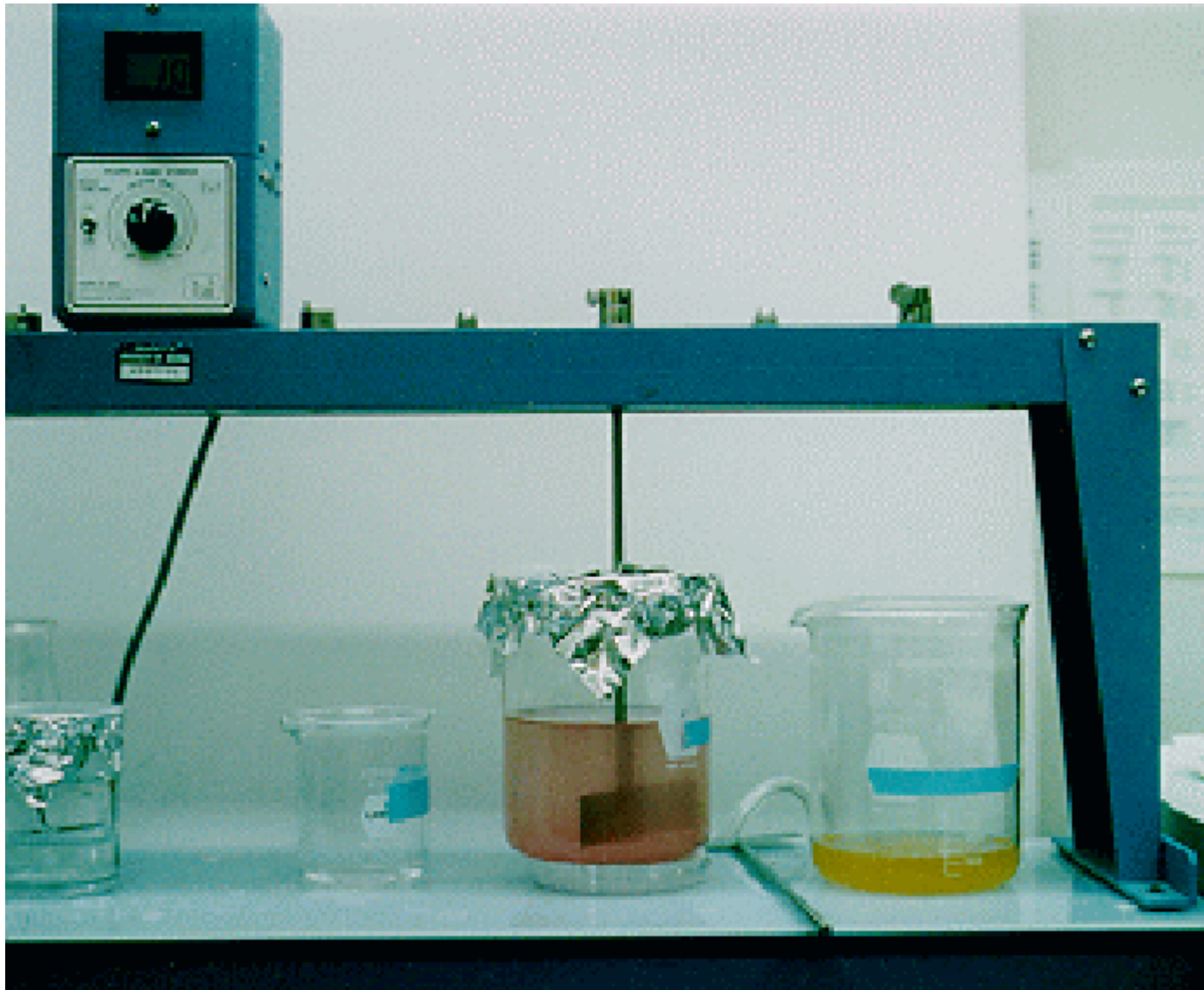
Laboratory studies: Inorganic aggregates

Couette device: laminar shear



From: Jiang and Logan (1996) J. AWWA

Paddle mixer: turbulent shear



Rolling cylinder: gravitational sedimentation

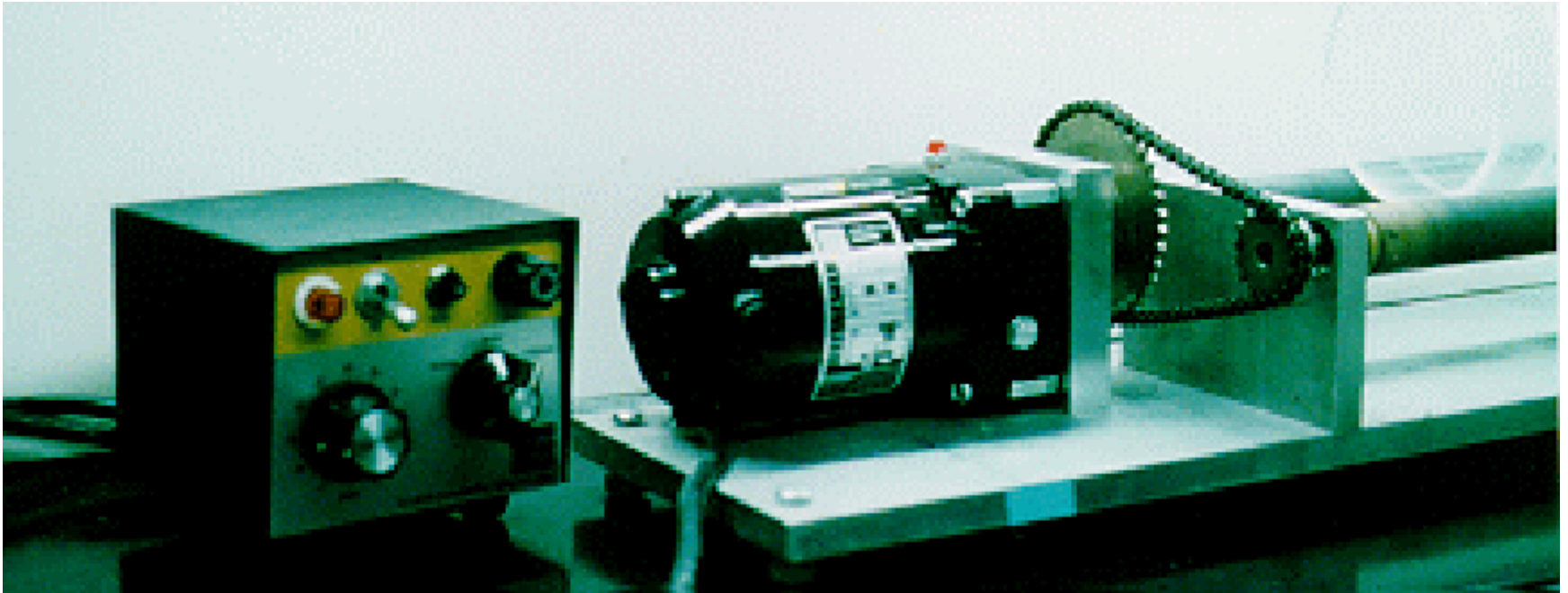
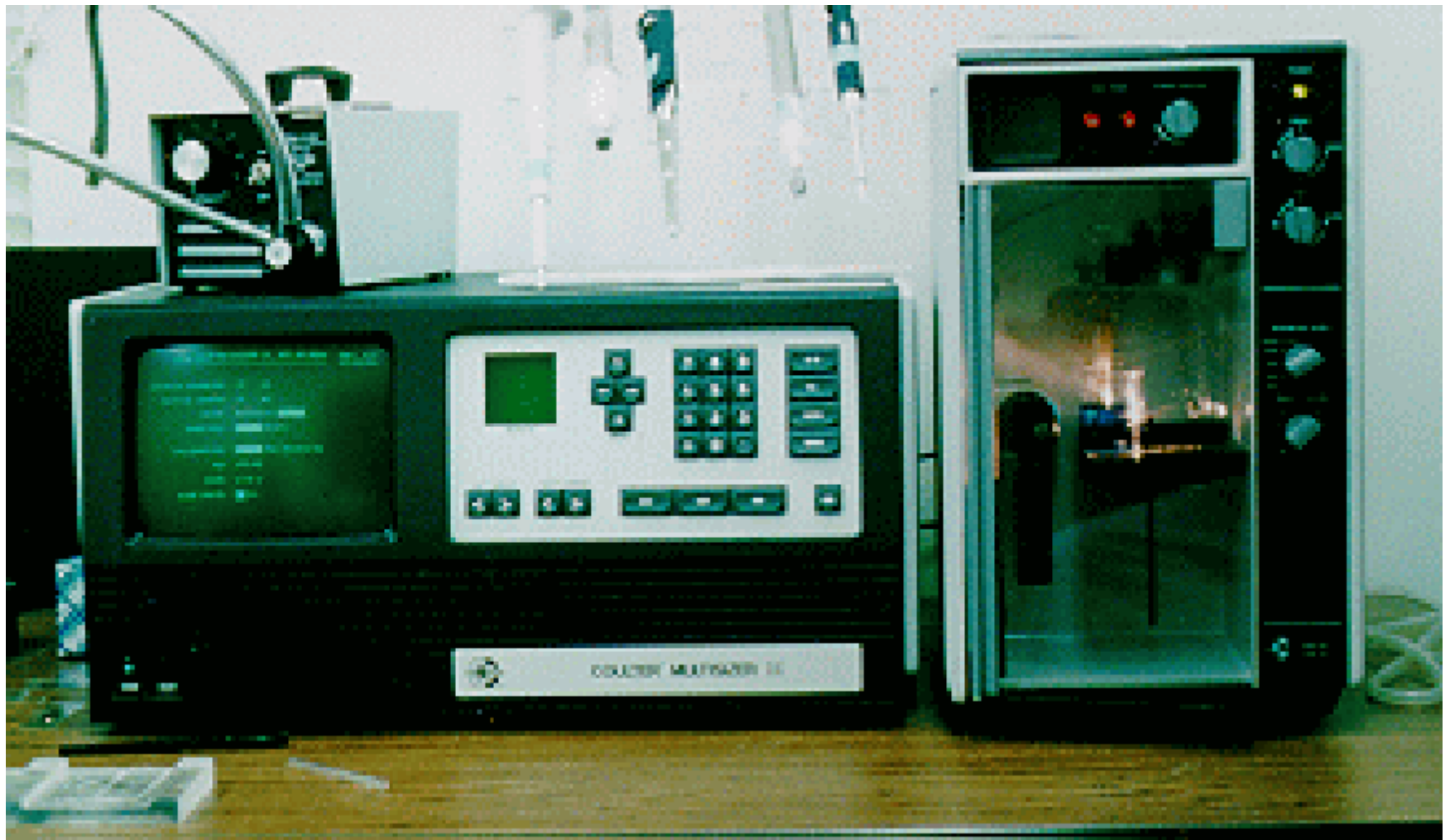


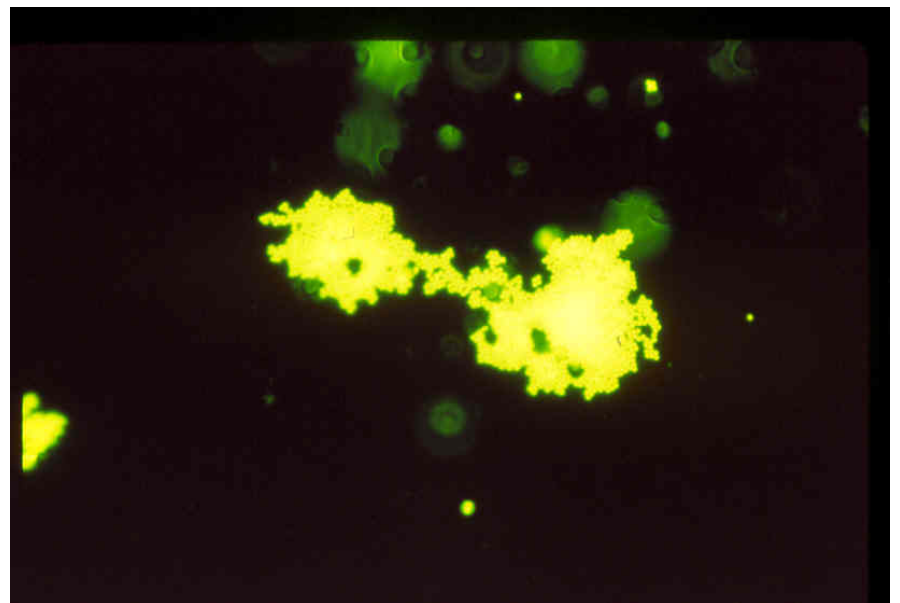
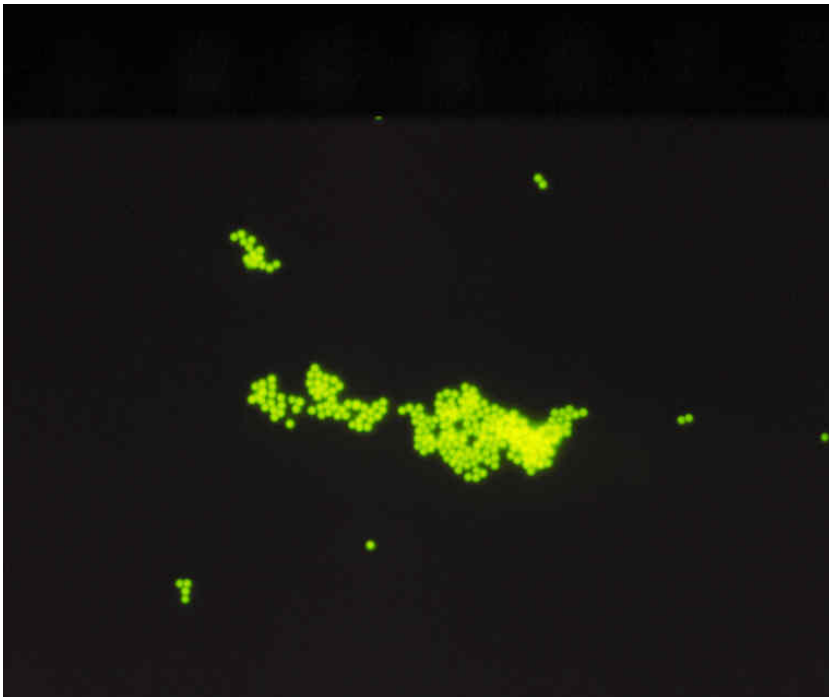
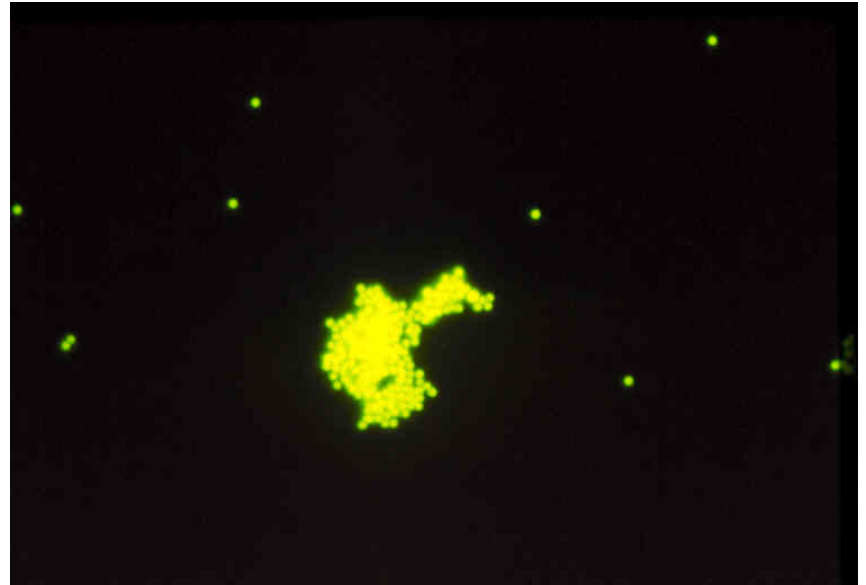
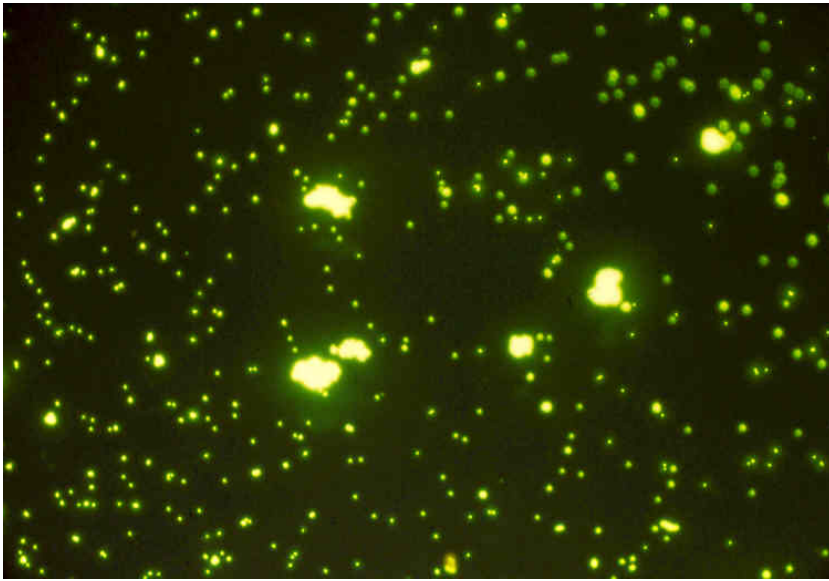
Image Analysis System- Particle length (Galai- Microscope system)



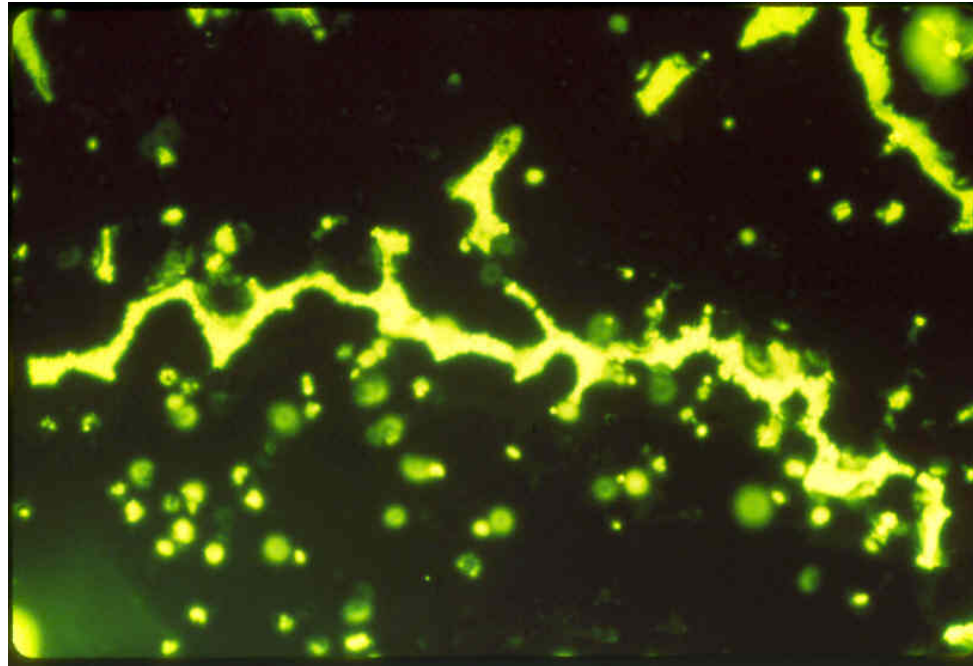
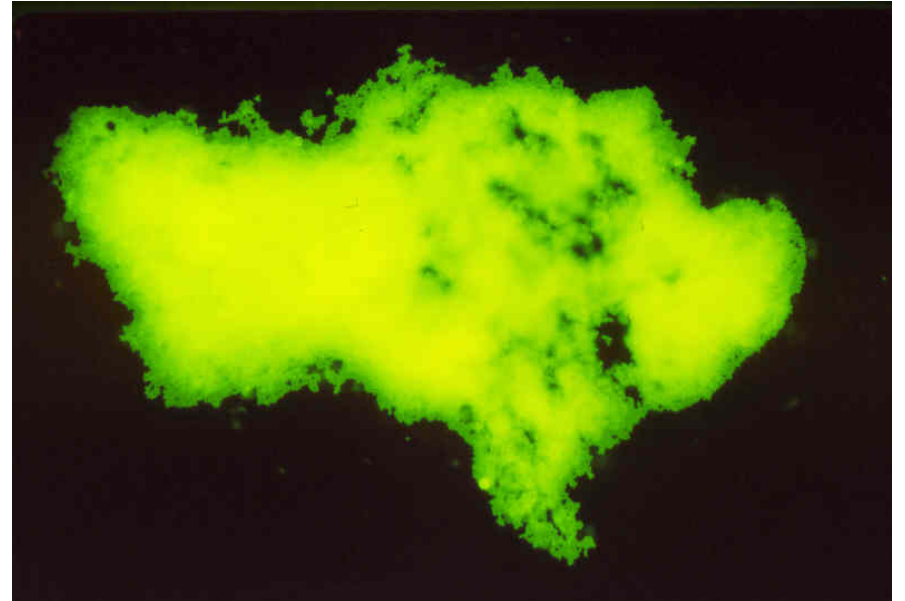
Resistance-type Particle Counter-solid volume (Coulter Counter)



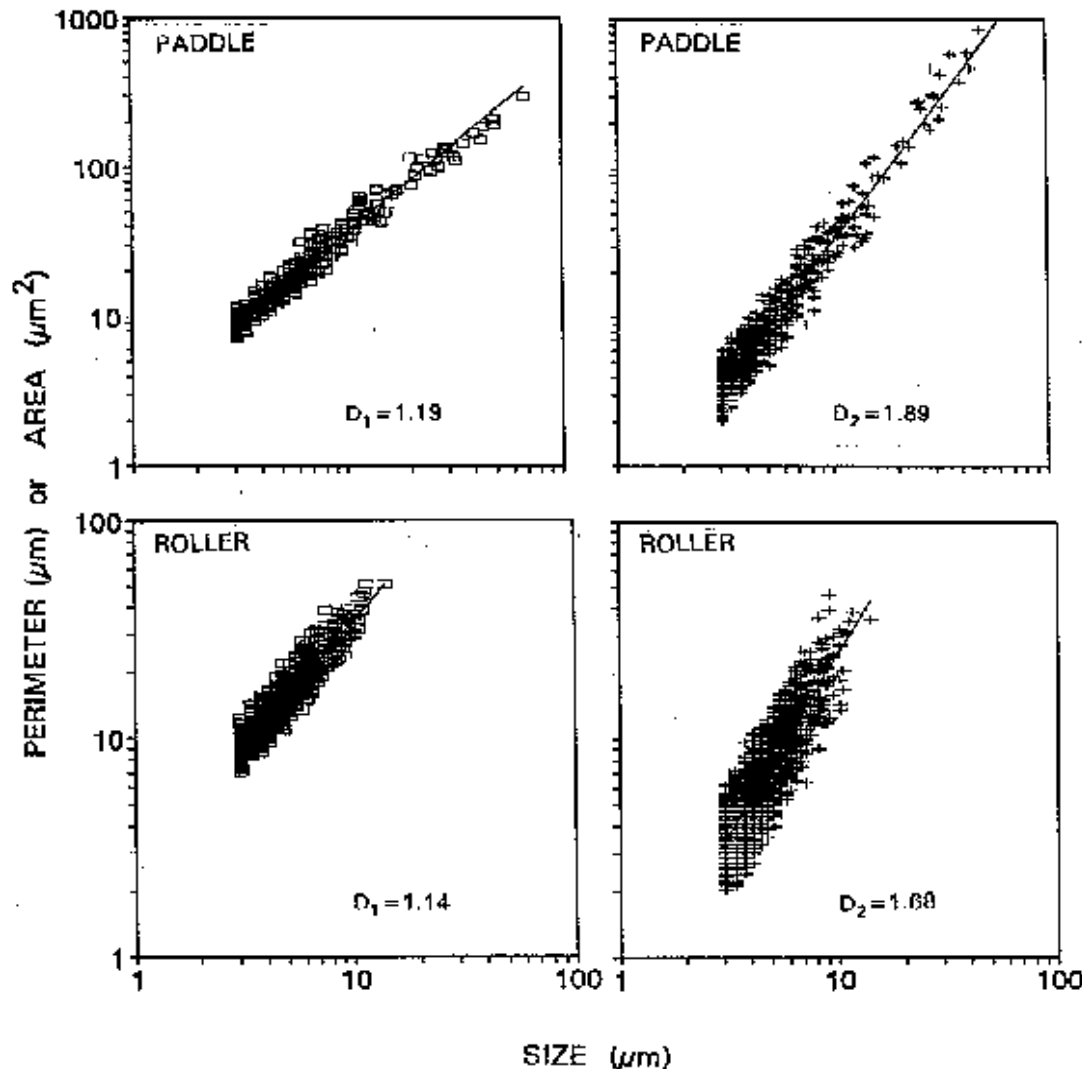
Fluorescent Microsphere Coagulation Experiments



Fluorescent Microsphere Coagulation Experiments



Fractal dimensions of microsphere aggregates from power laws



Paddle Mixer
 $D_2 = 1.89$

Roller
 $D_2 = 1.68$

From: Logan and Kilps (1995)
Water Research

Methods to calculate fractal dimensions

👍 Power law relationships:

☐ $A \sim l^{D_2}$

☐ $N \sim l^{D_3}$

👍 **Size Distributions:**

☐ Steady State (SS)

☐ Two slope method (TSM)

☐ Particle concentration technique (PCT)

TSM (Two-Slope method)

If the same population of particles are measured, the two size distributions must be equal, or

$$N(l) = N(V) \quad \text{or} \quad B_l l^{S_l} = B_V V^{S_V}$$

From fractal geometry,

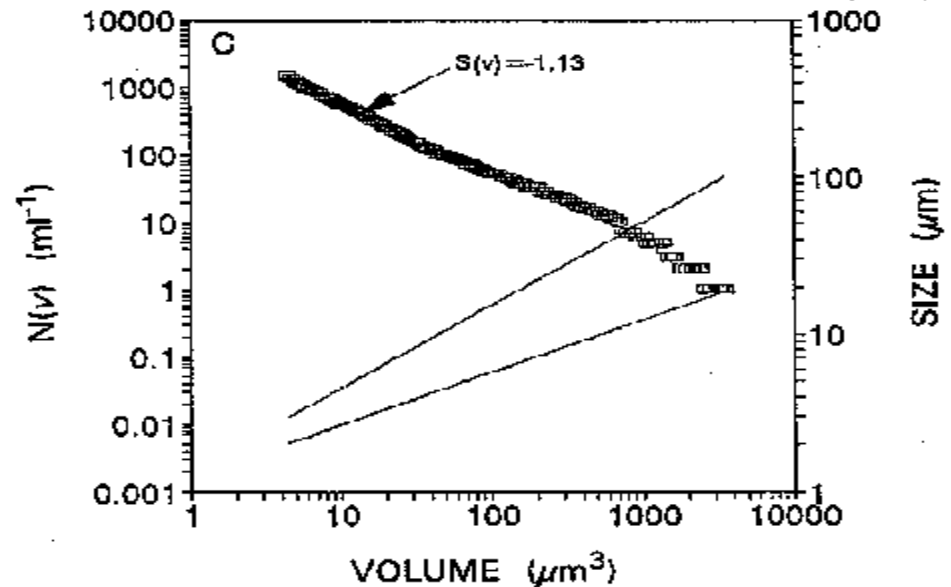
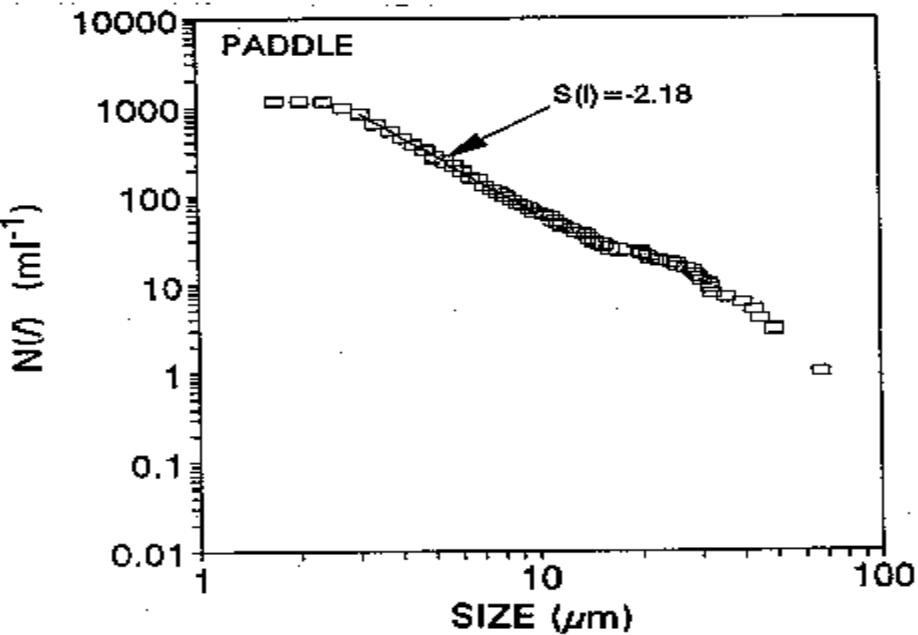
$$B_l l^{S_l} = B_V \left(\xi_p l_p^3 b_D l_p^{-D} l^D \right)^{S_V}$$

The exponents on l must be the same, so that

$$S_l = D S_V \quad \text{or}$$

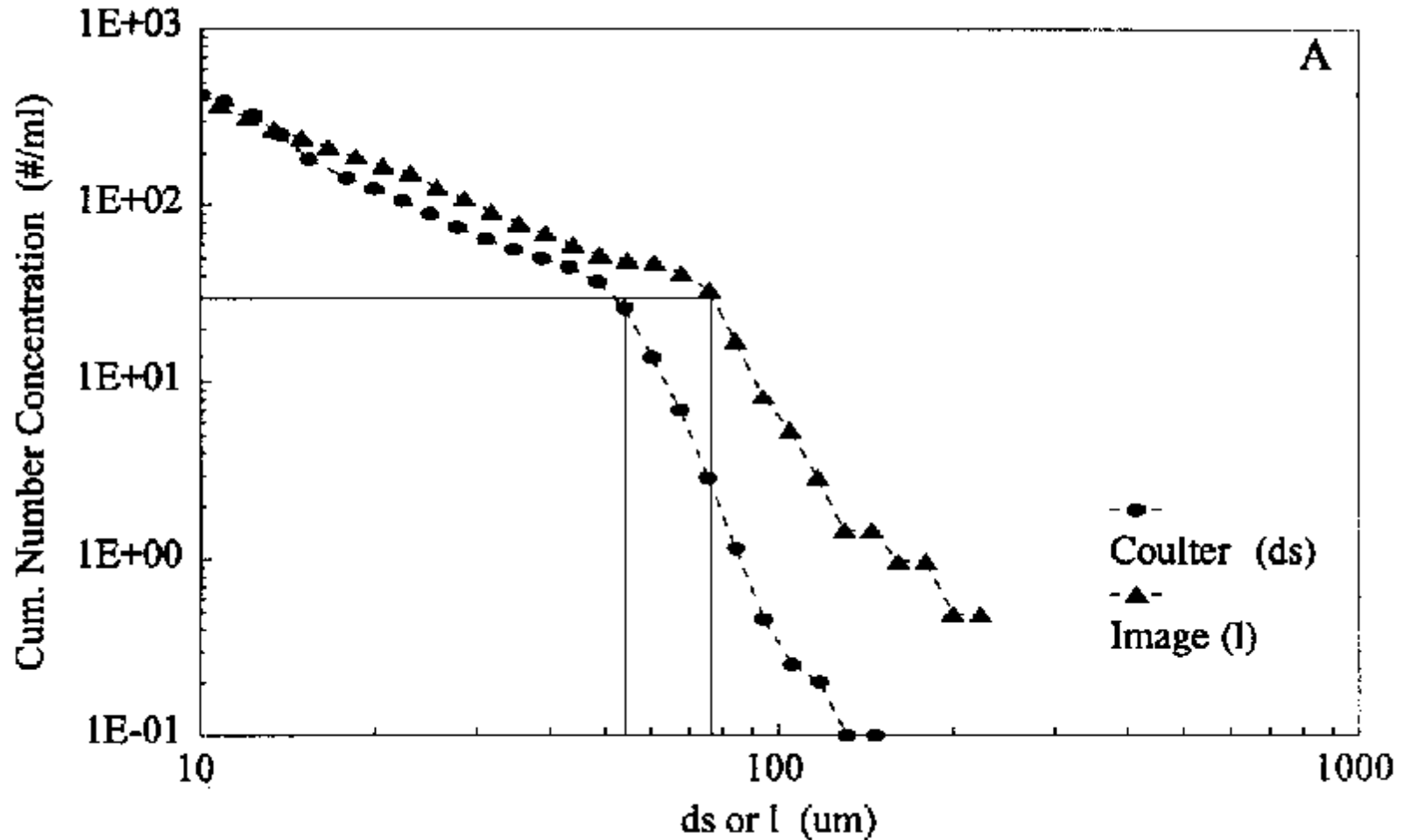
$$D = \frac{S_l}{S_V} \quad (TSM)$$

TSM: a direct method for calculating D_3 if the slope is constant

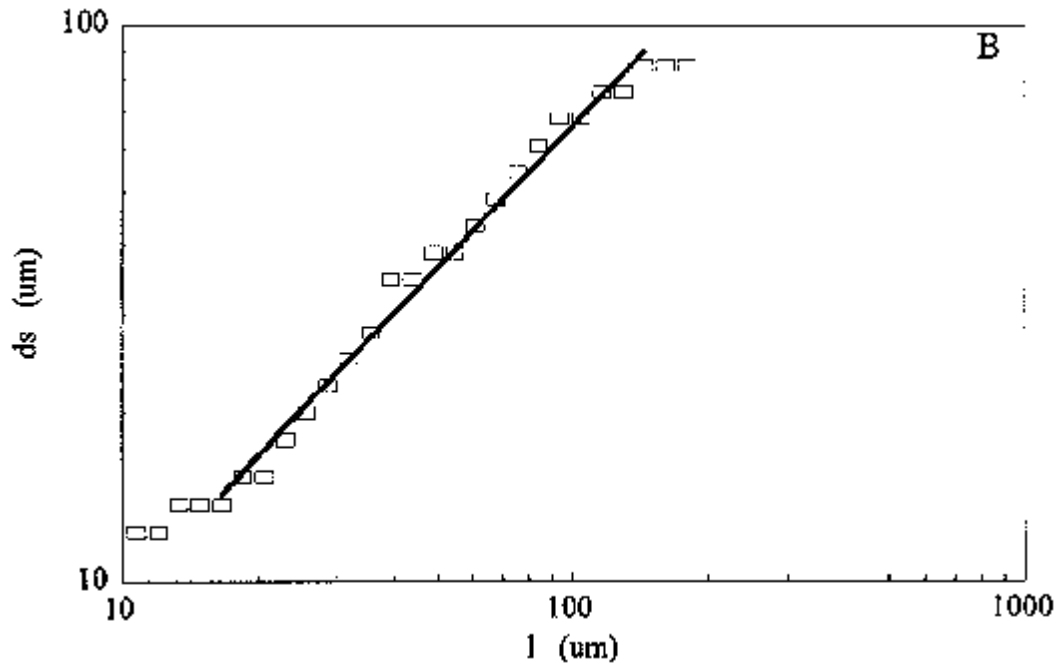


From: Logan and Kilps (1995)
Water Research

PCT (Particle Concentration Technique): used for non-linear size distributions



PCT: linked data from two size spectra



D_3 calculated as the slope of a line generated from a plot of solid volume (ds) versus length (l)

Fractal Dimensions of microsphere aggregates vary for different fluid environments

Aggregate Type	Method	Fractal dimension	Ref
Laminar shear	TS (high salt)	1.43 - 1.74 ^a	b
	TS (low salt)	1.92 (± 0.04)	b
Turbulent Shear	TS	1.92 (± 0.04)	c
	Power (Size-area)	1.89 (± 0.02)	c
Sedimentation	TS	1.59 (± 0.16)	c
	Power (Size-area)	1.68 (± 0.02)	c

a- D varies as a function of shear rate

b- Jiang and Logan (1996) *JAWWA*

c- Logan and Kilps (1995) *Water Research*

CONCLUSIONS

- 👍 There is no “universality” of fractal dimensions for biological aggregates
- 👍 D_3 varies from 1.4 - 3.0

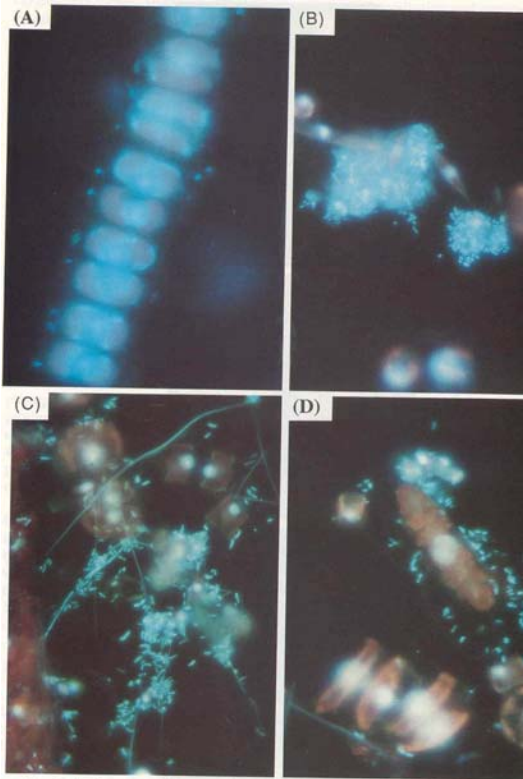
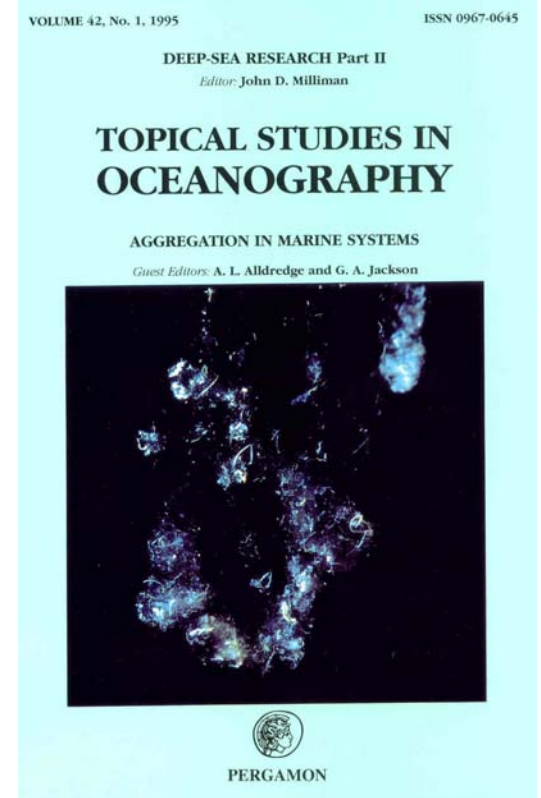


Fig. 11. Epifluorescence micrographs of DAPI-stained bacteria and diatoms during the course of the bloom. (A) Day 7. (B) Day 10. (C) Day 12. (D) Day 13. Scale bar = 10 μ m.



Natural Systems:

Tank Experiment

Fractal dimensions during a coagulation event: a simulated phytoplankton bloom

Hypothesis:

Marine snow aggregates formed by physical coagulation.

👍 Fractal dimensions should decrease during coagulation

📄 Start: $D_3=3$

📄 Finish: $D_3<2$

👍 Tank experiment conducted by SIGMA group to monitor a coagulation event.

A phytoplankton bloom was simulated in a mesocosm (tank) in the laboratory to study coagulation

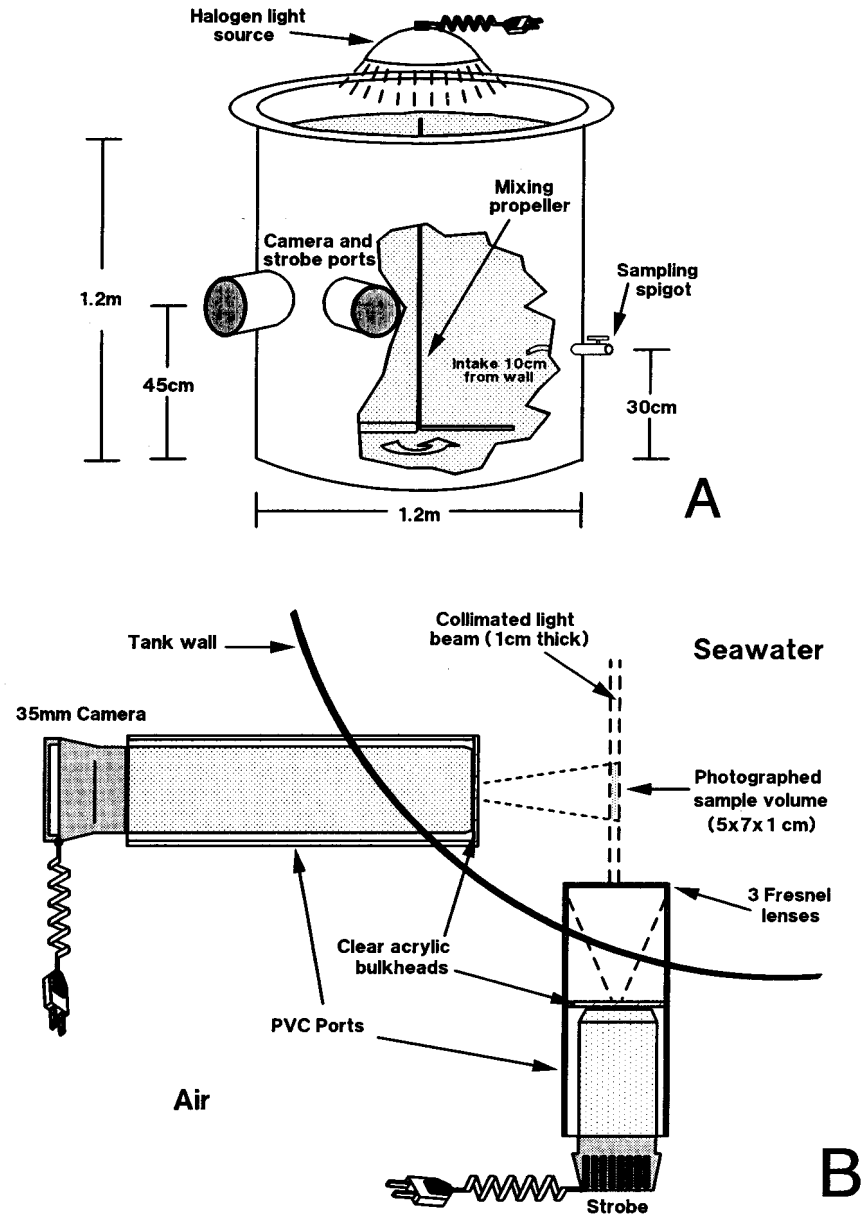


Fig. 1. Diagram of the 1400 liter mesocosm. (A) Entire mesocosm with cut away to show mixing propeller within. (B) Close-up of the camera and strobe configuration.

Tank Inoculated on
“Day 0” with:

-Seawater from
near UC Santa
Barbara

-Nutrients

Tank was mixed
and lighted to
match existing
photocycle

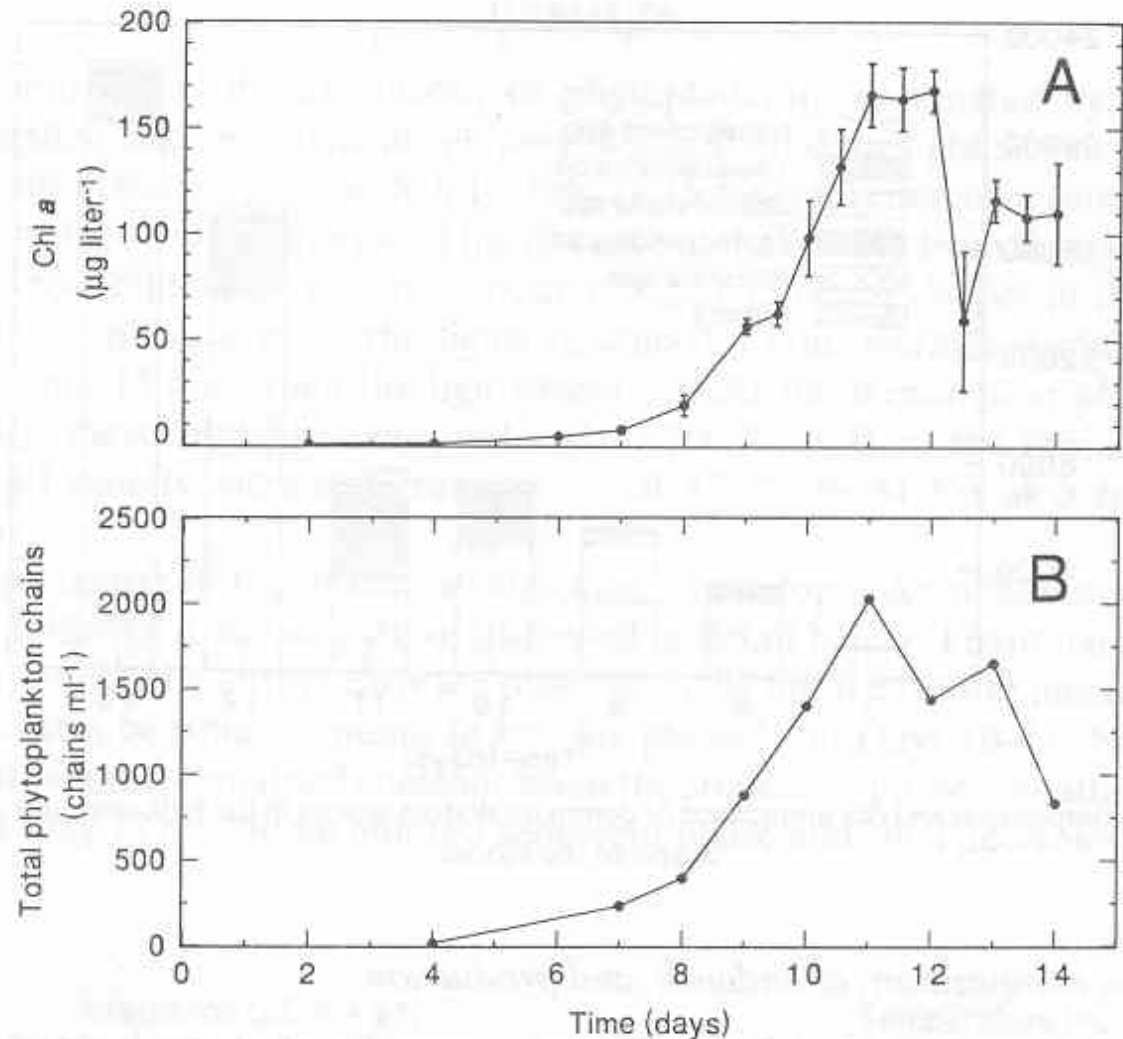


Fig. 4. Phytoplankton biomass and particle number. Bars represent 95% confidence intervals. (A) Chlorophyll *a*; (B) phytoplankton abundance expressed as discrete particles, i.e. numbers of chains and single cells.

Nutrients were
depleted by
day 12

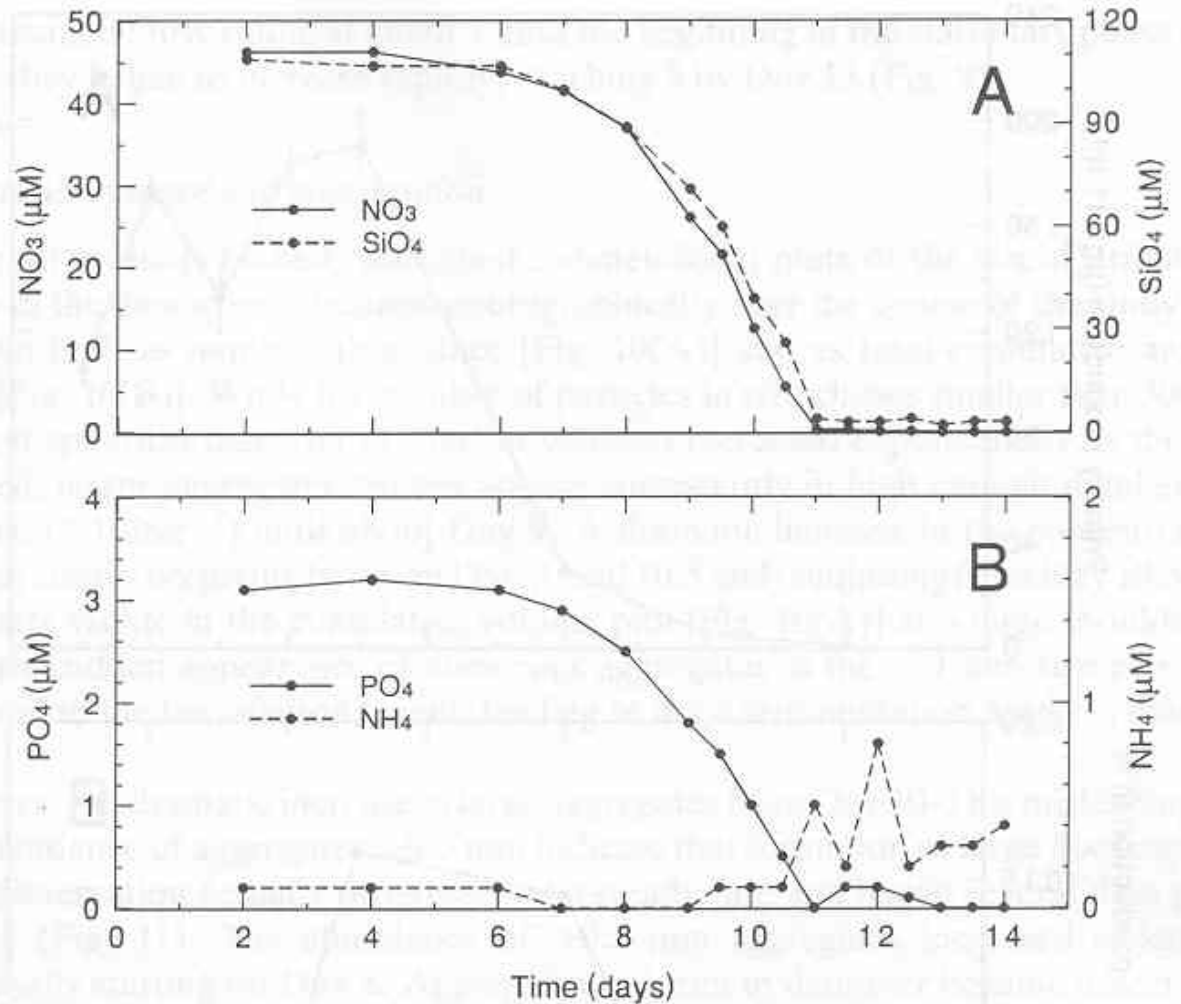


Fig. 5. Nutrient concentrations over the study. (A) Nitrate and silicate. (B) Phosphate and ammonium. Error bars were too small to be resolved graphically and are not shown.

Diatom bloom dominated by *Chaetoceros* spp.

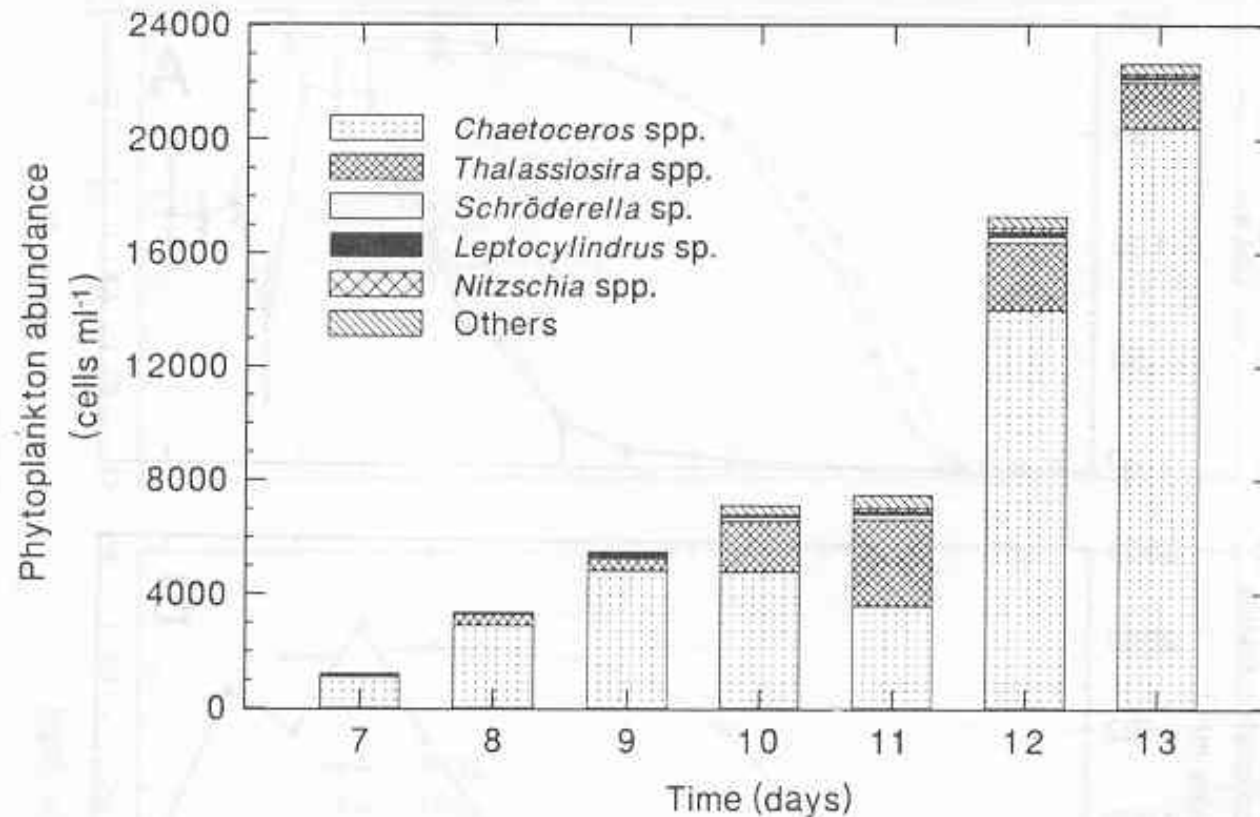


Fig. 3. Composition and cell abundance of dominant diatom genera in the bulk seawater over the course of the bloom.

The particle spectra indicated large increases in particles after day 6

Particles measured here were 2-300 μm in length (by image analysis)

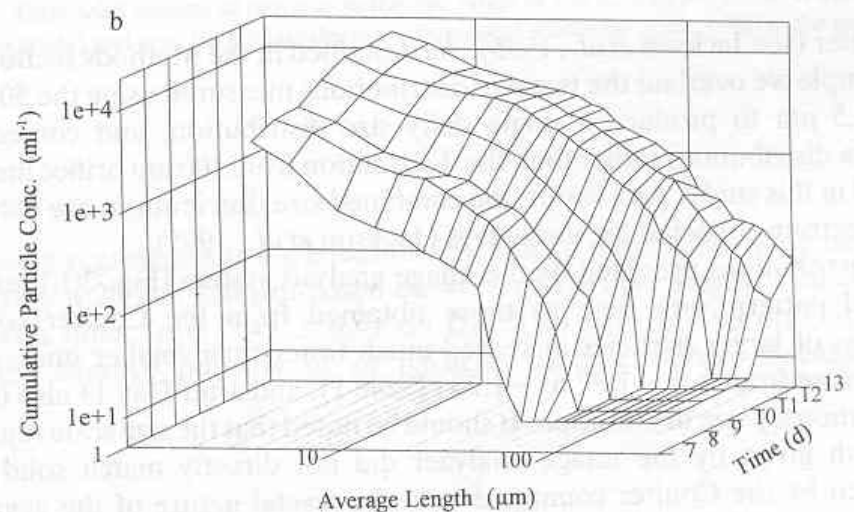
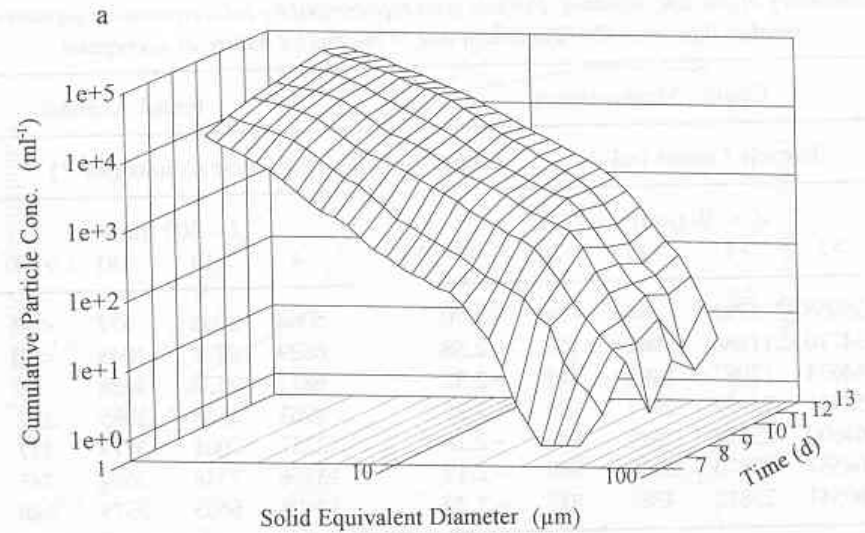
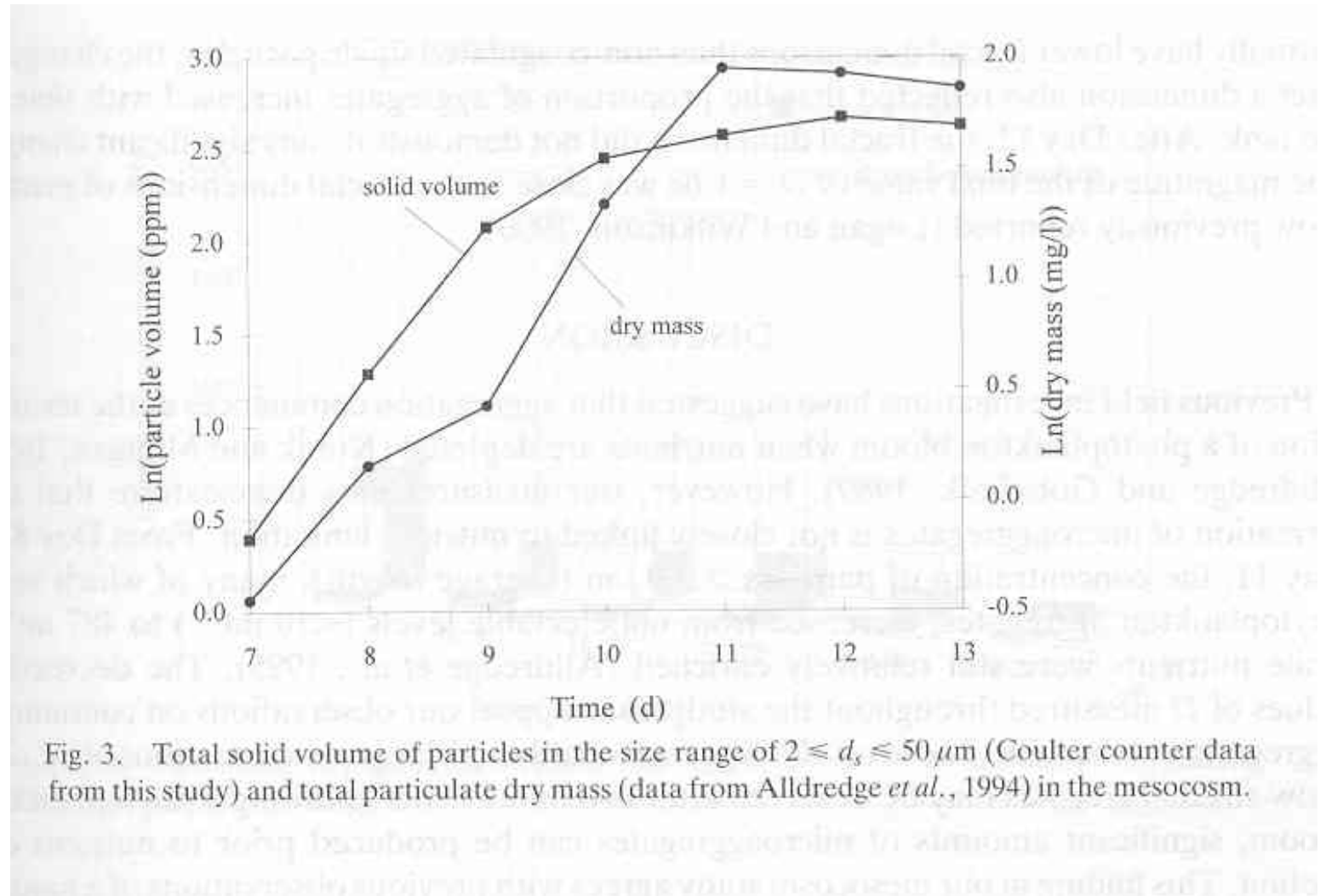


Fig. 2. Cumulative particle size distributions during the phytoplankton bloom in the mesocosm: (a) in terms of solid equivalent diameter obtained using the Coulter counter; (b) in terms of average length obtained using the image analyzer.

The measurements of solid particle volume
(Coulter Counter, 2-300 μm size fraction)
parallel the measurements of dry weight



Note the largest size particles
(aggregates) developed after day 6.

Particles measured
here were >0.5 mm
(by photographic
system in situ)

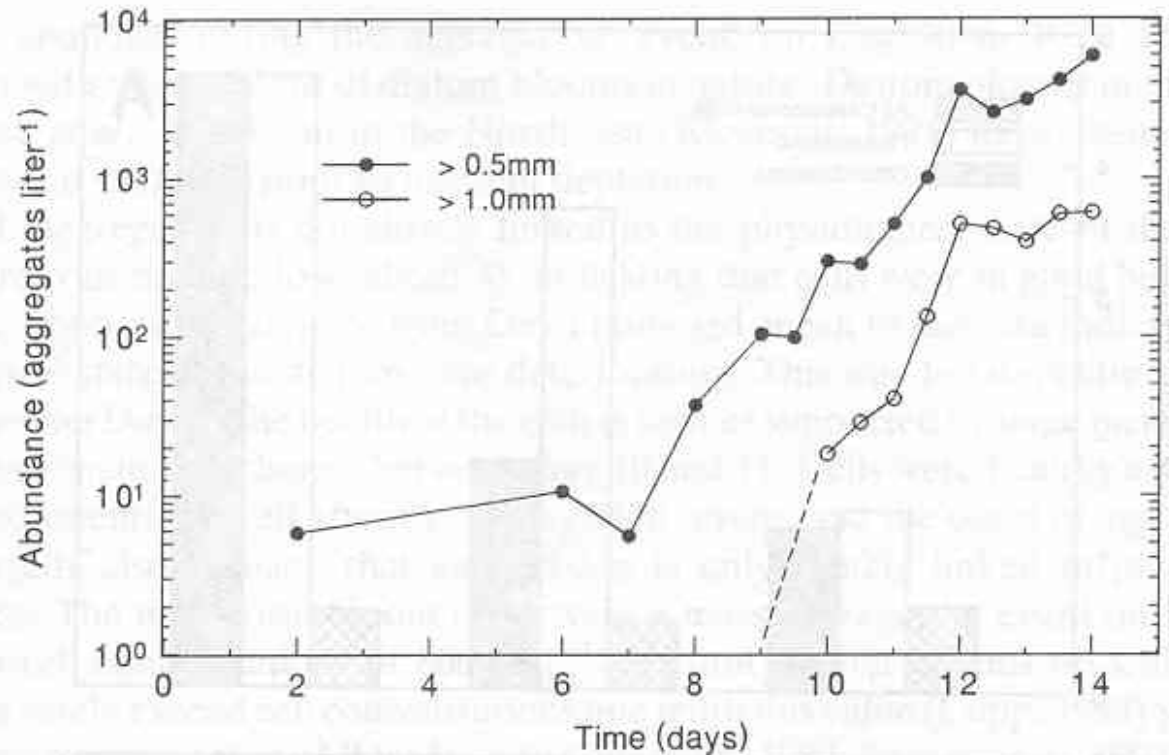


Fig. 11. Abundance of particles >0.5 mm and >1 mm in size over the course of the study as determined photographically through the mesocosm wall.

Half lives of TEP in a mesocosm during a simulated phytoplankton bloom

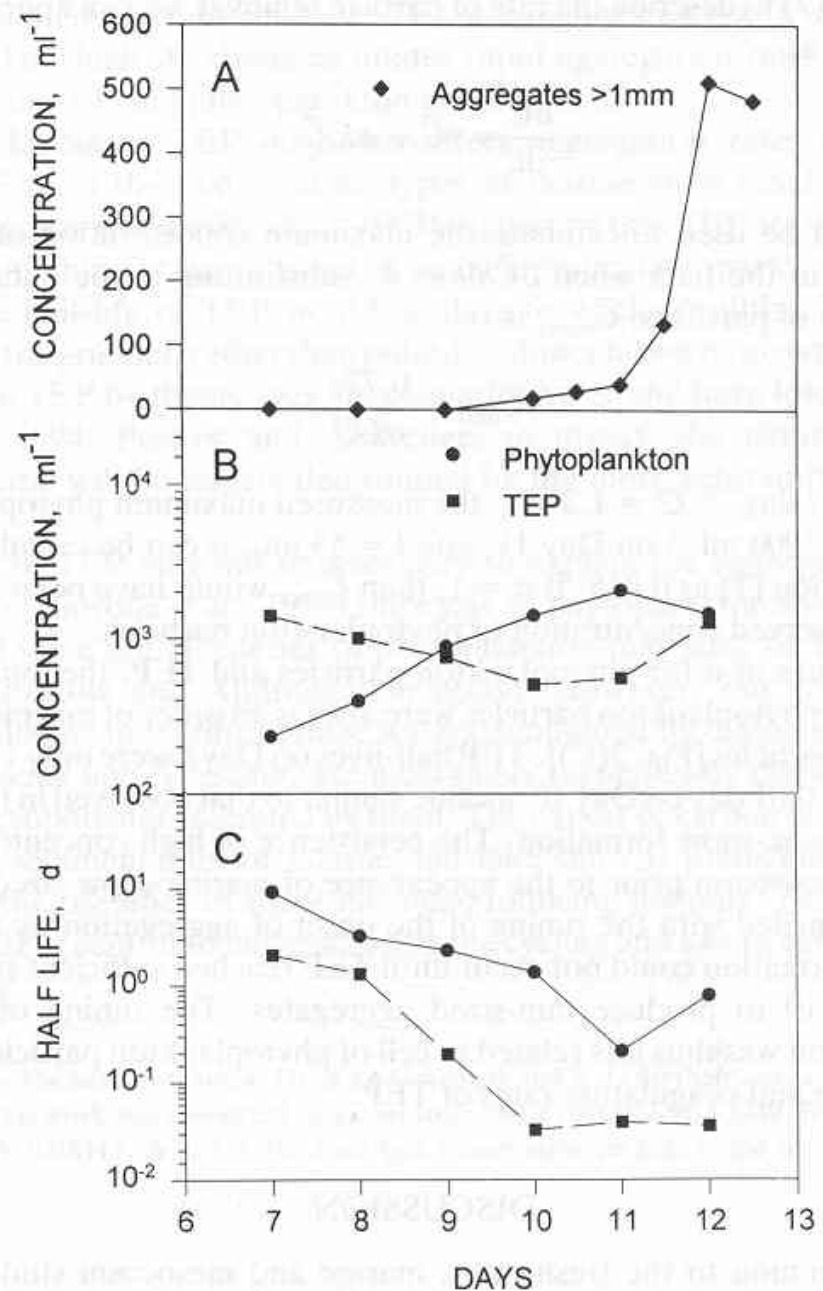
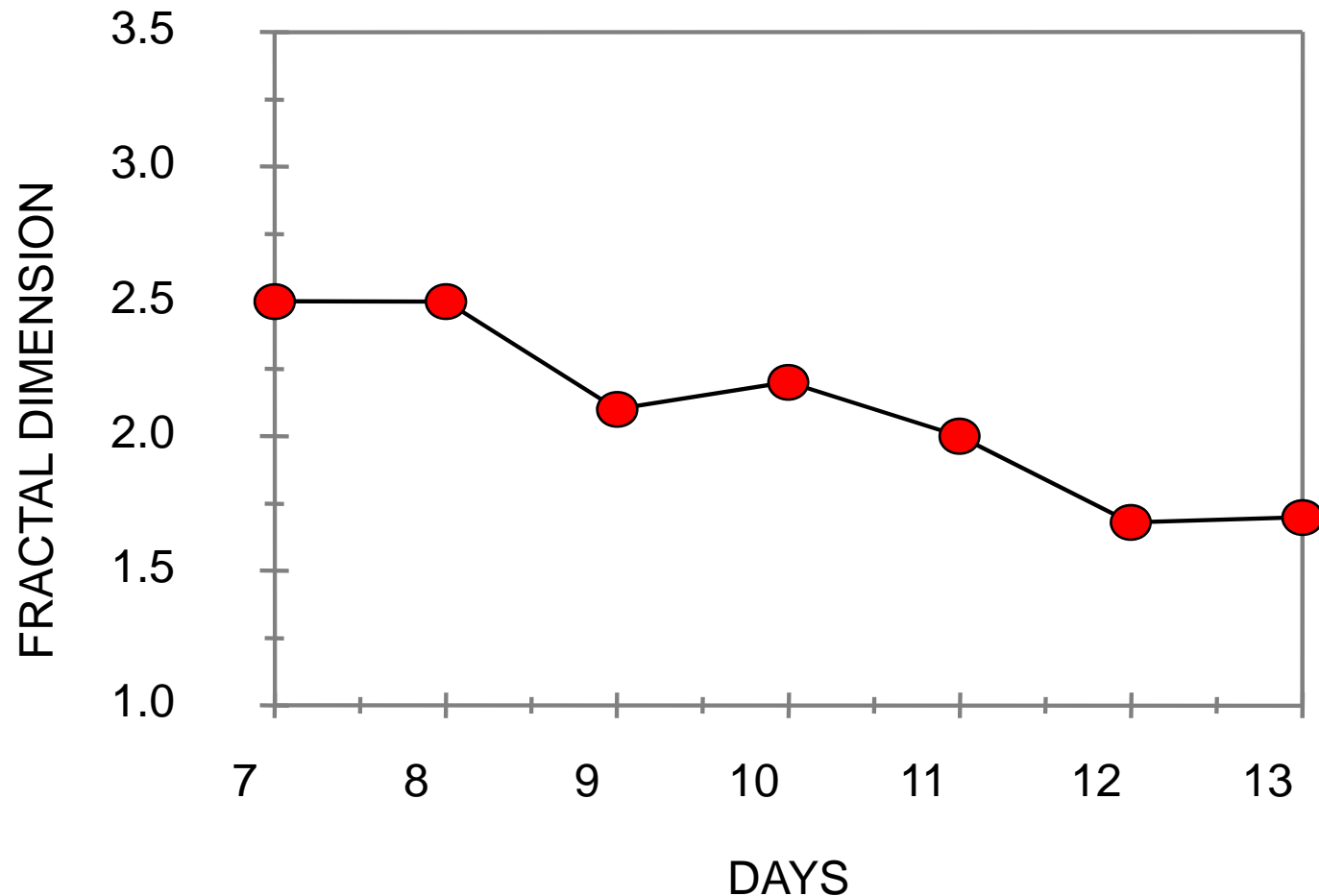


Fig. 2. (A) Size distributions, (B) concentrations, and (C) half-lives of TEP and phytoplankton particles in the mesocosm.

Fractal dimensions of particles (2-200 μm) decreased during the phytoplankton bloom in the tank as predicted.



Many of the particles measured in the 2-300 μm size fraction were not phytoplankton

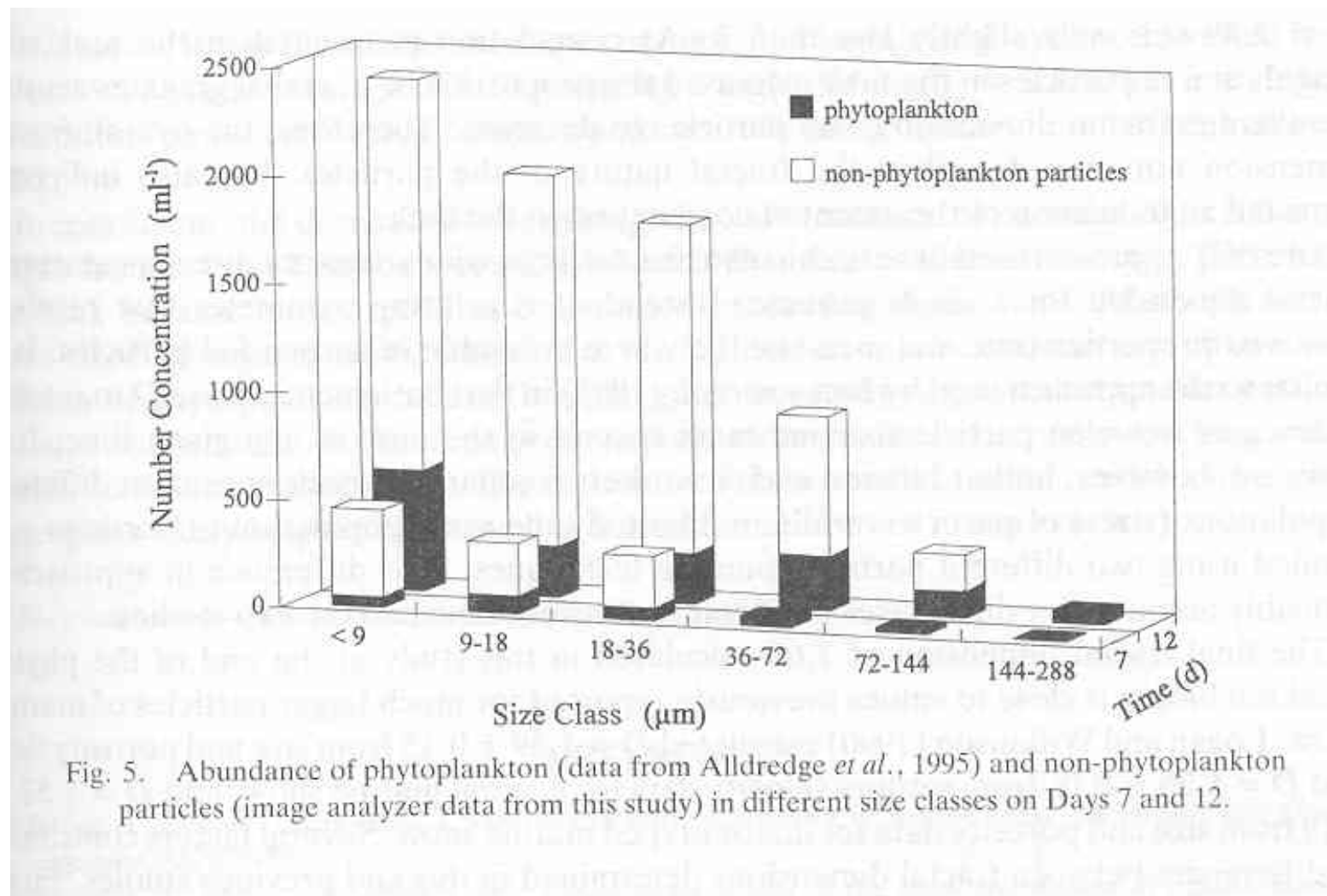


Fig. 5. Abundance of phytoplankton (data from Alldredge *et al.*, 1995) and non-phytoplankton particles (image analyzer data from this study) in different size classes on Days 7 and 12.



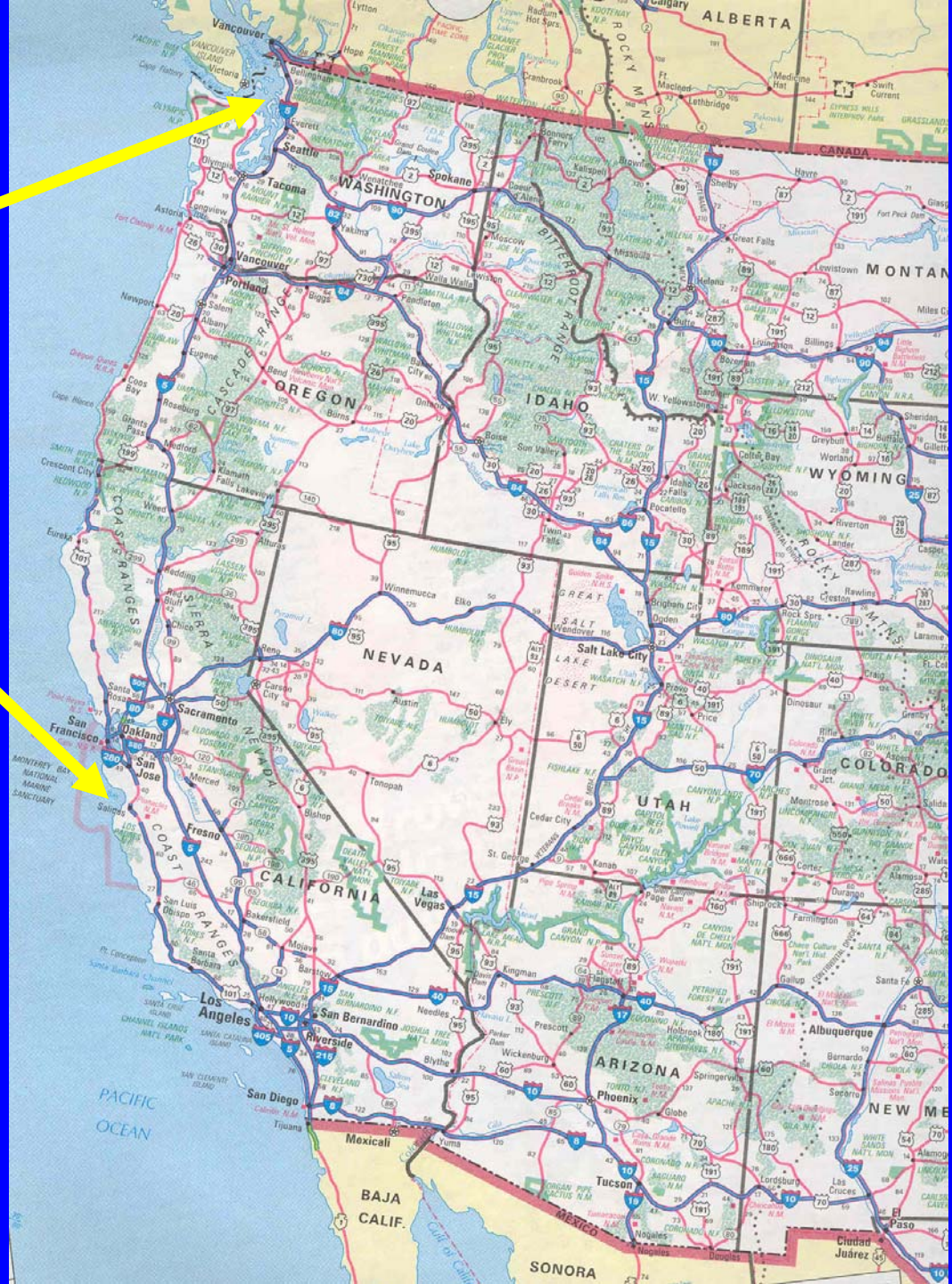
Natural Systems: Field Measurements

Fractal dimensions of particles formed in natural systems

- Are large aggregates formed in lakes and marine systems fractal?
 - Ocean Cruises (10-day) off S. California (UCSB)
 - Field studies (daily excursions):
 - Monterey Bay, CA
 - Friday Harbor, (near Seattle, WA)
 - Lake Constance, Germany
- Formation of aggregates was found to be linked to the abundance of TEP

Friday Harbor,
WA

Monterey Bay,
CA



Oceanographic Cruises- Two Week Studies off the Coast of Southern California



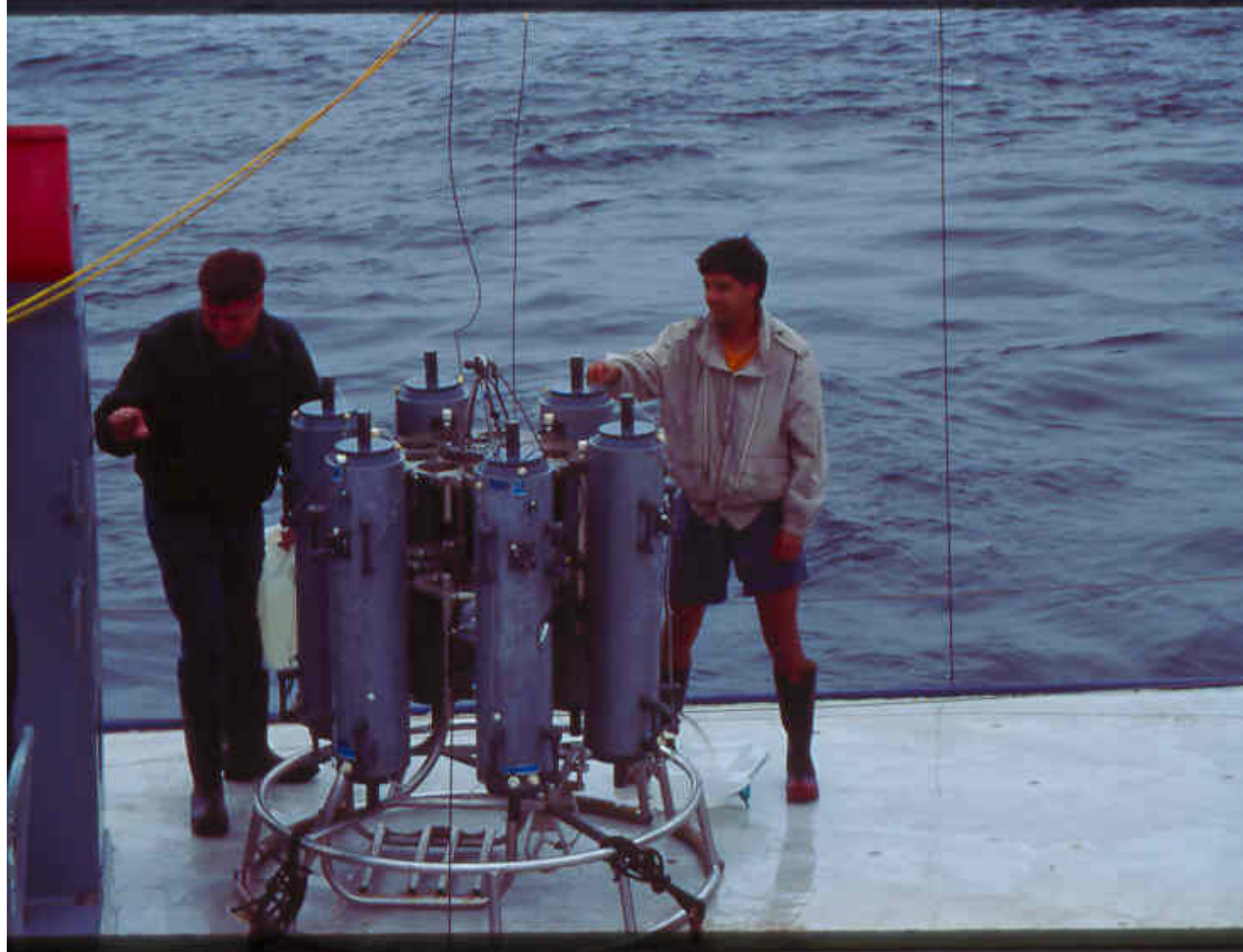
Multi-investigator study included launching camera systems...

Alice Alldredge and Chris Gottchalk launch Sno-cam



...and on-board laboratory studies (Point Sur)



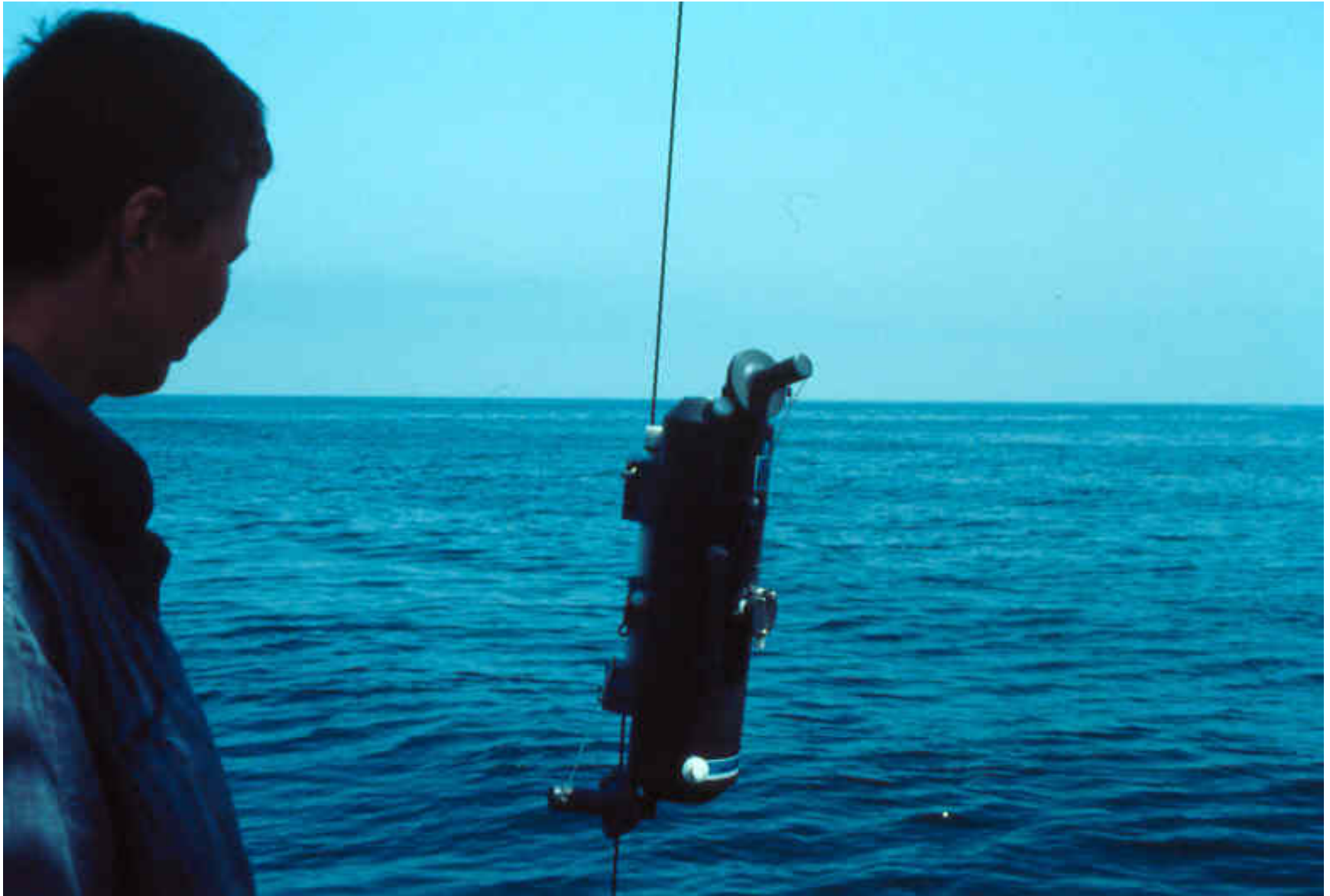




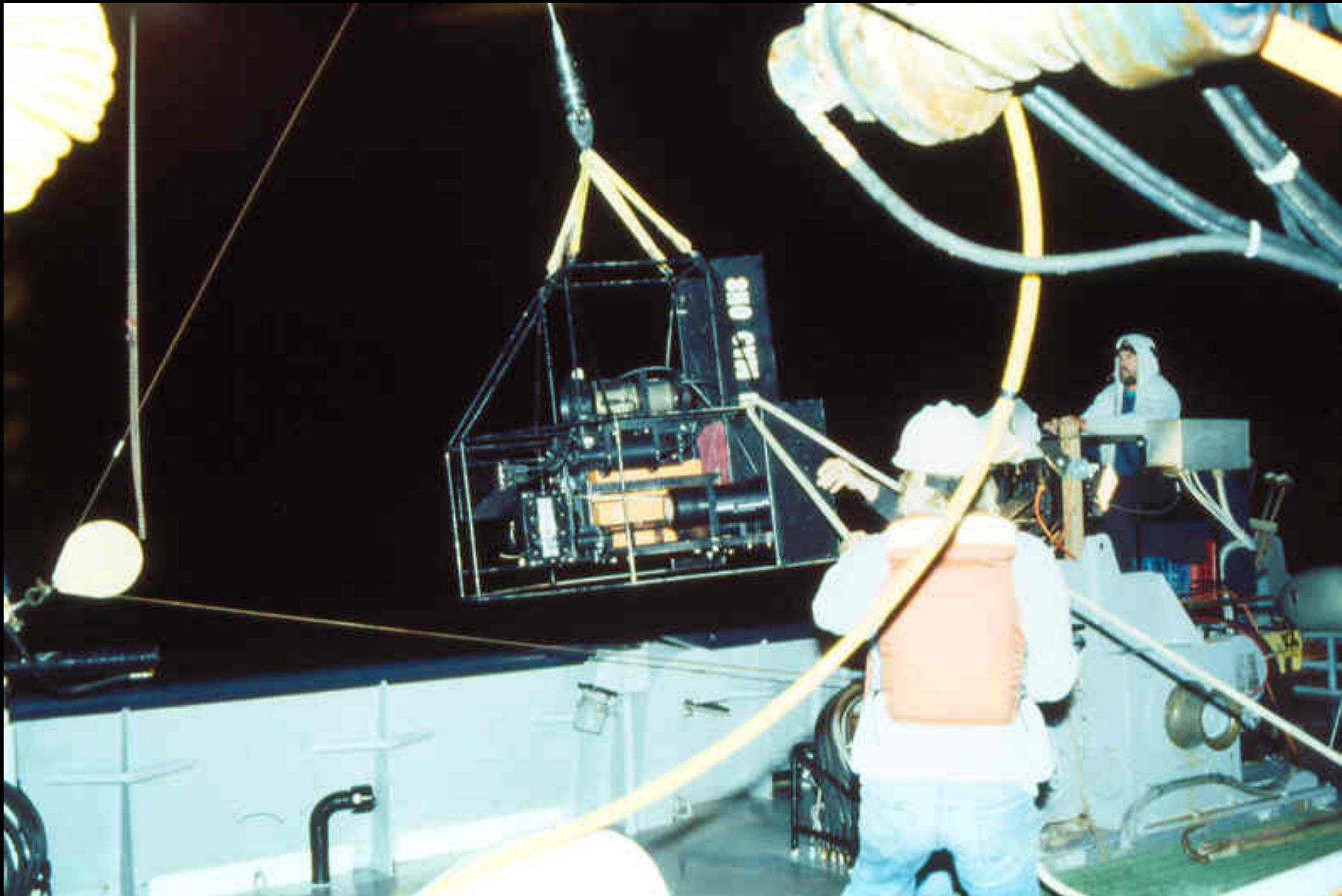
Smaller ships were used in the Monterey Bay Study



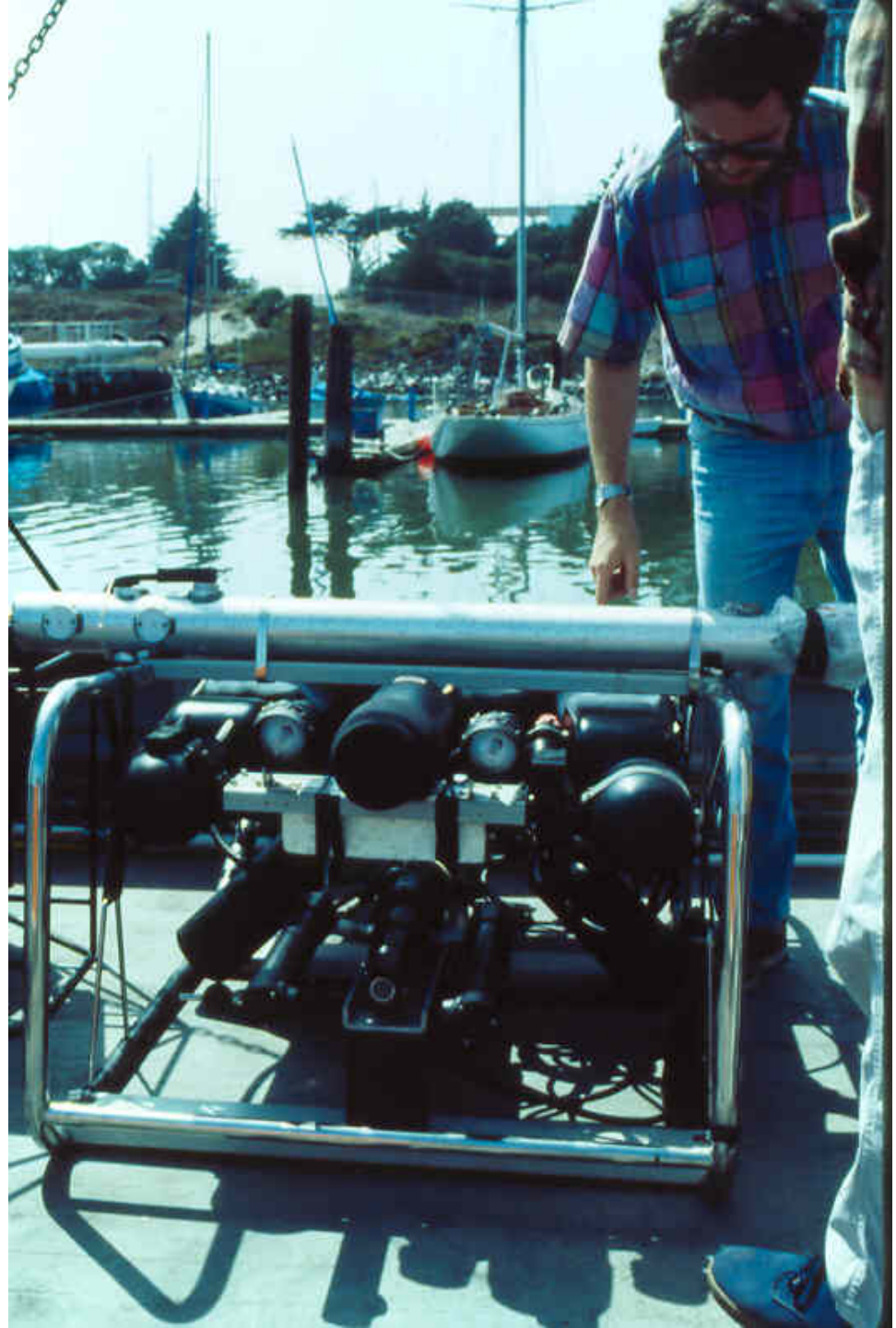
A smaller ship meant individual samples



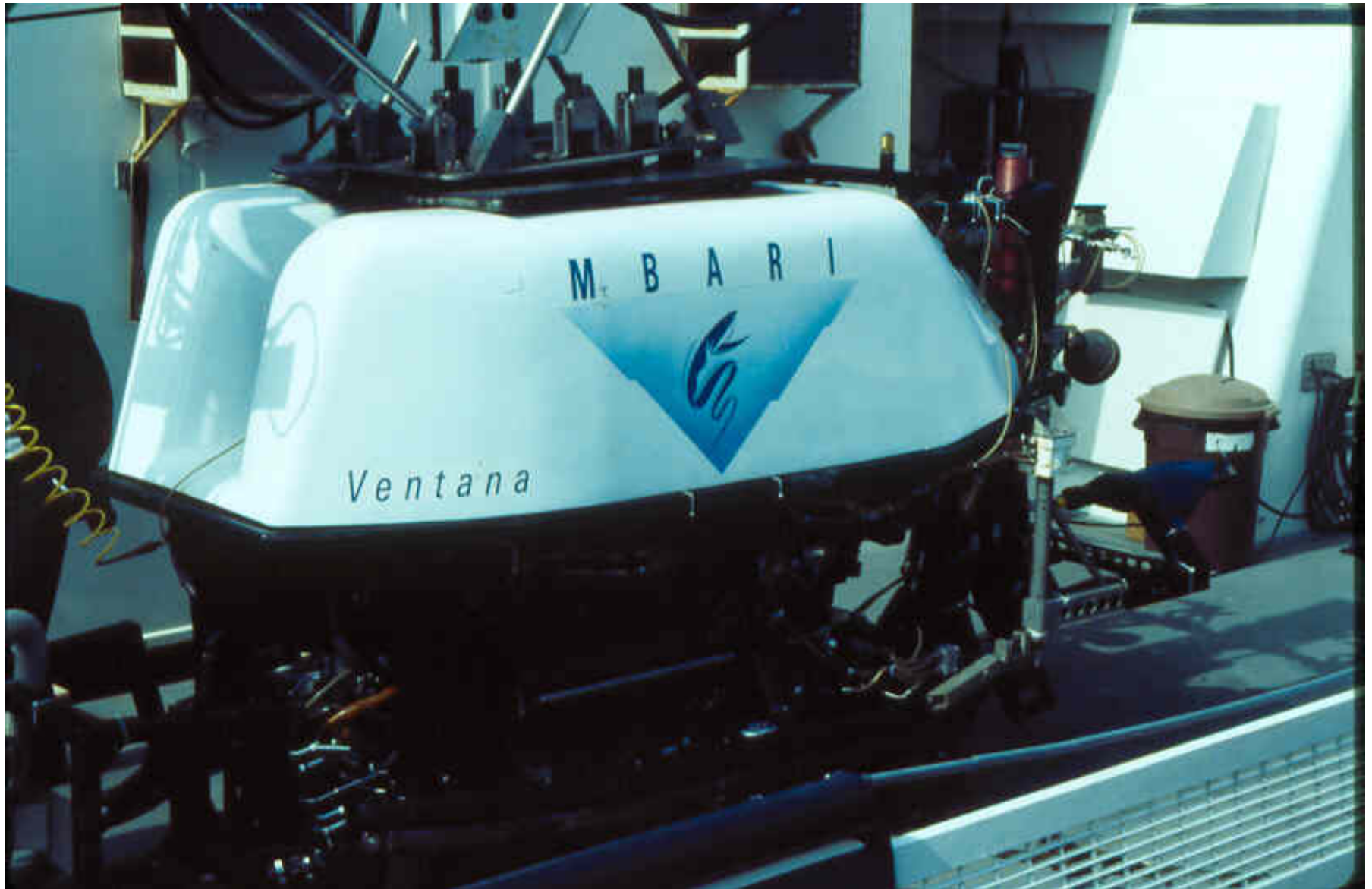
A number of camera systems were used in the Monterey Bay Study: The UCSB Sno Cam

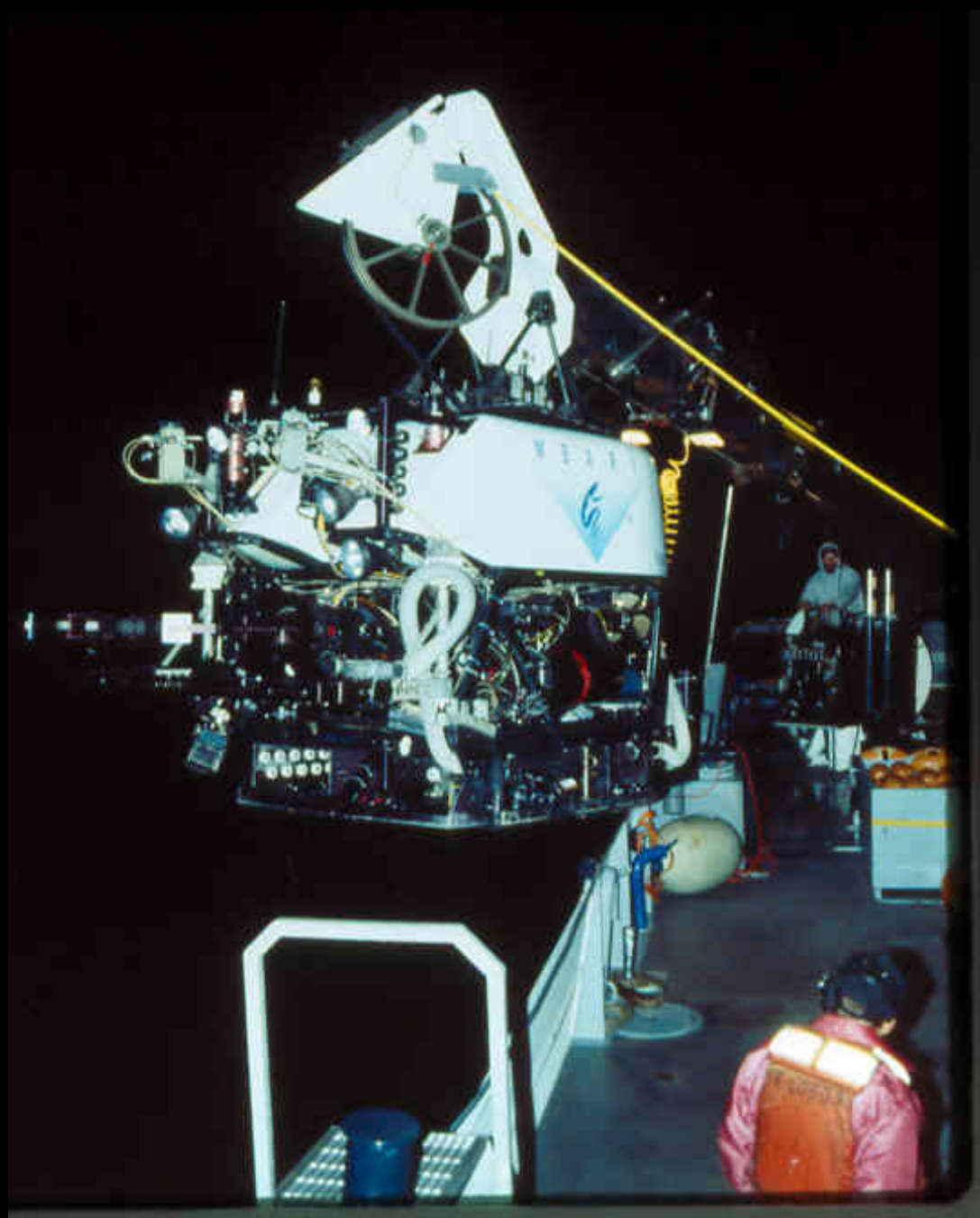


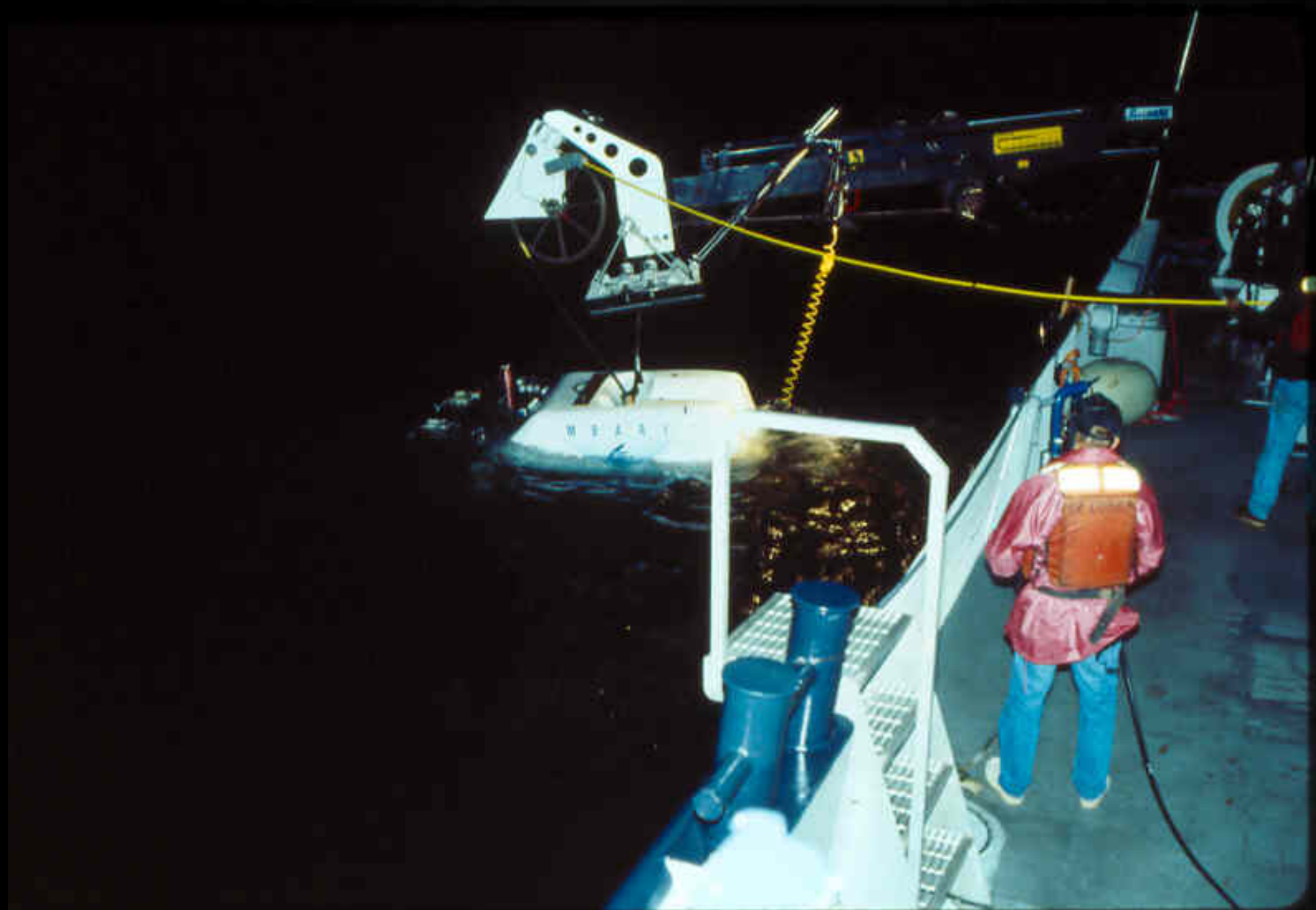
Camera system
used by group
from University of
Florida



The Monterey Bay Aquarium Bay Research Institute (MBARI) Camera System



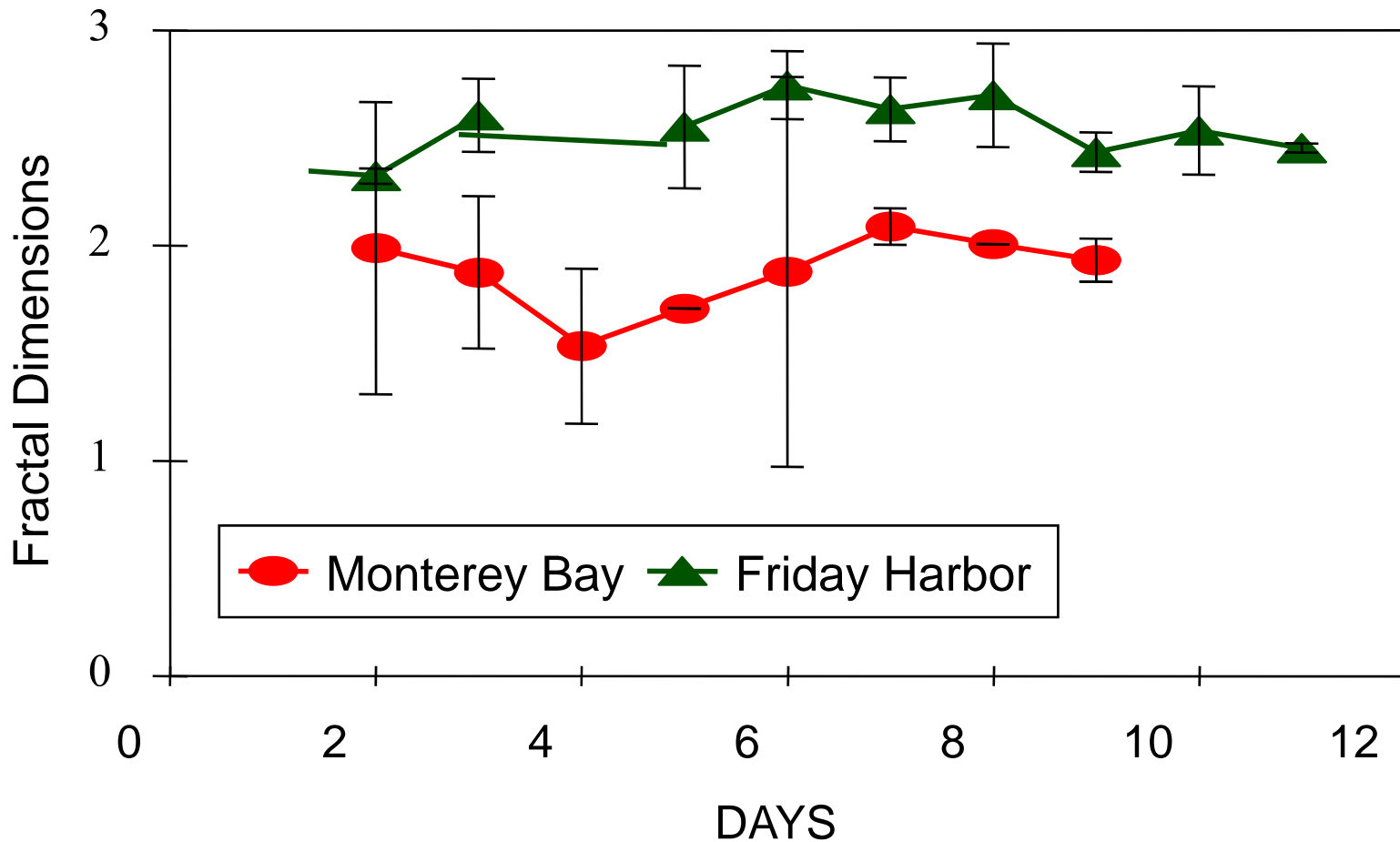




The depth and location of the camera system was remotely controlled from onboard the ship.



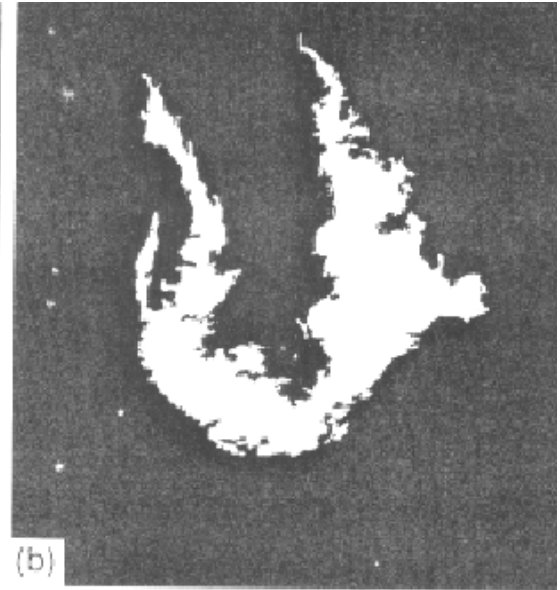
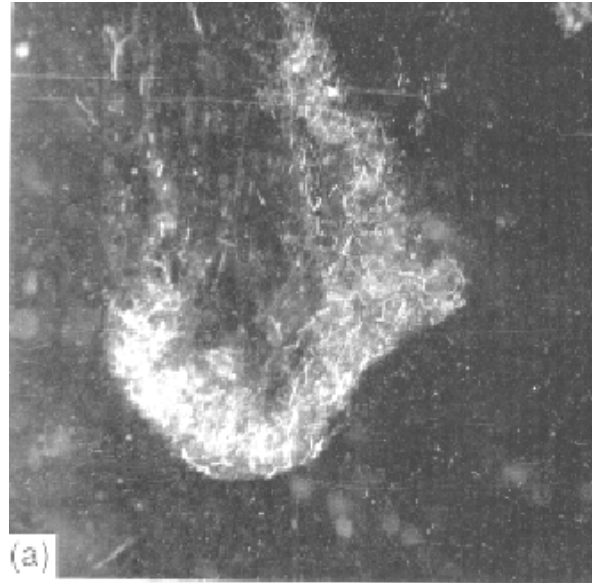
Field Measurements of Fractal dimensions (D_3) using PCT



Source: Li and Logan (1995) *Deep Sea Res*

Image analysis of Marine Snow using Photographs taken by Divers: Determining D_2

Diatom floc



Larvacean house

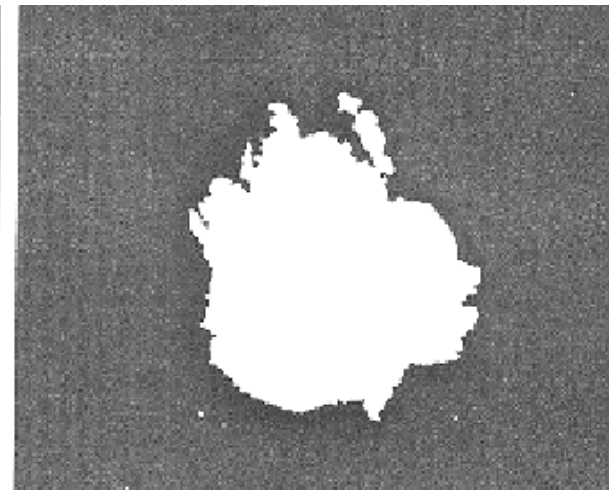
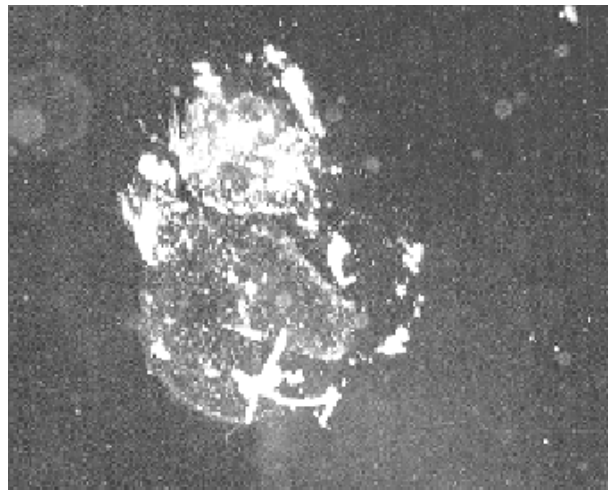
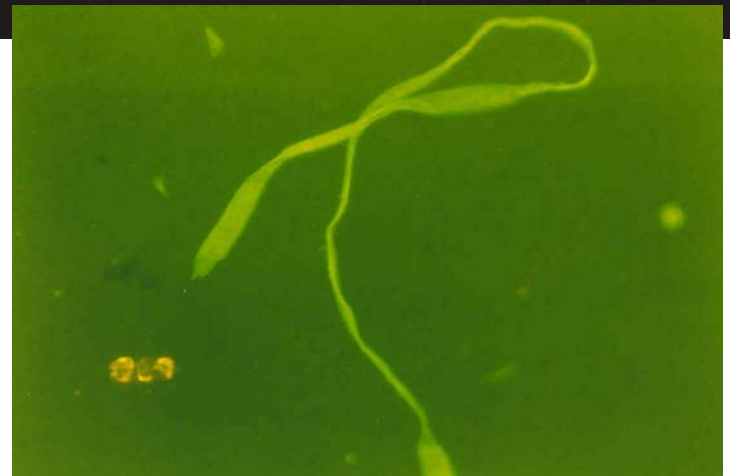
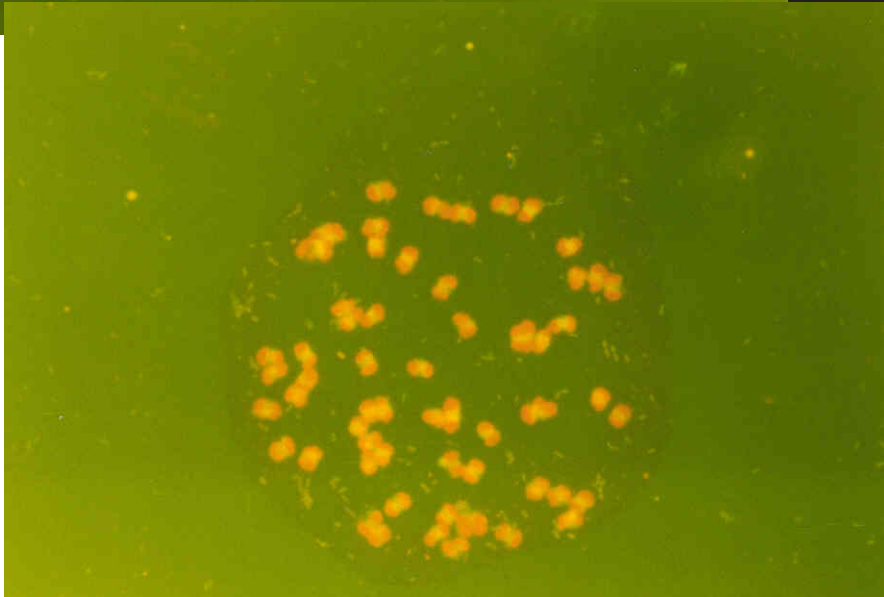
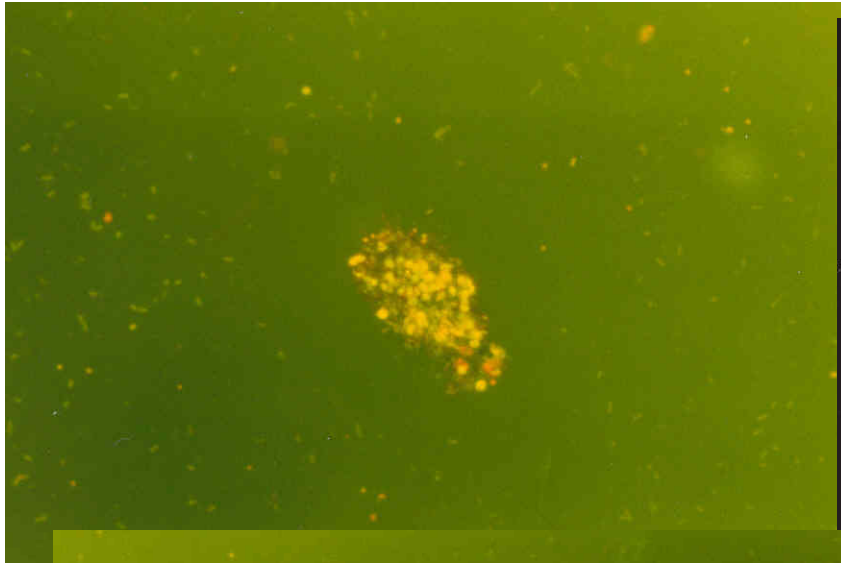


Image analysis done on particles in seawater by staining all particles with Acridine Orange



Fractal dimensions from Monterey Bay and UCSB studies: Marine Snow and Smaller Particles

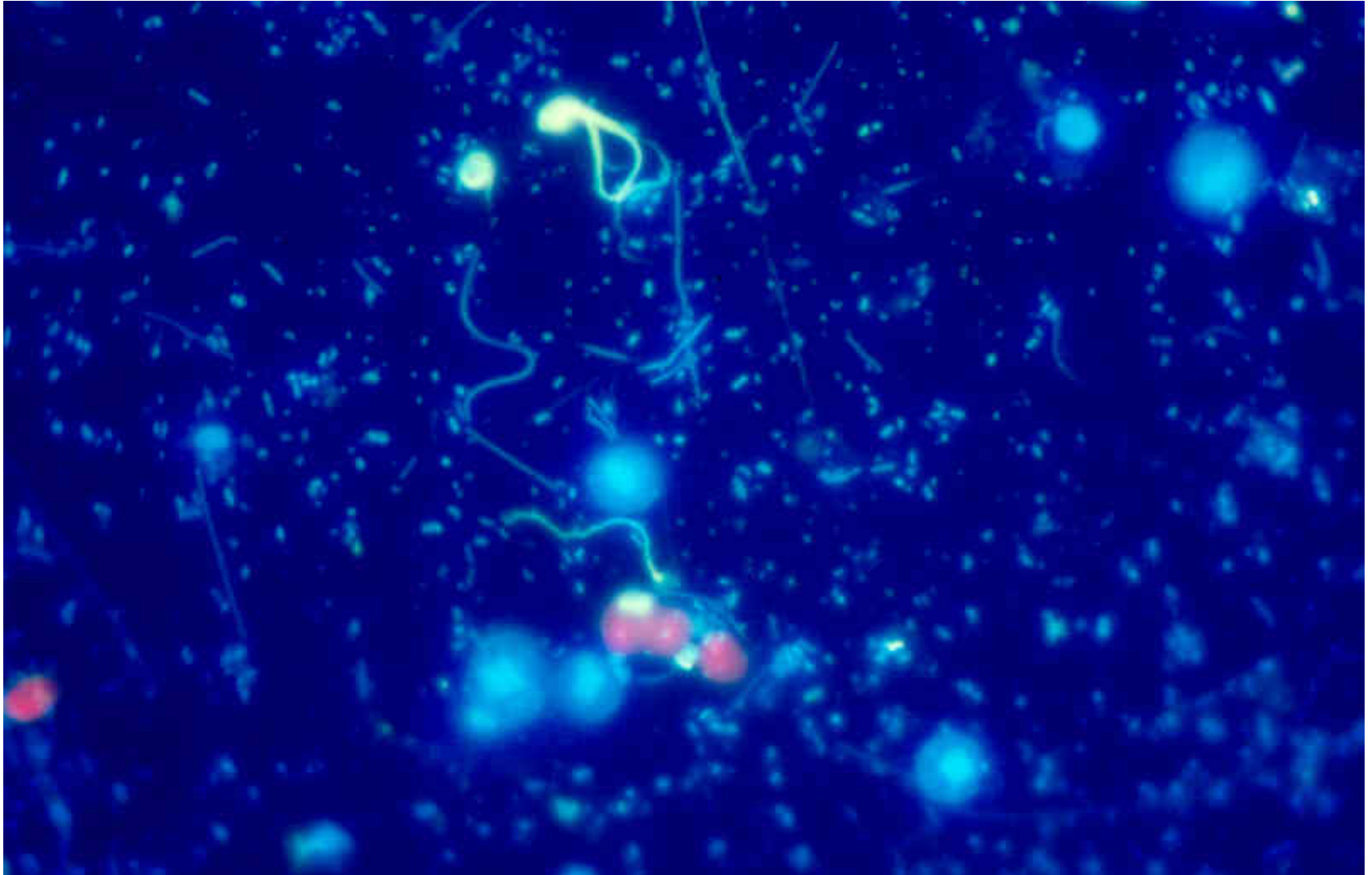
Aggregate Type	Method	Fractal dimension	Ref.
MARINE SNOW (Divers photographs, large aggregates)			
Miscellaneous	Power (area)	1.28 (± 0.11)	a
Fecal pellets	Power (area)	1.34 (± 0.16)	a
Amorphous	Power (area)	1.63 (± 0.72)	a
Diatoms	Power (area)	1.86 (± 0.13)	a
General	Power (mass)	1.52 (± 0.19)	b
OCEAN PARTICLES (Particle size spectra; <300 μm particles)			
>40 μm	SSM (size distrib.)	1.48 - 1.92	c

a- Kilps et al. (1993), b- Logan and Wilkinson (1990), c- Jiang and Logan (1991).

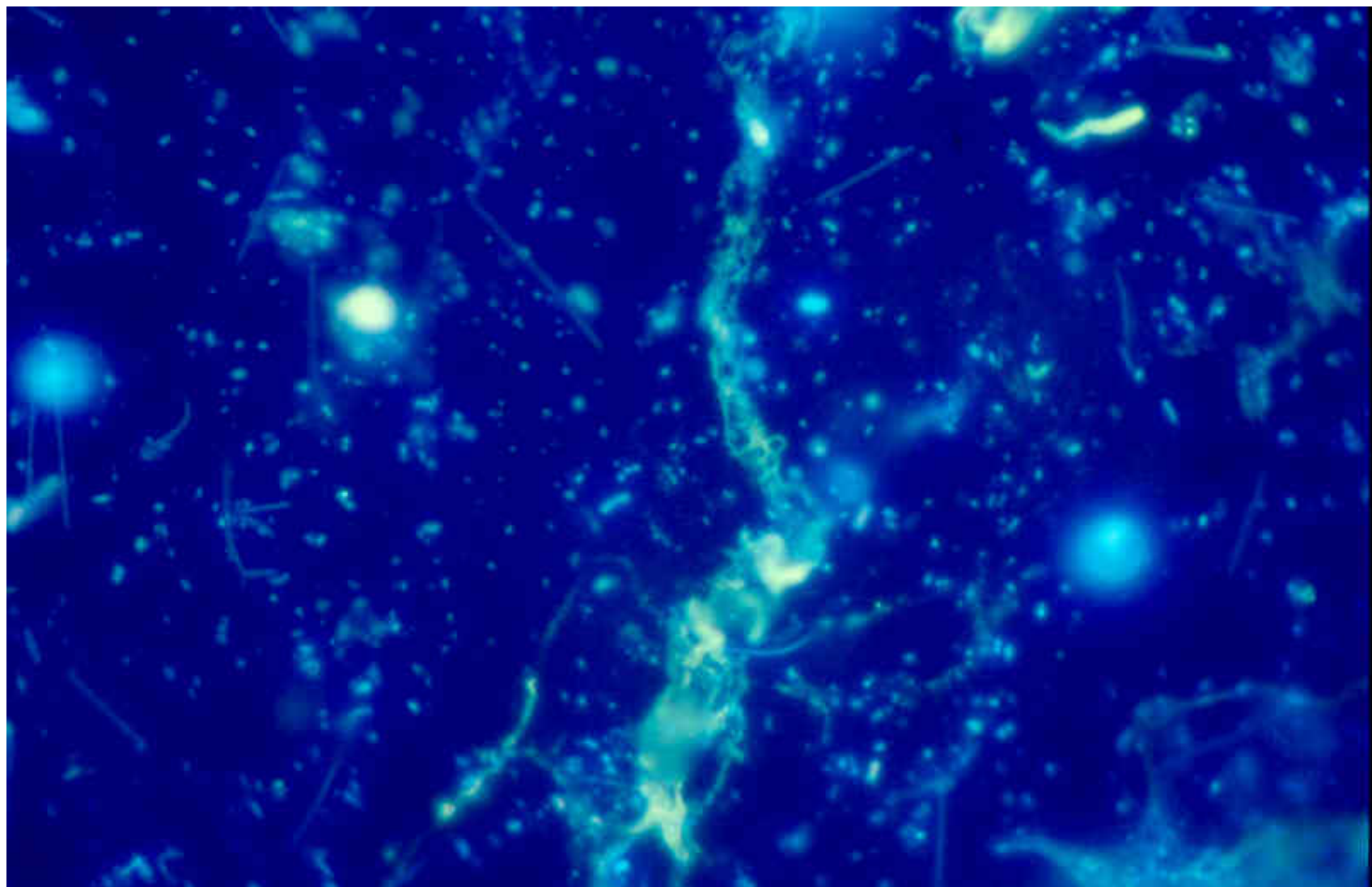
Particle Formation & Lake Snow

- Lake Constance (Konstanz, or the Bodensee) is located at the intersection of Germany, Switzerland, and Austria
- It is a deep, oligotrophic Lake formed by runoff from the Swiss Alps.
- Large aggregates, or Lake snow, have been observed to form there.
- In 1993, we studied particle formation during the spring to determine if TEP contributed to snow formation in the manner observed in California.

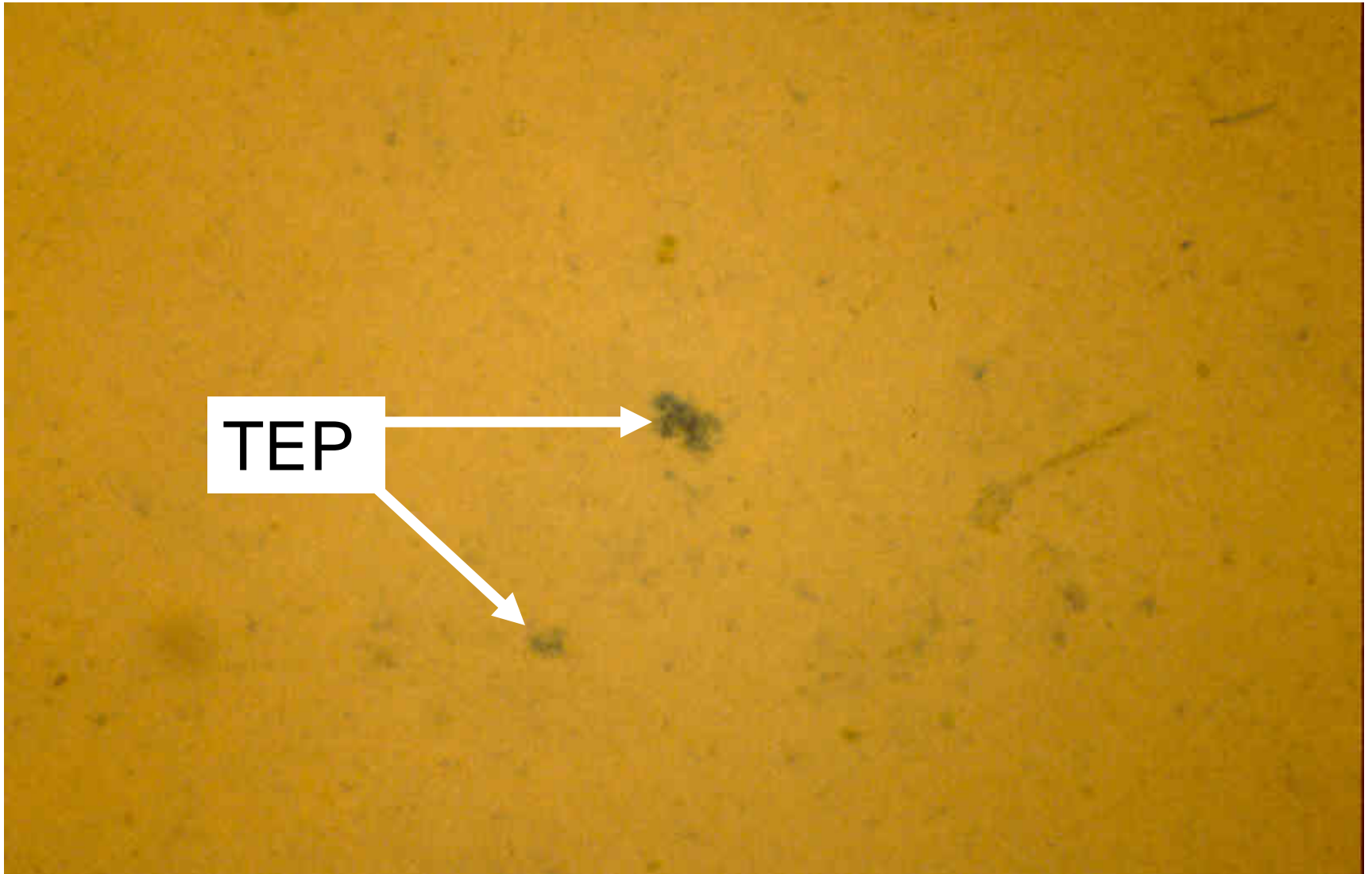
Particles in Lake Constance: Sample was double-stained with DAPI (fluorescence) for total bacteria and alcian blue



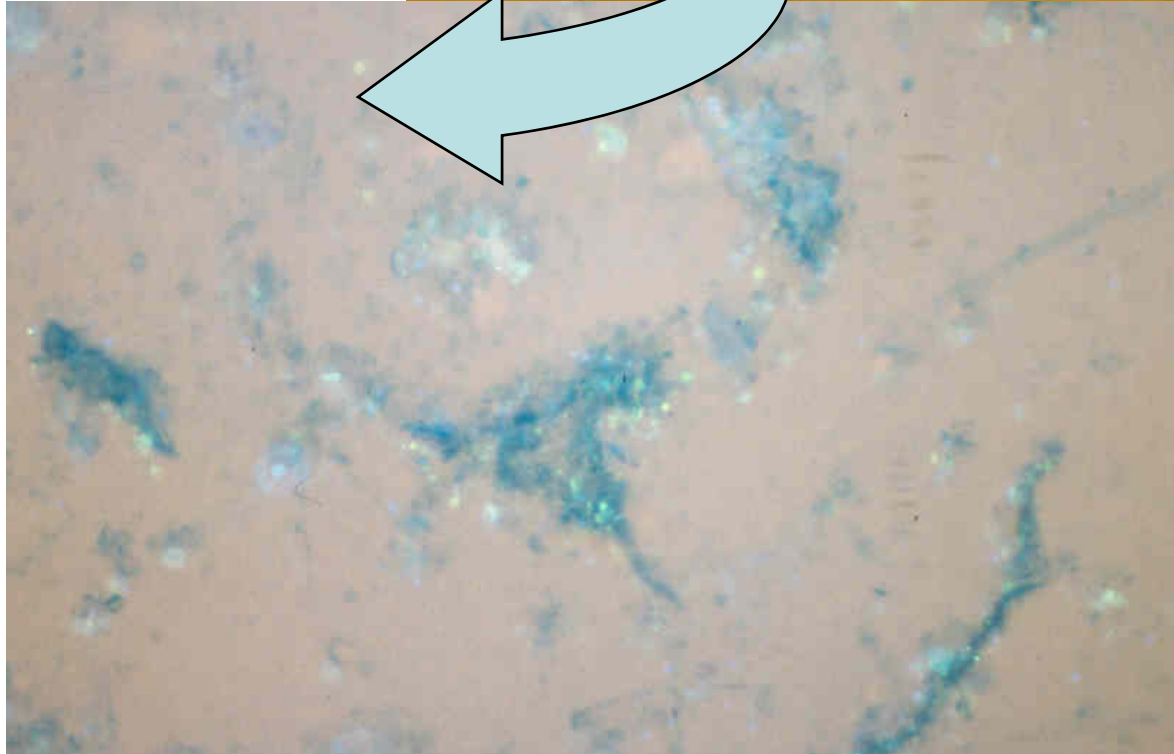




Particles in Lake Constance: Alcian blue (AB) was used to count TEP particles (AB stains negatively-charged polysaccharides)



Notice how the
concentration
and size of TEP
increased
during the
spring season



Half lives of TEP in Lake Constance

In the last week of April,
there was a storm that
increased shear in the water.

This produced a massive
coagulation event and loss
of TEP.

TEP loss was reflected in
sediment trap data taken
(data not shown).

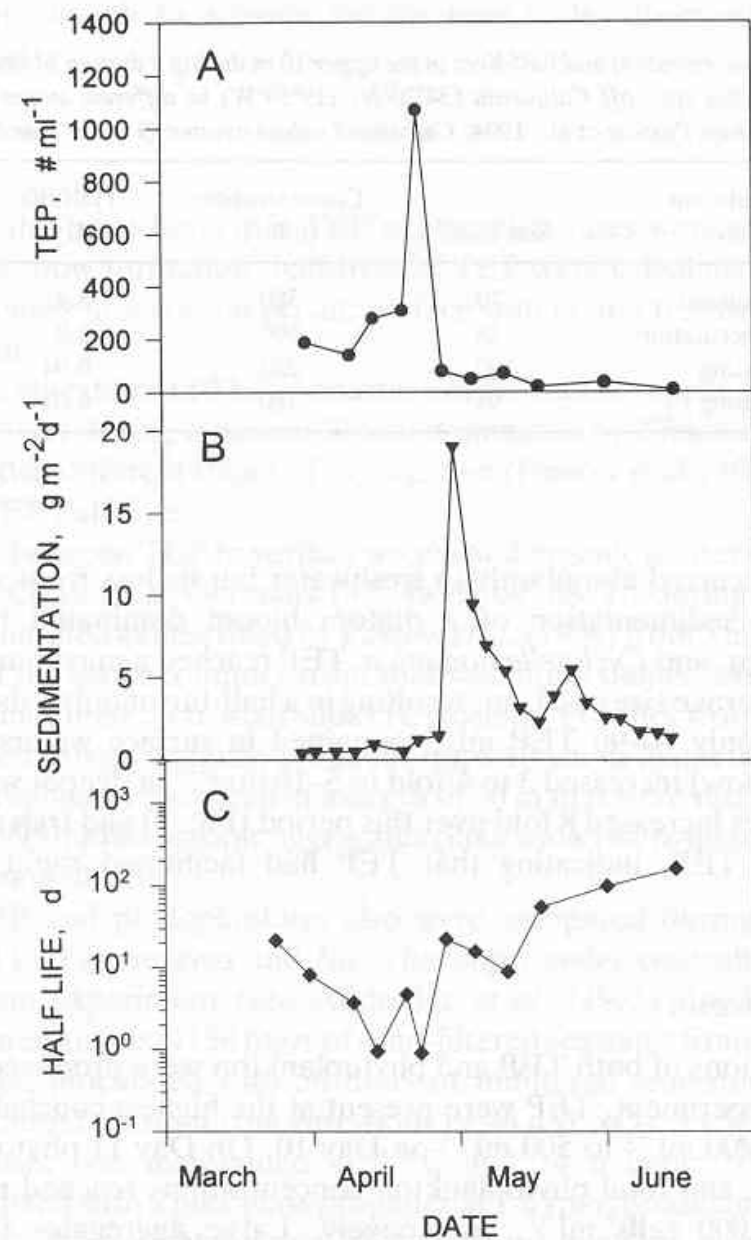


Fig. 1. (A) The concentration of TEP; (B) sedimentation rates of particulate mass; and (C) the half-lives of TEP particles in surface waters of Lake Constance during the spring of 1993. The peak in sedimentation follows the peak and disappearance of TEP from surface waters. Short half-lives (<1 day) support high TEP coagulation rates. (Calculations assume $G = 1 \text{ s}^{-1}$ and $\alpha = 1$.)

Conclusions From Lab & Field Studies

👍 D_3 is lower for aggregates formed in natural systems than those made in the laboratory

📁 Natural systems: $1.28 < D_3 < 1.92$

📁 Paddle mixers: $1.89 < D_3 < 1.92$

👍 D_3 are lower for aggregates formed by sedimentation than by shear

📁 Sedimentation: $1.6 < D_3 < 1.7$

📁 Shear: $1.8 < D_3 < 2.5$

👍 Low fractal dimensions of particles typical of systems where coagulation is important

📁 Monterey Bay: $D_3 = 1.6$

📁 Friday Harbor: $D_3 = 2.5$

Implications of the Fractal Structure of Aggregates

Settling Velocities
Coagulation Rates

Settling velocities of fractal aggregates versus spheres

👉 Settling velocities power laws differ:

📁 Sphere: $U_s \sim d^2$

📁 Fractal: $U_s \sim d^x$ where $x < 2$

👉 Fractal aggregates settle faster than spheres

Settling velocity: Spheres

From Stokes' Law, the settling velocity of a sphere is:

$$\dot{U}_s = \frac{g \Delta \rho (1 - \theta_{ag})}{18 \nu_w \rho_w} d_{ag}^2$$

or in terms of number of particles in an aggregate,

$$\dot{U}_s = \frac{g \Delta \rho \nu_\rho}{3 \pi \nu_w \rho_w} \frac{N^*}{d_{ag}} \quad \text{where} \quad N \sim d_{ag}^3$$

Therefore, $\dot{U}_s \sim d_{ag}^2$

Settling velocity: Fractals

From fractal scaling relationships,

$$U_s = \left[\frac{\Pi^2 g \xi_\rho I_\rho^3}{18 b_{d1} \rho_w \xi_2 v^{b_d}} (\rho_\rho - \rho_w) b_D I_g^{D_2-D-2} I_{ag}^{D-D_2+b_d} \right]^{\frac{1}{2-b_d}}$$

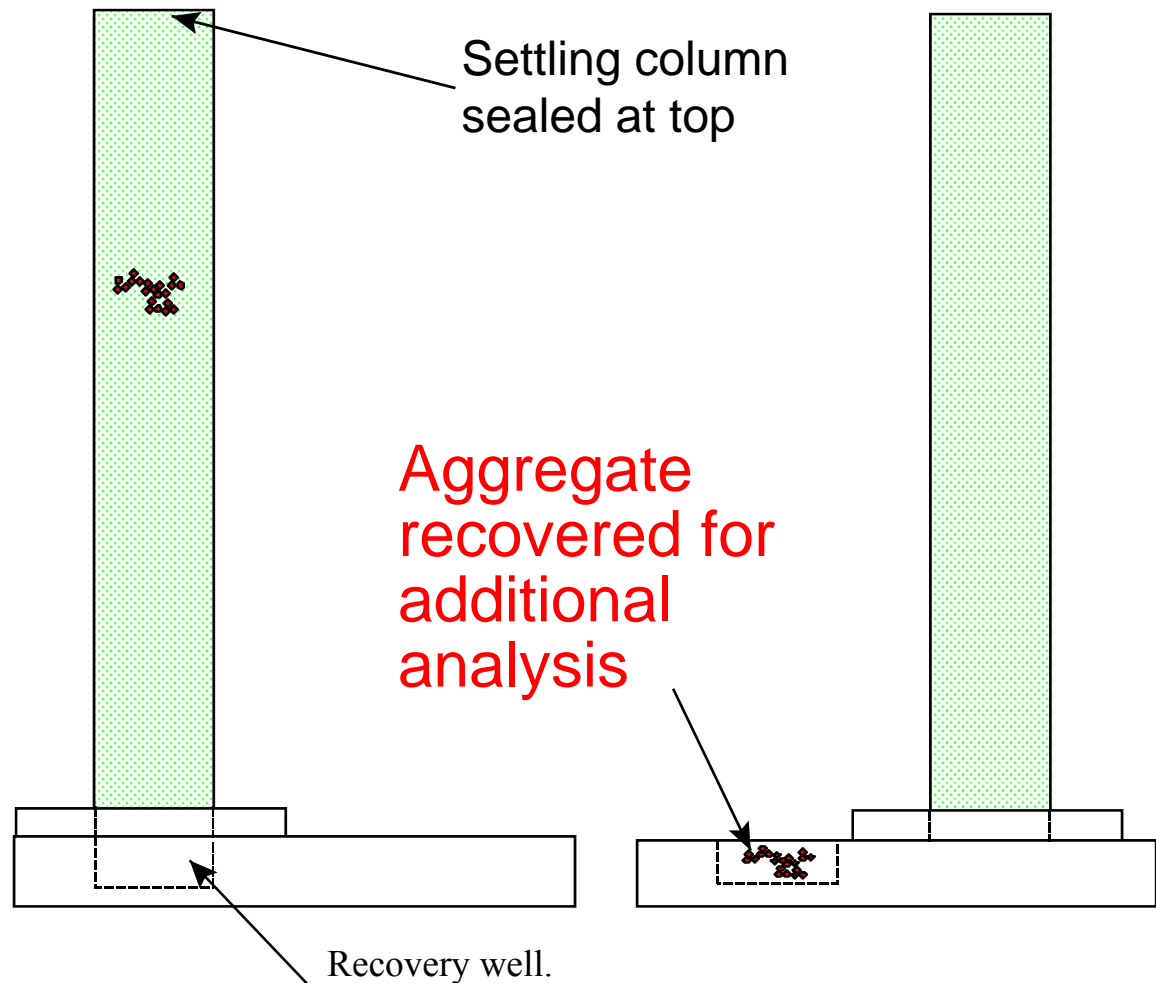
The scaling relationship between U_s and I_{ag} is therefore

$$U_{set} \sim I^{\frac{D_3-D_2+b_d}{2-b_d}}$$

where b_d is a drag coefficient (unknown for fractals, but known for spheres).

Experimental measurement of settling velocities of fractal aggregates

Aggregates introduced one at a time. Settling velocity measured using a camera system.



Parameters measured for each aggregate

l = size of aggregate

A = cross-sectional area

U_s = settling velocity

N_p = number of particles in aggregate, and therefore,

m = mass of aggregate

v = solid volume of aggregate

Settling velocities of microsphere aggregates

Fractals settle 4-10 times faster than predicted by Stokes' law

From: Johnson et al. (1997) *ES&T*

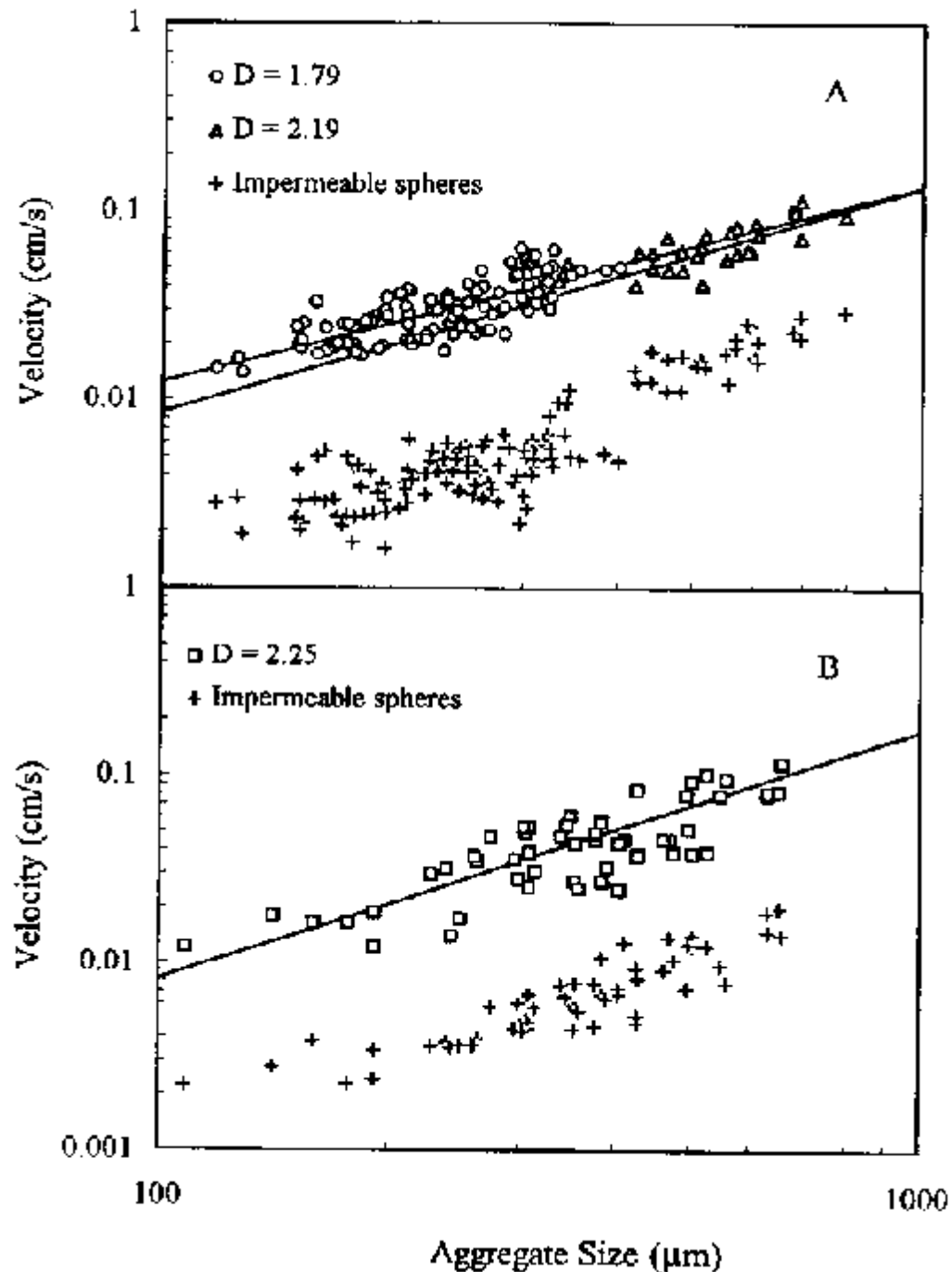


FIGURE 4 Settling velocities of aggregates predicted using fractal models

Implications of the Fractal Structure of Aggregates

Settling Velocities
Coagulation Rates

Aggregate coagulation rates

Particle coagulation rate can be described by

$$\frac{dn_h}{dt} = \frac{1}{2} \sum_{i=j=h} \alpha\beta(v_i, v_j) n_i n_j - \sum_{i=1}^{\infty} \alpha\beta(v_i, v_h) n_i n_h$$

where: n = particle concentration in a size interval

α = sticking efficiency

β = collision efficiency

$$\beta = \beta_{Br} + \beta_{sh} + \beta_{ds}$$

Collision function: spheres

Mechanism	Collision Function
Brownian motion	$\beta_{Br} = \frac{2 k_B T}{3 \mu_w} \frac{(d_i + d_j)^2}{d_i d_j}$
Turbulent shear	$\beta_{sh} = \frac{G}{6 \cdot 18} (d_i + d_j)^3$
Differential sedimentation	$\beta_{ds} = \frac{g \pi \Delta \rho}{72 \nu \rho} d_i^2 - d_j^2 (d_i + d_j)^2$

Collision function: fractals

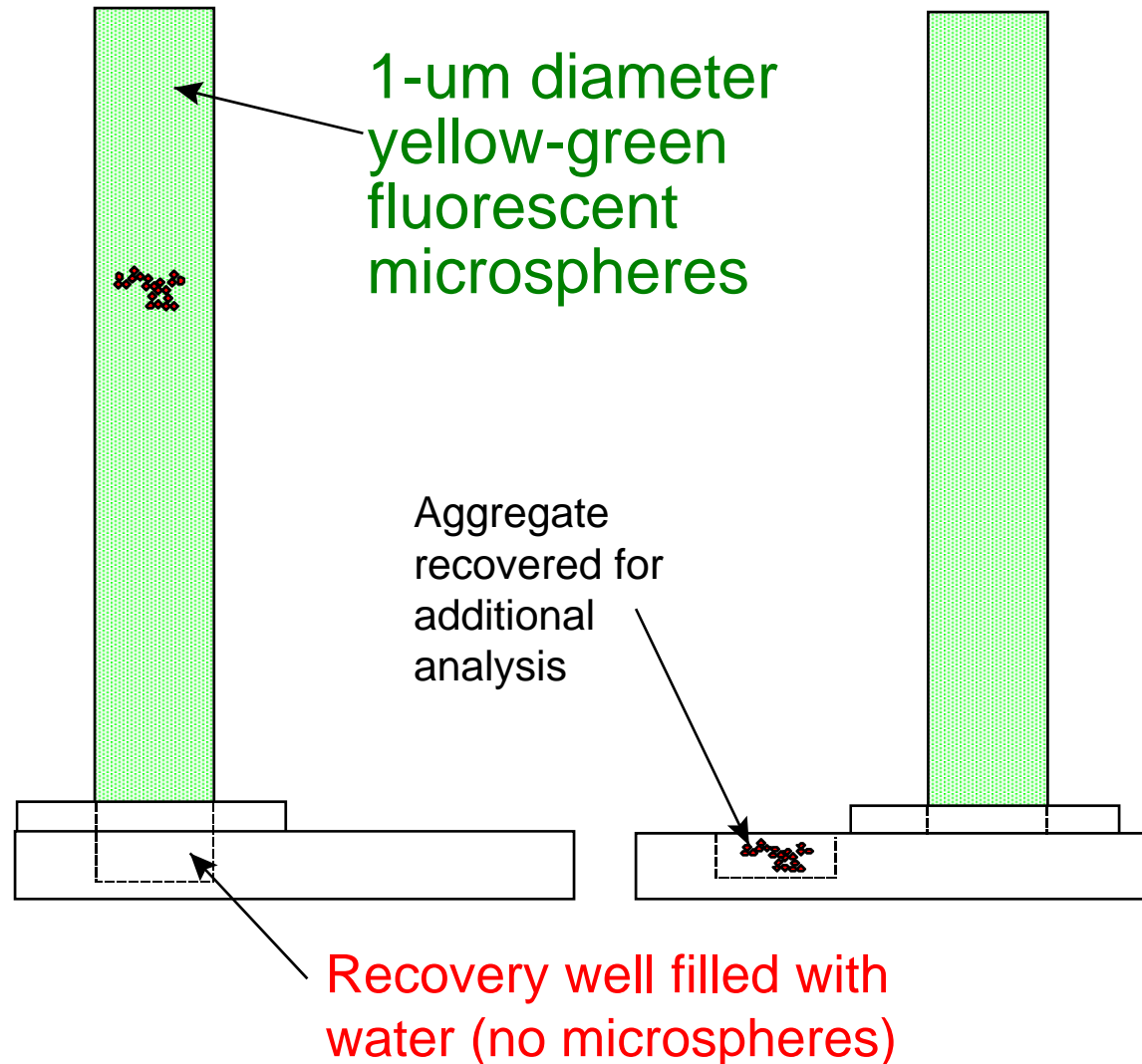
$$\beta_{Br} = \frac{2k_B T}{3\mu_w} \left(v_i^{-1/D} + v_j^{-1/D} \right) \left(v_i^{1/D} + v_j^{1/D} \right)$$

$$\beta_{sh} = \frac{G}{6 \xi p b_D^{3/D}} v_\rho^{1-(3/D)} \left(v_i^{1/D} + v_j^{1/D} \right)^3$$

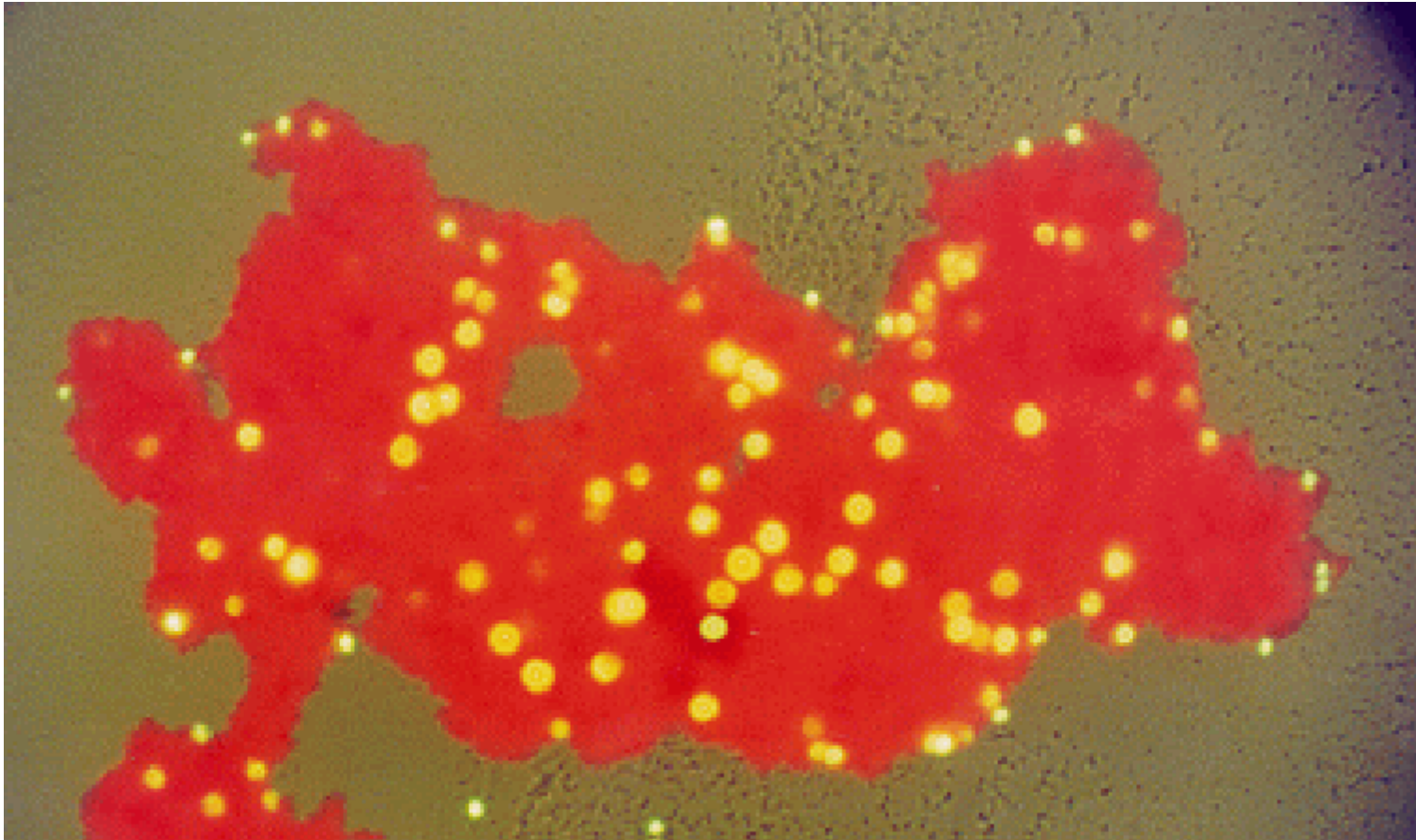
$$\beta_{ds} = \frac{\pi}{4} \left[\frac{2 g (\rho_\rho - \rho_w)}{b_{d1} \rho_w \xi_2 v^{b_d}} \right]^{\frac{1}{2-b_D}} \xi_\rho^{-\frac{1}{3}} b_D^{-\left(2 + \frac{b_d - D_2}{2-b_d}\right)} v_\rho^{\frac{1}{3} - \frac{1}{D} \left(2 + \frac{b_d - D_2}{2-b_d}\right)} \bullet$$

$$\left| v_i^{\frac{1}{D} \frac{D+b_d-D_2}{2-b_d}} - v_j^{\frac{1}{D} \frac{D+b_d-D_2}{2-b_d}} \right| \left(v_i^{\frac{1}{D}} + v_j^{\frac{1}{D}} \right)^2$$

Experimental measurement of fractal collision function: **Sedimentation**

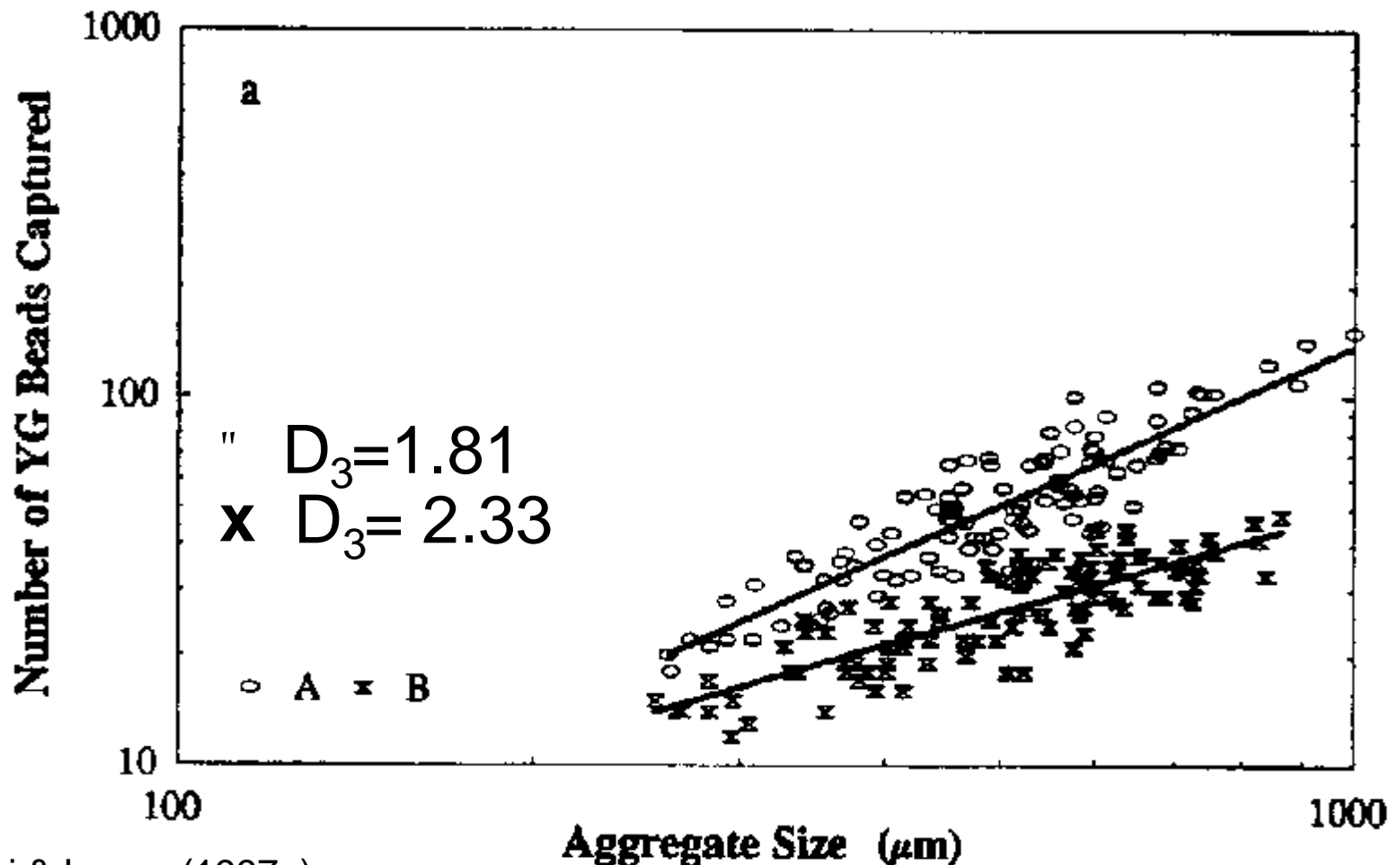


Example of fractal aggregate



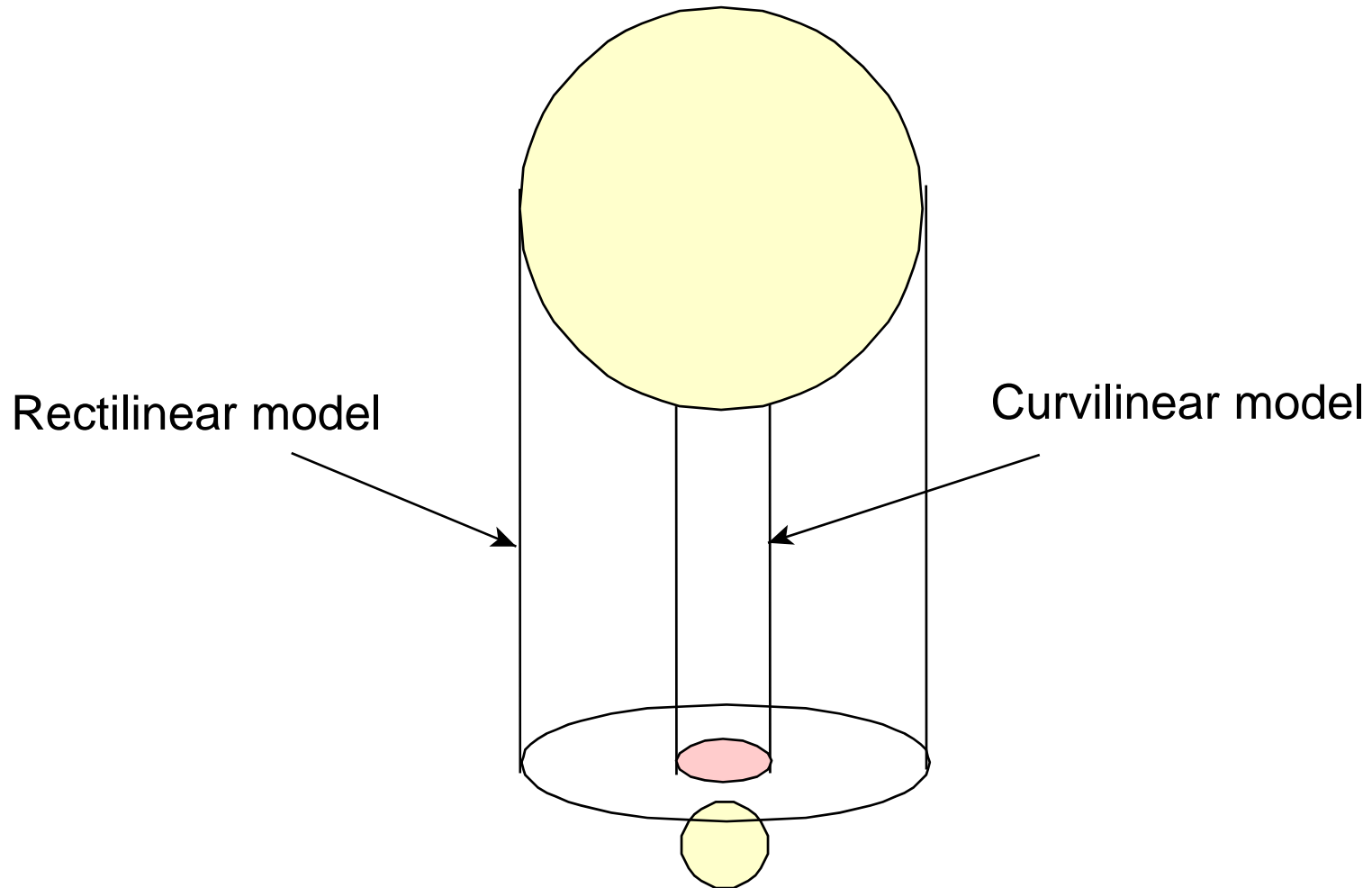
Results: Differential sedimentation

Bead capture is a function of D_3

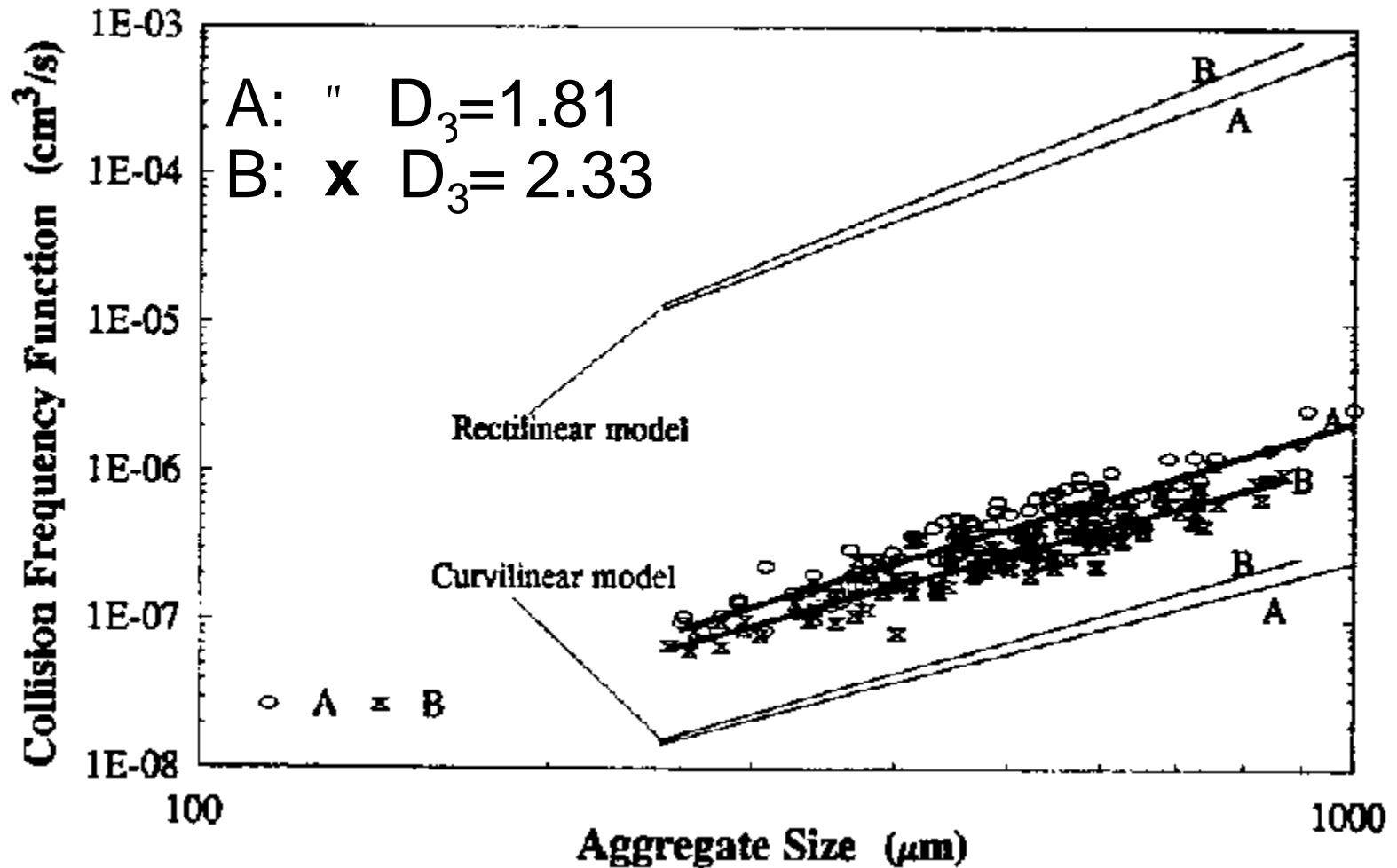


From: Li & Logan (1997a):
ES&T 31(4):1229-36, Figure 7a

Explanation of curvilinear versus rectilinear collision model

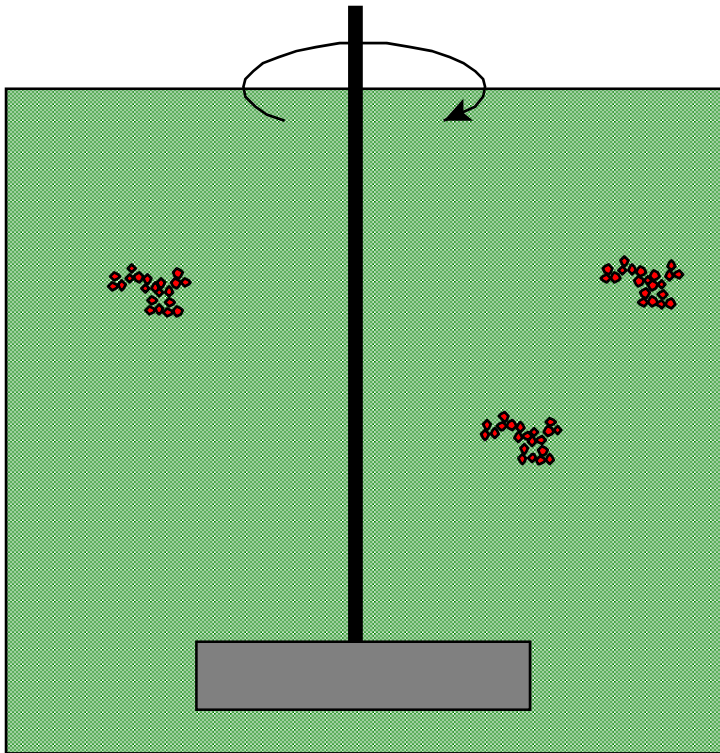


Results: Differential sedimentation



From: Li & Logan (1997a):
ES&T 31(4):1229-36, Figure 7b

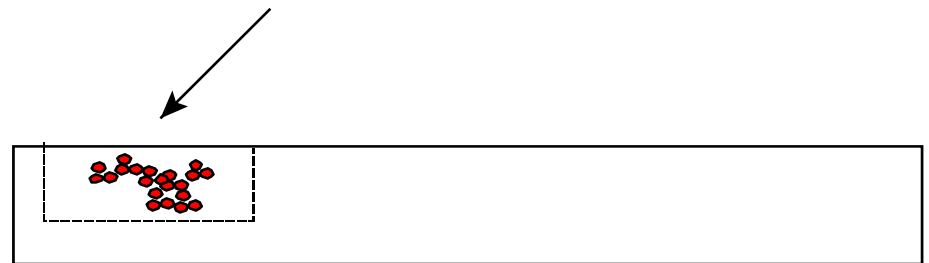
Experimental measurement of fractal collision function: Shear



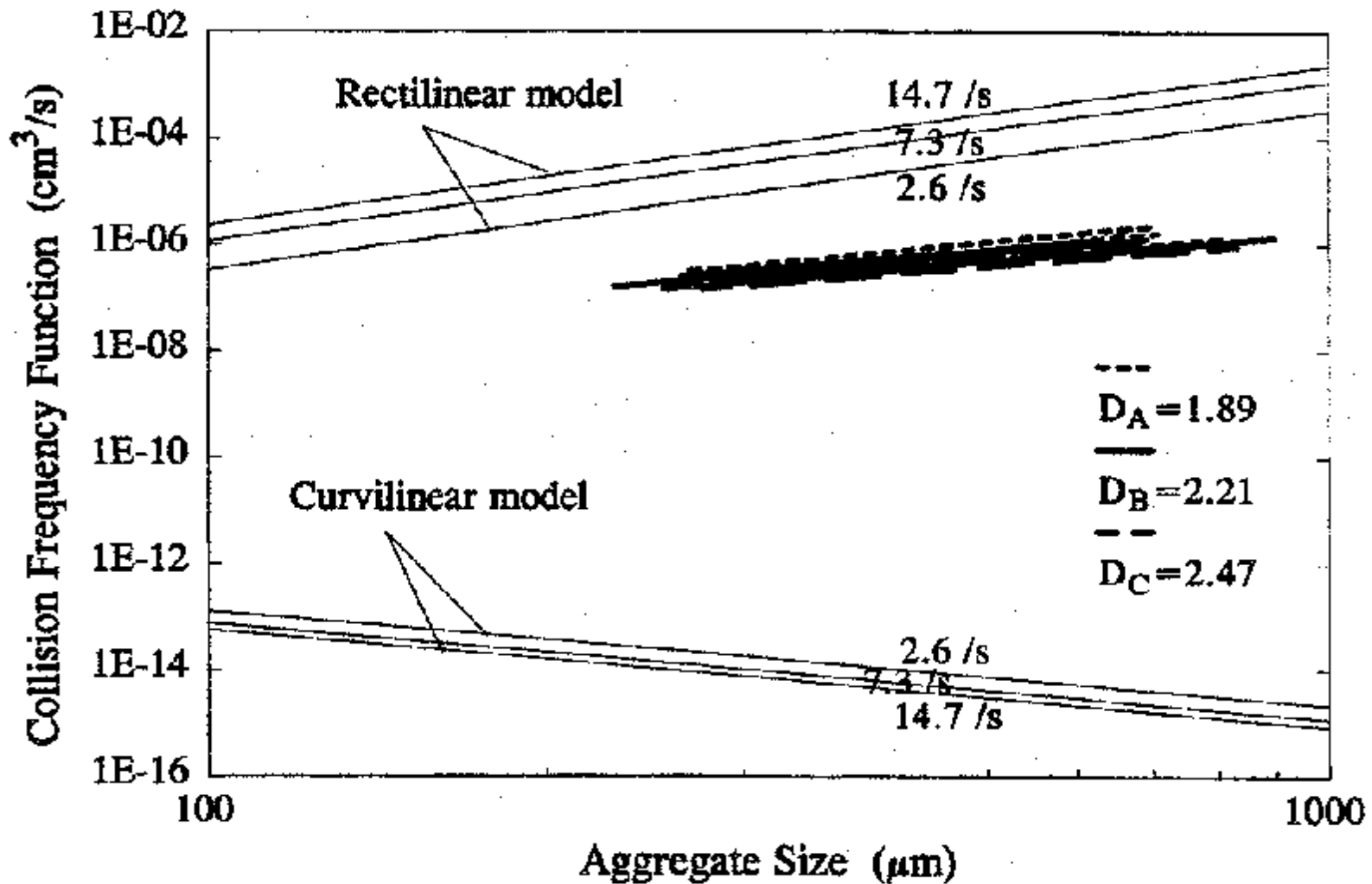
Beaker filled with 1- μm diameter yellow-green fluorescent microspheres

Paddle mixer apparatus used to measure collision efficiencies

Aggregate recovered for additional analysis after exposure time t in beaker



Results: Shear

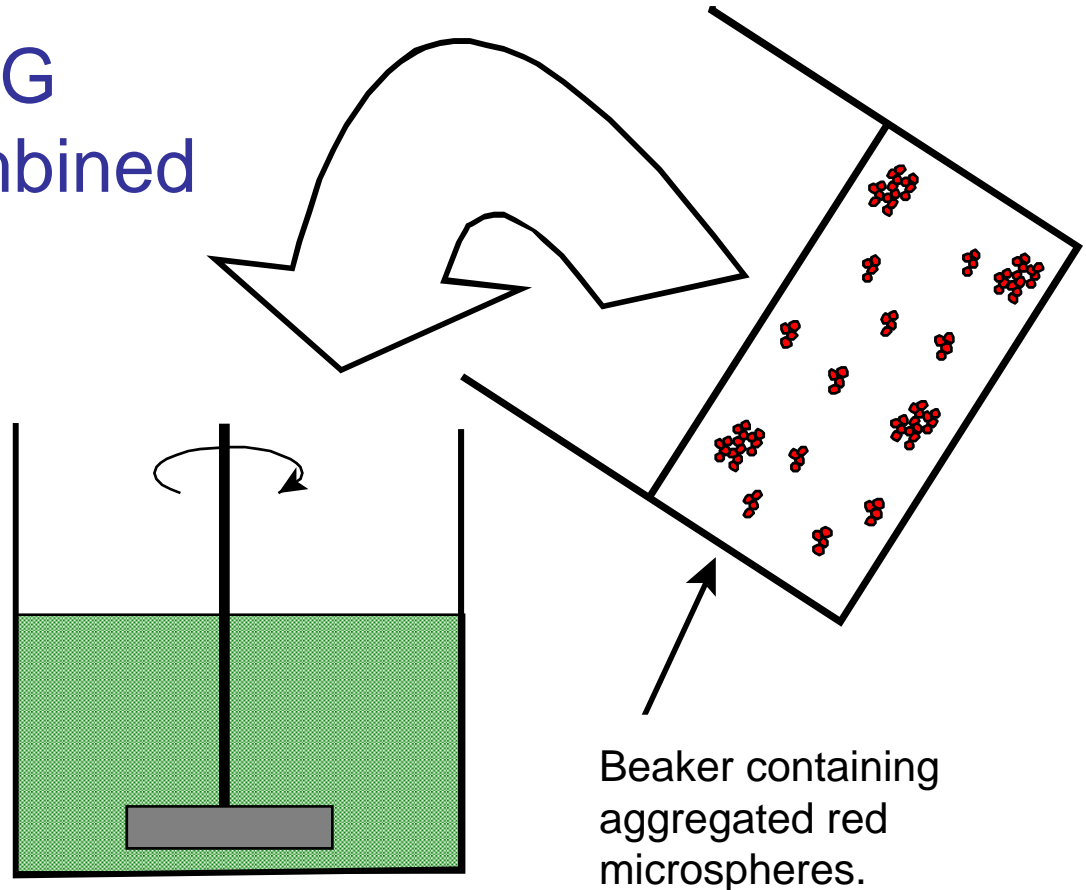


From: Li & Logan (1997b): ES&T 31(4):1237-42, Figure 7b

Experimental fractal collision functions: Shear, smaller particles

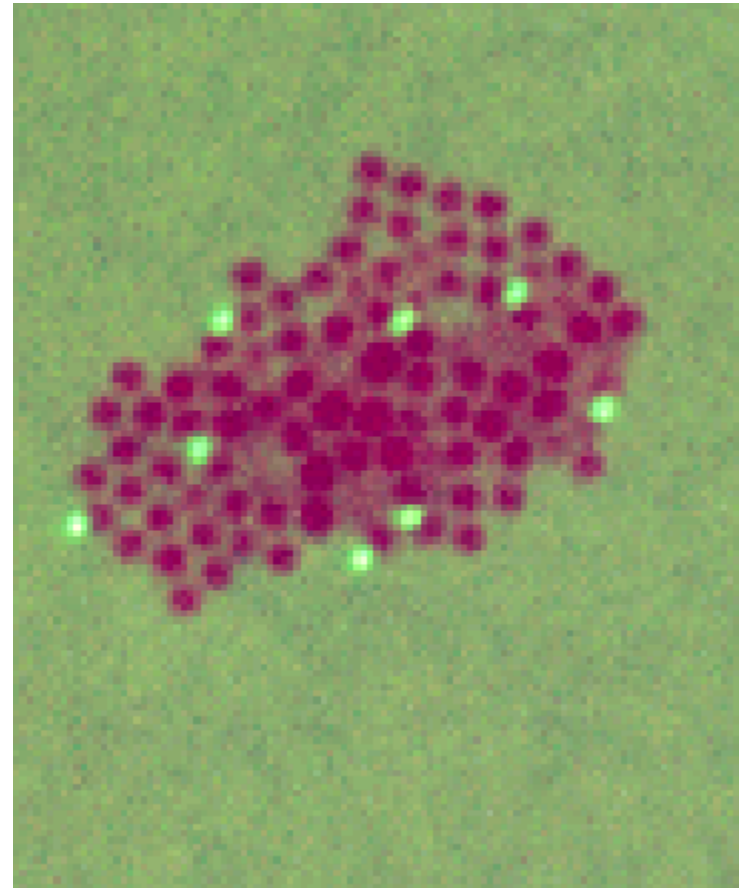
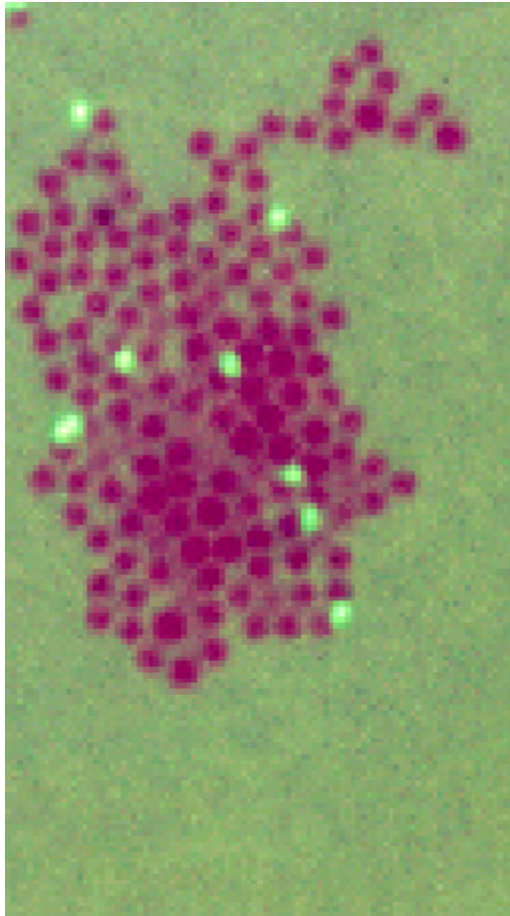
Aggregates and YG
microspheres combined
and coagulated.

Samples withdrawn,
filtered, and
aggregates examined
on microscope.

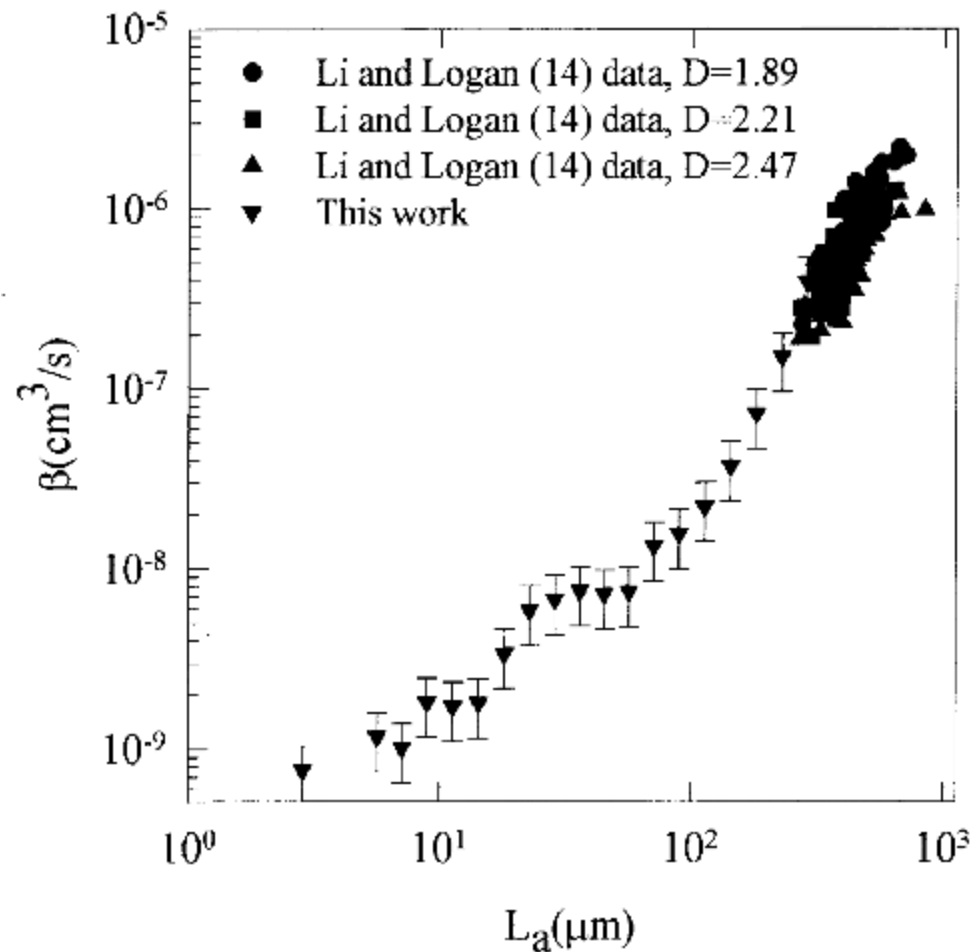


Beaker filled with 1- μm diameter
yellow-green fluorescent microspheres

Examples of small RB aggregates coagulated with monodisperse YG beads



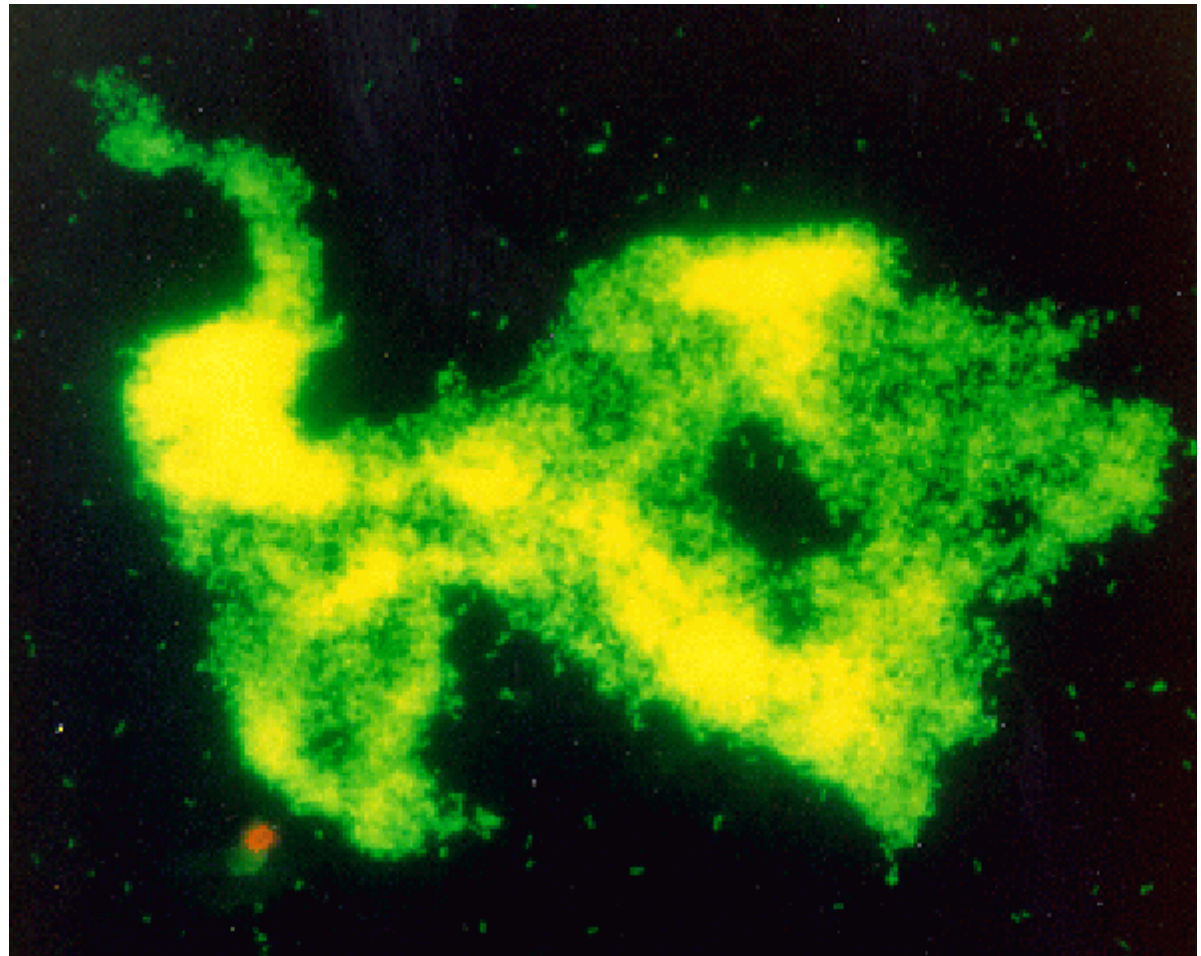
Results: Fluid shear with small and large microsphere aggregates



From: Serra & Logan (1999),
Environ. Sci. Technol.
Figure 5

Shear coagulation experiments repeated with bacterial aggregates and a monodisperse suspension of beads

Bacterial
aggregate
stained with a
fluorescent dye
(acridine orange)



Results: Fluid shear with microsphere and bacterial aggregates

From: Serra & Logan (1999),
Environ. Sci. Technol.
Figure 6

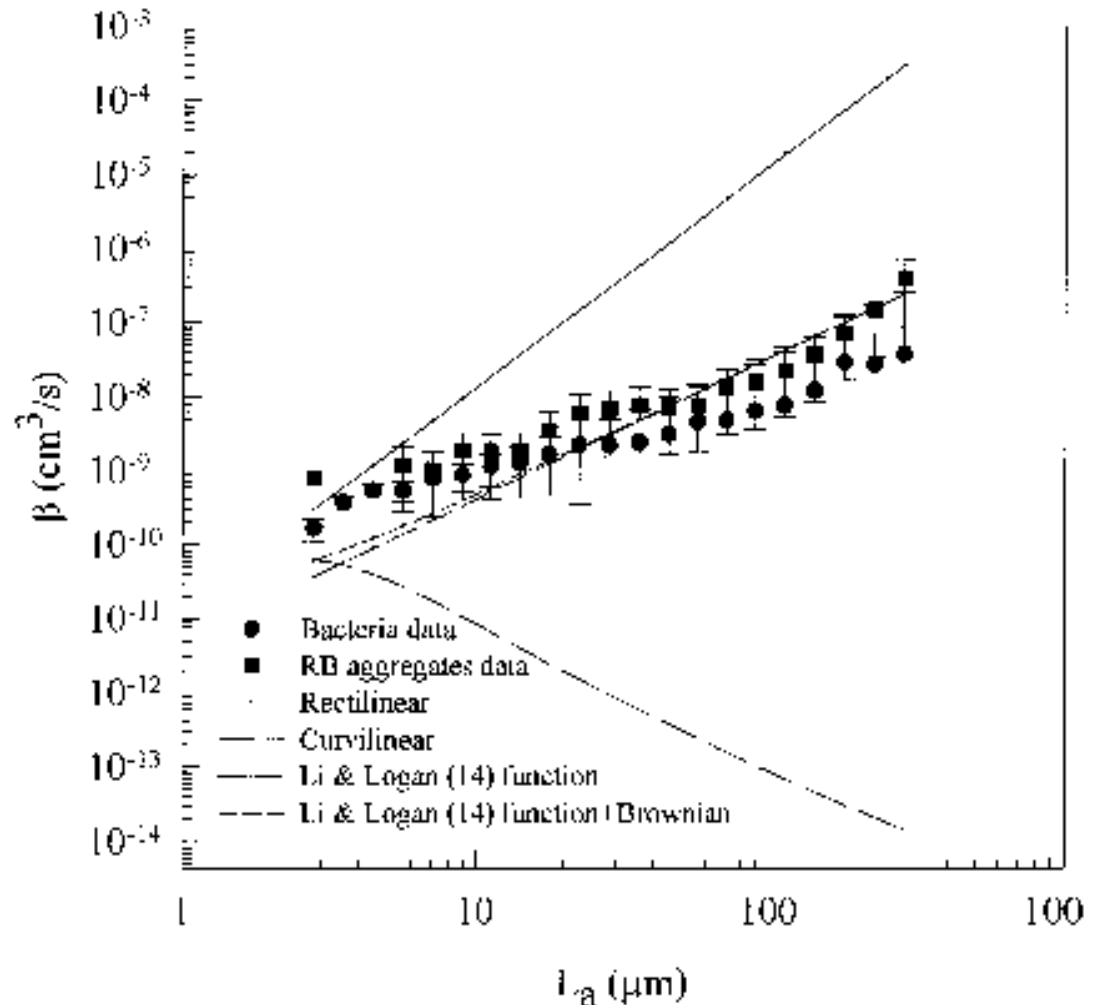


Figure 6

CONCLUSIONS

1. Microbial and inorganic aggregates have fractal geometries with fractal dimensions ranging from ~ 1.5 - 2.5 .
2. The fractal dimension, D , is a function of reactor type (paddle mixer, laminar shear, roller), particle type, and particle stickiness.

CONCLUSIONS ... cont'd

3. Settling fractal aggregates have lower drag coefficients than impermeable spheres (larger permeabilities) resulting in settling velocities that are an order-of-magnitude larger than spherical aggregates (of identical size and mass).
4. Collision frequencies of large fractal particles with much smaller particles are many times larger than those between spheres:
 - ~ $10 \times$ larger for differential sedimentation
 - ~ $10^6 \times$ larger for turbulent shear

Acknowledgements

Funding

Office of Naval Research (ONR) (to B.E. Logan) Comissió Interdepartamental de Recerca i Innovació Tecnològica (CIRT)(to T. Serra)

Students and Collaborators: SIGMA team, especially:

D. Wilkinson
J. Kilps
Q. Jiang
C. Johnson
X. Li
T. Serra

A.L. Alldredge
G. Jackson
U. Passow